COST

European cooperation in the field of scientific and technical research

COST Action 733

Proceedings from the 5th annual meeting of the European Meteorological Society

Session AW8 – Weather types classifications

Edited by
Ole Einar Tveito and Massimiliano Pasqui
Utrecht, Netherlands

12-16 September 2005

EUR 22594

Cataloguing data can be found at the end of this publication.

Luxembourg: Office for Official Publications of the European Communities, 2007

ISBN 978-92-898-0025-9

Printed in Belgium

PRINTED ON WHITE CHLORINE-FREE PAPER

Preface

This publication present the scientific papers from the session AW8 "Weather types classifications" at the 5th annual meeting of the European Meteorological Society (EMS). This session was initiated by COST Action 733 "Harmonization of weather types classifications in Europe" and convened by Dr. Ernst Dittmann and Dr. Massimiliano Pasqui.

In the session eight oral and nine posters were presented. Twelve of these presentations are published in this proceeding of the session.

Oslo, 7.June 2006

Ole Einar Tveito

Chair of
COST733 Management Committee.

Content.

Foreword

Dr. Ernst Dittmann
Former Chair of COST Action 733

The definition of Weather Types is connected to the development of Synoptic Meteorology during the second half of the 19th century. The establishment of national meteorological services with the conseqence of operating synoptic observational networks and the immediate exchange of data in an international frame was the basis of constructing actual daily weather maps in a continental scale.

Although it is true, that weather situations do never repeat exactly, a lot of characteristic features can be found in a series of synoptic weather maps over a long period of time. One of the first practical meteorologists to detect, define and publish systematic behaviour of the atmospheric circulation was W. J. van Bebber (1885). Other well-known classifications, based on daily weather maps since 1861 respectively 1881, were defined by H. H. Lamb (1972) and Hess&Brezowsky (1952). These subjectively compiled series are still maintained up to date.

In our computer age, a new classification method on weather types has to be '***objective***'. This means, that the basic data sets are numerical weather analyses and the criteria for defining weather types are numerically fixed. This guarantees identical results when repeating the application of a certain method to the same input data.

Since the last decades, weather types classifications mostly had been developed for special purposes like air quality problems, human health, fog situations, heat waves, droughts, cold spells, windy weather, periods of intense rainfall or others. This fact is reflected by any reference list on weather types classifications as well as by the content of the following articles.

COST Action 733 started in 2005 and took the opportunity of presenting its scope and objectives during the 5th scientific conference of the European Meteorological Society in Utrecht in September last year. A fundamental task was the evaluation of a questionnaire on the current use of weather types classifications in meteorological organisations and institutions in Europe. The results are documented in the first contribution of this publication. The following articles demonstrate the variety of actually used classification methods and of the application purposes.

The main objective of COST Action 733 is to achieve a general numerical method for assessing, comparing and classifying typical weather situations in European regions. The resulting procedure should be scalable in space and time from 200 km to 2000 km and from half a day to 3 days respectively, and it should be applicable to as much as possible purposes.

I would like to express my thanks to the Chair of COST Action 733, Ole Einar Tveito, and to all other members of the Management Committee for giving me the opportunity to this foreword. At last, I wish all participants in the Action a successful continuation of their work.

Inventory of Circulation Classification Methods and Their Applications in Europe within the COST 733 Action

Radan Huth[1,*], Zbigniew Ustrnul[2,3], Ernst Dittmann[4],
Peter Bissolli[4], Massimiliano Pasqui[5], Paul James[6]

[1] Institute of Atmospheric Physics, Prague, Czech Republic
[2] University of Silesia, Katowice, Poland
[3] Institute of Meteorology & Water Management, Krakow, Poland
[4] Deutscher Wetterdienst, Offenbach, Germany
[5] IBIME – CNR, Florence, Italy
[6] Meteorological Office, Exeter, United Knigdom
[*] email: huth@ufa.cas.cz

Abstract

The first step within the COST Action 733 "Harmonization and Applications of Weather Types Classifications for European Regions" was an inventory of already existing classifications by submitting a questionnaire to the scientific community. The outcome of this questionnaire provides a first overview about the spatial and temporal resolution, methods, number of types, and purpose of the classifications.

1. Introduction

Classification is one of the most commonly used statistical methodologies in the atmospheric sciences. For a review and intercomparison of various classifications, including their applications, refer to a couple of papers and textbooks dating back to the mid 1990's and earlier: Key and Crane (1986), Yarnal (1993), El-Kadi and Smithson (1992), and Huth (1996). Because of a wide variety of different classification methodologies, approaches, target regions, spatial scales, target variables, applications, etc., it appeared feasible to launch a new COST Action, aimed just at circulation and weather classifications. The first task of the COST Action, "Harmonization and Applications of Weather Types Classifications for European Regions" (COST733), is to compile an inventory of weather types (circulation pattern) classifications and its applications used in Europe. For this purpose, a questionnaire was made up and sent to relevant persons and institutions. Our aim is to cover different criteria, spatial areas and applications of circulation classifications for both research and operational purposes in as many European countries as possible. This contribution attempts to summarize the outputs of the questionnaire and provides information necessary for a forthcoming work within the COST733 Action.

2. Questionnaire and response

Based on the agreement made at the COST kick-off meeting in Brussels in April 2006, a questionnaire on the existing circulation / weather classifications, their applications, and comparison studies, was prepared. The questionnaire consists of 40 questions, concerning different aspects of the classifications (methods, datasets, spatial and temporal resolution, references, etc.), experience with the ERA-40 dataset, comparisons between different methods, and basic personal information about the respondent. The questionnaire was sent out to the members of the Management Committee, other persons who had expressed their interest to participate, and those suggested by members of the MC as potential contributors.

73 responses were received: in many cases, these were multiple responses from a single person or institution. This ensures a satisfactorily good coverage as to the topics and region. The countries from which a response was received are: Austria, Belgium, Czech Republic, Estonia, Finland, France, Germany, Greece, Hungary, Italy, Lithuania, Norway, Poland, Portugal, Romania, Serbia and Montenegro, Slovenia, Spain, Sweden, Switzerland, United Kingdom. Of the relevant large and medium-sized European countries (except for former U.S.S.R.), only Ireland, the Netherlands, Denmark, Slovakia, Croatia, and Bulgaria did not provide a response.

3. Analysis of the response

General remarks. A trivial and expected observation is that the classifications are varied in all of their aspects. A few procedures were reported, which in fact are not classifications; the possible implication is that the terms 'classification' and 'weather / circulation types' are not perceived by all meteorologists and climatologists in the same way. Such procedures are excluded from further analysis. The inventory reflects three different activities relevant for the COST Action, i.e., the development of own classifications, the application of already existing classifications to new regions / datasets, and comparison studies of several classifications. The most frequently used classifications are the Lamb and Hess-Brezowsky catalogues, including their various modifications and objectivized versions; among the objective methods, the k-means method of cluster analysis prevails.

Temporal resolution (Fig.1). The large majority (84% of reported classifications) operate on a daily basis. Altogether 9% of classifications operate on a shorter time scale, viz., 12 and 6 hours. However, the difference is not due to a specific methodology, but results mainly from data availability. Only 5% of classifications were operated on a monthly basis, but all with a remark that a daily timestep is also possible or has already been applied.

Spatial scales (Fig.2). The information about the horizontal scale, resolution, and geographical coordinates of the database was somewhat subjectively transformed into general qualitative information on the spatial scale in five different classes: continental (involving whole Europe with adjacent parts of the Atlantic Ocean, or at least a major part of Europe – typically more than 30° of latitude by 40° of longitude), sub-continental (involving large parts of Europe – typically of about 20° by 20°), country (involving a single country or a group of small countries, possibly including its / their close neighbourhood), regional (only a part of a single country), and local (single station). Larger-scale classifications prevail: The half of all classifications are of a continental scale, about 20% of them are of sub-continental and of country scale. The rest (8%) includes regional and local scales. All the local-scale classifications are based on weather, not circulation variables (see below).

What is classified (Fig.3). The largest number of classifications (84%) is based on variables describing baric fields (SLP, geopotential heights), usually gridded or in a map form, in some cases together with other variables (typically thickness, temperature, humidity). These are referred to as 'circulation classifications' and are principally what the COST 733 Action is supposed to concentrate on. One classification is based on cyclone trajectories. The 'weather classifications' (8%) are based on surface weather variables at a single station or a group of close stations, and frequently employ the diurnal cycle of the variables. One classification can be referred to as 'airmass' since it utilizes variables suitable for characterizing airmasses, viz., temperature and humidity, over a small area. One classification combines 'circulation' and 'weather'. Another classification is based on regional precipitation patterns. It is important to note that the share of classifications other than the circulation-based ones is likely to be

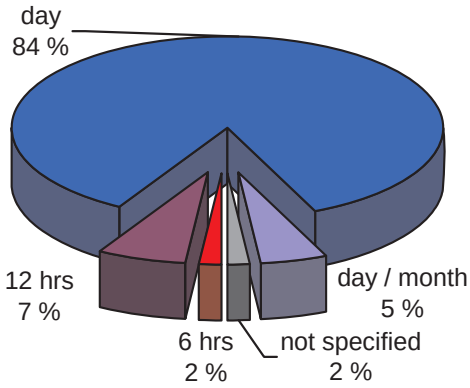

Figure 1. *Percentage of reported classification methods as for their temporal resolution.*

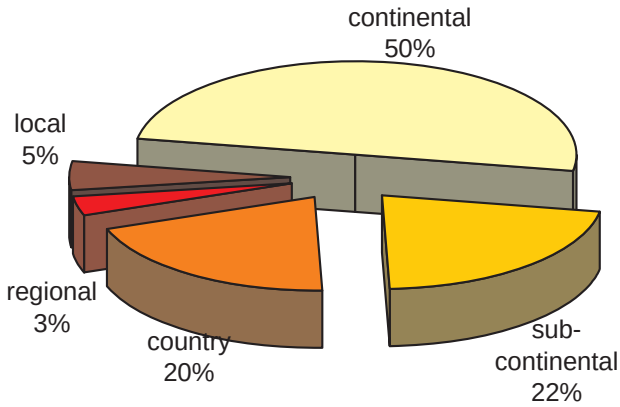

Figure 2. *Percentage of reported classification methods as for their spatial scale.*

underestimated because the majority of respondents seem to have concentrated just on circulation, while having overlooked the airmass- and weather-based classifications.

*Approach (Fig.4 to 6)***.** Three basic approaches to classification may be distinguished according to whether the definition of types and the attribution to them is done in a subjective or objective manner (e.g., Huth 1996): (i) subjective – the types are defined and patterns are classified subjectively; (ii) objective – the types are defined and patterns are classified objectively; (iii) mixed – the types are defined subjectively but the classification procedure is objective. The mixed approach is typically used in the objectivized subjective catalogues. Of the classifications, 30% are subjective, 25% are mixed, and 45% are objective (Fig.4). Several objective methods are used is classification studies (Fig.5): cluster analysis (most frequently k-means method is used, but also hierarchical methods of average linkage are reported) has the largest share (30% of the total). Other methods are represented by PCA (2 responses), correlation (Lund) method (one response), and classifications based on physical criteria, which have not been clearly described (one response). In 8% of cases, the objective method is not specified or its description is more or less misleading. The mixed methods (Fig.6) include

7 cases of the objectivized Lamb catalogue (Jenkinson-Collison method and its derivatives), 2 are objective versions of the Hess-Brezowsky catalogue, and 6 others are based on authors' own subjective classifications.

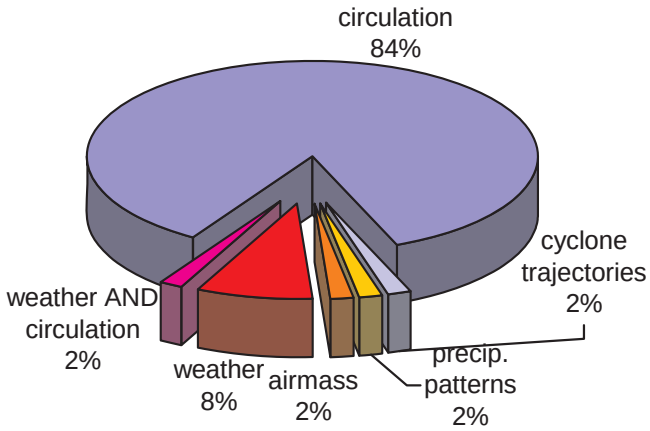

Figure 3. Percentage of reported classification methods as for the data on which classification is performed.

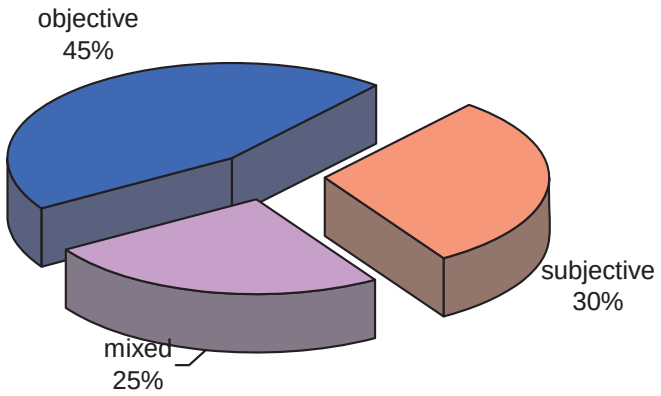

Figure 4. Percentage of reported classification methods as for the approach.

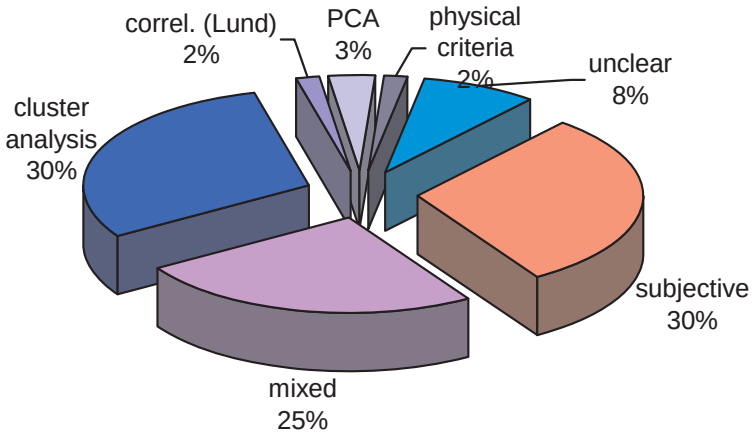

Figure 5. As in Fig.4 with a subdivision of objective methods.

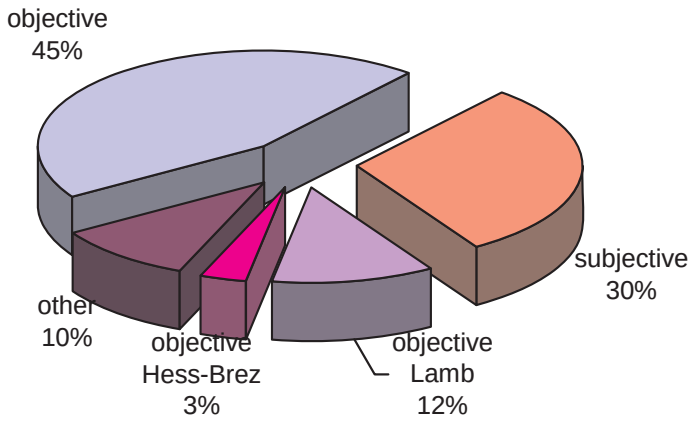

Figure 6. As in Fig.4 with a subdivision of mixed methods.

Number of types (Fig.7). The number of resulting types varies widely from 4 to 40. Some of the methods allow also sub-types to be determined, of which the largest number is 209. Several objective methods produce variable numbers of clusters, depending on the dataset subject to classification; their respondents either do not specify possible numbers of classes or indicate their usual range. The numbers of types are distributed fairly evenly in the groups of classifications with 4 to 8, 9 to 14, 15 to 20, 21 to 29, and over 30 classes.

Purpose. Many different purposes of classifications have been reported. Many respondents used the wording suggested as an example, which is rather general (e.g., applied synoptic climatology, weather prediction), others were fairly specific. Anyway, two broad, partially overlapping families of purposes can be identified: meteorological and climatological. Among the meteorological purposes, weather prediction includes specific answers such as verification, forecast adjustments, seasonal forecasting, and avalanche forecasting. Other meteorological purposes include air pollution / quality, objective analysis of precipitation, and medicine meteorology. Climatological purposes include applied synoptic climatology, which is very general; its several specifications include precipitation, forest fires, and human health.

Other general responses are dynamical climatology and climatology / climate analysis. More specific climatological purposes include long-term climate and circulation changes, climate model validation, analysis of relationships between circulation and surface weather / climate, statistical downscaling, conditional weather generator, wind atlas, and (one may wonder if it can really be included among climatological purposes) fish capture. A few other general purposes were reported: research, documentation, and teaching.

Comparisons. Slightly more than a half of the responses claim that the respondent has an experience with comparisons among different classifications. However, it is frequently unclear whether the comparison relates to the classification method reported or to respondent's general knowledge. Many responses omit stating any more details and results of the comparison, e.g., which methods were compared, which method to prefer, etc. The comparison studies are difficult to count since in multiple responses from a single respondent, the same information on the comparison regardless of the method reported is typically given. Useful for further work in the COST 733 Action are a couple of references to intercomparison studies the respondents are aware of.

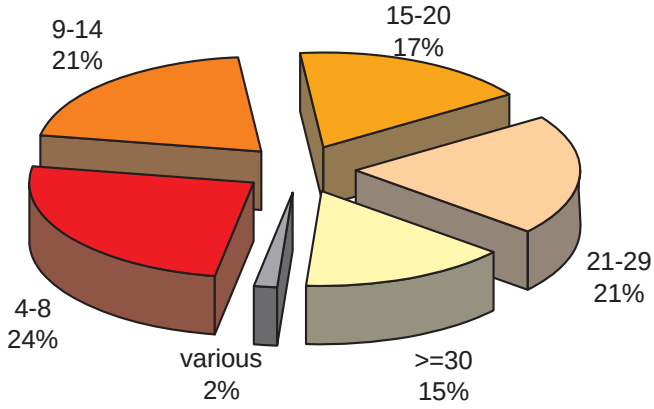

Figure 7. Percentage of reported classification methods as for the number of types.

4. Concluding remarks

The number of responses to the questionnaire and their geographical and topical coverage are quite satisfactory and provide a generally good idea of the classification studies having been in use in Europe recently. However, many classifications and their applications known from the literature have not been reported and some countries where classifications have certainly been employed are not represented in the inventory for the moment (e.g., the Netherlands). Therefore, in order to make the picture of the classification methods more complete, it appears important to carry out an additional search in open scientific literature.

The classifications reported are so varied that the exercise of mutually comparing them on a unified dataset seems to be very useful and of great importance for a broad meteorological and climatological community.

The recommendation of some of the authors is to consistently distinguish between circulation, weather, and airmass types (classifications) because these terms are not interchangeable and each is supposed to refer to a different database on which the classification is developed. Indeed, the three groups are not strictly disjunctive and there can be an overlap among them.

Acknowledgement
The participation of Radan Huth in the COST733 Action is supported by the Ministry of Education, Youth, and Sports of the Czech Republic under contract OC115.

References

El-Kadi, A.K.A., Smithson, P.A., 1992: Atmospheric classifications and synoptic climatology. *Progr. Phys. Geogr.,* **16**, 432-455.

Huth, R., 1996: An intercomparison of computer-assisted circulation classification methods. *Int. J. Climatol*., **16**, 893-922.

Key, J., Crane, R.G., 1986: A comparison of synoptic classification schemes based on 'objective' procedures. *J. Climatol.,* **6**, 375-388.

Yarnal, B., 1993: *Synoptic Climatology in Environmental Analysis.* A Primer. Belhaven Press, London, 195 pp.

Classifying reconstructed daily pressure patterns for the period 1850 to 2003 in the North-Atlantic - European Region by Simulated Annealing Clustering

A. Philipp (1), J. Jacobeit (1) and P.M. Della-Marta (2)

(1) University of Augsburg, (2) University of Bern

Abstract

In order to assess long-term changes of daily circulation variability, different classification methods are applied to a recently reconstructed Sea Level Pressure (SLP) dataset reaching back to 1850. Both the reconstruction and the classification is part of the ongoing EU project EMULATE (European and North Atlantic daily to MUL-Tidecadal climATE variability) which has the final aim to examine changes of circulation-climate-relationships with particular respect to extreme climatic events. This study deals with classification methods suitable for assessing long-term changes in the SLP fields. In order to account for the varying reconstruction skill, an error weighting scheme is applied to the SLP fields before submitting them to the classification procedure. Since statistical methods applied to the classification results (e.g. trend analysis of pattern frequencies) may be quite sensitive to small changes in the classification, robust results have to be achieved. Conventional Cluster Analysis (e.g. k-means clustering) does not meet these requirements: Depending on the dataset as well as on the number of clusters, the resulting partition is a matter of chance, and thus no robust evidence on long-term changes can be provided. In order to find a stable solution for this classification problem, a clustering method based on so called simulated annealing and multistart techniques is used. This allows for a reliable examination of circulation changes which are shown in their relevance for temperature variability as an example of applying results of this classification.

1. Introduction

In the context of assessments of climate change dynamics it is important to extend the study period on climatic variability back into time as far as possible. In order to keep a minimum level of data quality, the temporal resolution of most reconstruction approaches have been limited to monthly or seasonal time scales. Within the EU project EMULATE (European and North Atlantic daily to MULtidecadal climATE variability) a new dataset has been generated by reconstructing sea level pressure (SLP) fields on a daily basis for the period 1850 to 2003. This new dataset is expected to allow improved insights into long-term changes of high frequency variability of the North-Atlantic – European circulation. Therefore one objective of EMULATE is to identify leading atmospheric circulation patterns for assessing their trends and variations in time.

A very fundamental approach in this context is to create a pressure-pattern-classification which allows a sound analysis of the complex variability within the dataset based on well-defined categories. This approach is similar to so called weather-type-classifications but

differs in using only one parameter for classification (SLP) instead of attempting to represent the weather as a whole.
The classification method applied here is a non-hierarchical Clustering technique whose methodological aspects may affect similar classification techniques as well and therefore might have relevance to weather-typing approaches in general.

2. Data

The gridded SLP reconstruction has been done by Ansell et al. (2005) applying the Reduced Space Optimum Interpolation (RSOI) method (Kaplan et al. 2000) to quality checked and homogenized historical station time series and ICOADS marine data . The product provides a 5°x5° spatial grid for the daily mean SLP from the 1st of January 1850 in the sector 70°W-50°E/25°N-70°N. Additionally, RSOI-error estimates are provided for each grid point and each day (for further details see Ansell et al. 2005).
Before applying the classification scheme, all SLP-fields were weighted by the square root of the cosine of latitude to account for area differences in grid cells. Additionally the RSOI-error estimates have been used to weight the data in order to account for the varying confidence in the reconstructed data. The RSOI-error weight was calculated as the inverse of the mean RSOI-error divided by the standard deviation (both in hPa) of each grid point for the whole period 1850-2003. As an example, Figure 1 shows the error weighting field for the winter (DJF) season. With the highest values over western and central Europe the classification scheme is most sensitive to pressure configurations in these areas of high confidence on reconstructed SLP.

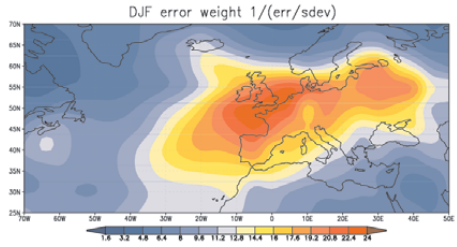

Figure 1: Error weights for the winter season as applied to the daily pressure patterns prior to their classification.

3. Classification by k-means cluster analysis

A conventional approach for classifying a set of objects (e.g. the daily pressure patterns of the reconstructed dataset) is to use non-hierarchical k-means cluster analysis (CA) which tries to find an optimal assignment of each pattern to a particular cluster by minimising the within cluster variances. Within cluster variance can be measured by the so called Explained Cluster Variance (ECV): ECV = 1 – WSS / TSS, where WSS is the sum of squares of distances between all objects within a cluster and the corresponding cluster centroid and TSS is the sum of squares of distances between all objects and the total centroid of the dataset.

The process can be split up into three steps:

1. Produce a starting partition, i.e. an assignment of each object to initial clusters.
2. Iteratively rearrange objects from one cluster to another if this reassignment increases the cluster quality (reduces within cluster variance).
3. Stop the iterations if no enhancement by reassigning objects is possible anymore. This means that a final convergence of the optimisation process has been reached.

a) b)

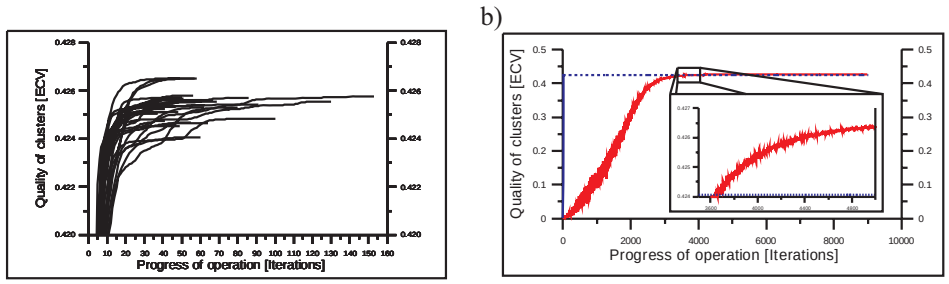

Figure 2: Visualisation of optimisation processes by k-means cluster analyses (CA) showing cluster quality as a function of progress of operation: a) several runs of conventional CA differing just by starting partition and ordering of objects (see text); b) Simulated Annealing CA run (the blue line indicates a conventional k-means CA run) . ECV is a measure of cluster quality and is calculated as 1 minus the within cluster variability (sums of squares of distances between objects and their cluster centroid) scaled by total variability (sums of squares of distances between all objects and the overall mean).

The result is always an optimized partition. But the main problem of this method – at least if a complex dataset is used as in our case – arises with the fact that there is a various number of possible solutions, called local optima, which are more or less different and generally worse than the so called global optimum which is the best one possible. Any dataset may be called 'complex' in the context of classification problems if it does not show clearly separated groups of objects inherent in the dataset .

In order to illustrate the behavior of conventional CA when applied to a complex dataset, figure 2a exemplarily presents the optimization process of different k-means CA runs differing just by two initial conditions:

1. The starting partition has been determined by different methods (hierarchical CA, PCA and by random),
2. The ordering of objects (days) has been changed by random.

The latter initial condition leads to a different ordering of checks to determine whether an object has to be moved to another cluster which in turn has a large impact on the outcome of all subsequent checks.

In figure 2a each single optimization process can be depicted by an individual line representing cluster quality (ECV) as a function of the progress of operation. If the method would be stable, all these lines would end up in one single point which should be the best solution, but conventional k-means CA is not able to realize this. Instead we can see that the result is unpredictable and found by chance. Thus, different ordering of objects and different starting partitions lead to different clustering results.

No method is known to determine the global optimum directly but only the brute force method of testing all possible combinations of objects, which is impossible for large datasets.

A method explicitly designed to approximate the global optimum (regardless of the ordering of objects or starting partitions) is the Simulated Annealing technique. This method can be utilized for k-means CA and systematically avoids bad local optima because it allows small steps backward (in terms of overall ECV) during the optimization process and therefore is able to get over these pitfalls as it is indicated in figure 2b. The idea behind this approach is to

move all objects randomly between the clusters like in a hot melt of particles and slowly reduce the probability of objects moving into a ill-suited cluster which is simulating the process of slow cooling. By moving all objects initially, the result should be ideal for the whole of the objects, in contrast to any approach looking just at the momentary advantage of each single reassignment (for details see Philipp et.al. 2006).

The computational effort of using Simulated Annealing for clustering a large dataset is relatively high, thus the question arises whether it is worth doing so. In order to give an answer, figure 3 shows an example of a cluster equivalently derived by conventional k-means (figure 3 upper panel) and by simulated annealing clustering (figure 3 lower panel). The centroid patterns in both cases show a blocking situation over the British Isles, but the simulated annealing result provides a better defined anticyclonic pattern which seems to be the product of a better assortment of daily patterns. Furthermore, the differences are even more significant if we look at the time varying seasonal frequencies of this cluster (Fig. 3, right column). Not only short-term variability, but especially the long term changes show remarkable differences: while the simulated annealing cluster has a significantly positive trend (Mann-Kendall-trend test at the 95% confidence level), this long-term change (also apparent from the time series of cumulative anomalies in figure 2) is not detected by conventional k-means CA . These differences are a direct result of the sub-optimal classification of the latter method. As a rule of thumb, the danger of achieving non-optimal results increases with the number of objects, with the number of clusters, and with the complexity (no clearly defined natural clusters) of the dataset, because all these factors tend to enlarge the number of local optima.

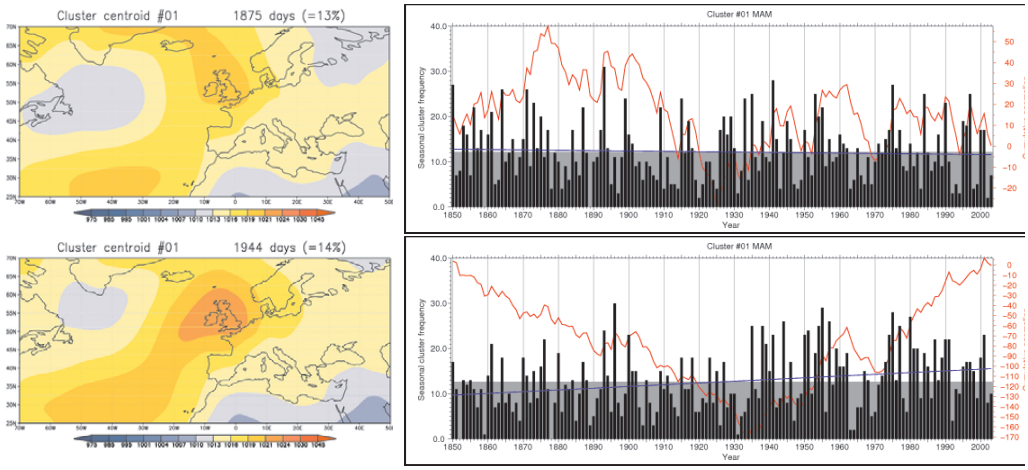

Figure 3: First of 11 cluster centroids and seasonal cluster frequencies derived for an example in spring by conventional k-means cluster analysis (upper level) and by cluster analysis using the simulated annealing technique (lower panel). The patterns (left column) are the mean raw data from the cluster members. The time series plots (right column) include in gray the overall long-term means, as blue lines the linear trends, and as red lines the cumulative anomalies of cluster frequencies.

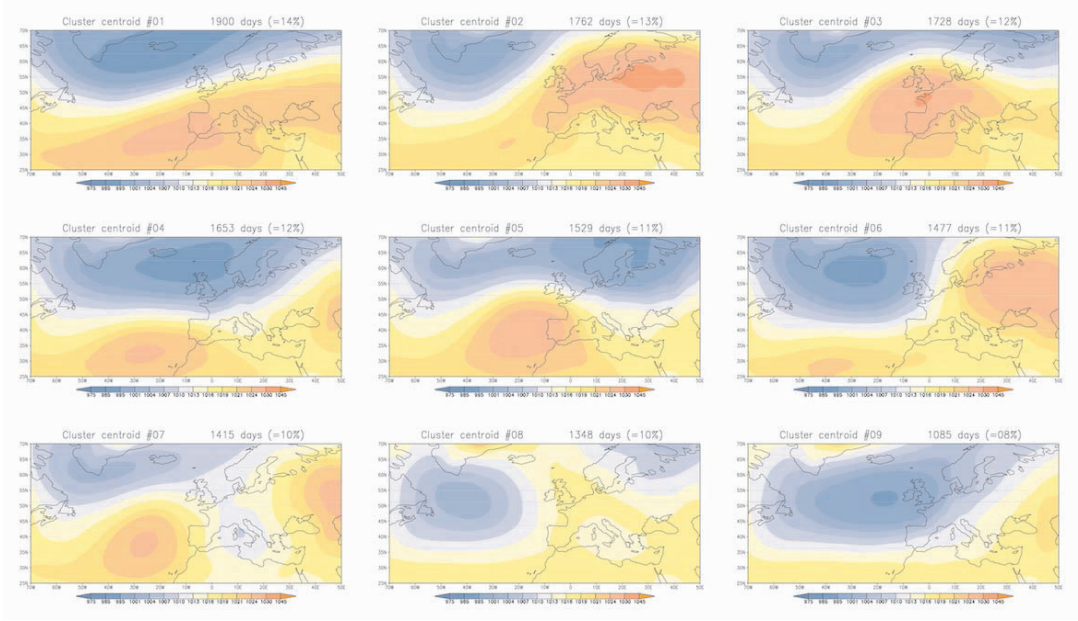

Figure 4: Simulated Annealing Cluster centroid patterns for clusters 1 to 9 in winter (DJF) 1850-2003. Patterns represent the average of all cluster members using non-weighted data in order to aid the interpretation of these patterns.

The numbers of clusters chosen to represent the winter season (DJF) was 9. While all commonly used indices for an appropriate number of clusters failed to give a reliable hint for this dataset (propably another consequence of the complexity of the dataset), it was determined by a PCA approach. This method tries to estimate the number of uncorrelated patterns fitting into the dataset. The detailed description of this method is beyond the scope of this report and will be published elsewhere.

The resulting classification for the winter (DJF) season is represented in figure 4 by the cluster centroid patterns. While the CA itself was performed with weighted data, the centroids are shown with original raw data for better interpretation. A wide range of pressure configurations is obtained comprising of zonal ones (clusters 1, 2 and 5) as well as anticyclonic and generally meridional ones. The temporal information for these patterns is given in figure 5 in terms of the seasonal cluster frequencies (SCF): significant long-term positive trends are indicated for the zonal flow pattern (cluster 4) and negative trends for cluster 6 - a pressure configuration of mainly meridional air flow and high pressure influence over Europe. The zonal cluster 1 resembles the recent positive phase of the North Atlantic Oscillation which is outbalanced by another positive phase at the very beginning - in the 1850s and 1860s. Therefore no significant overall linear trend is indicated for this cluster.

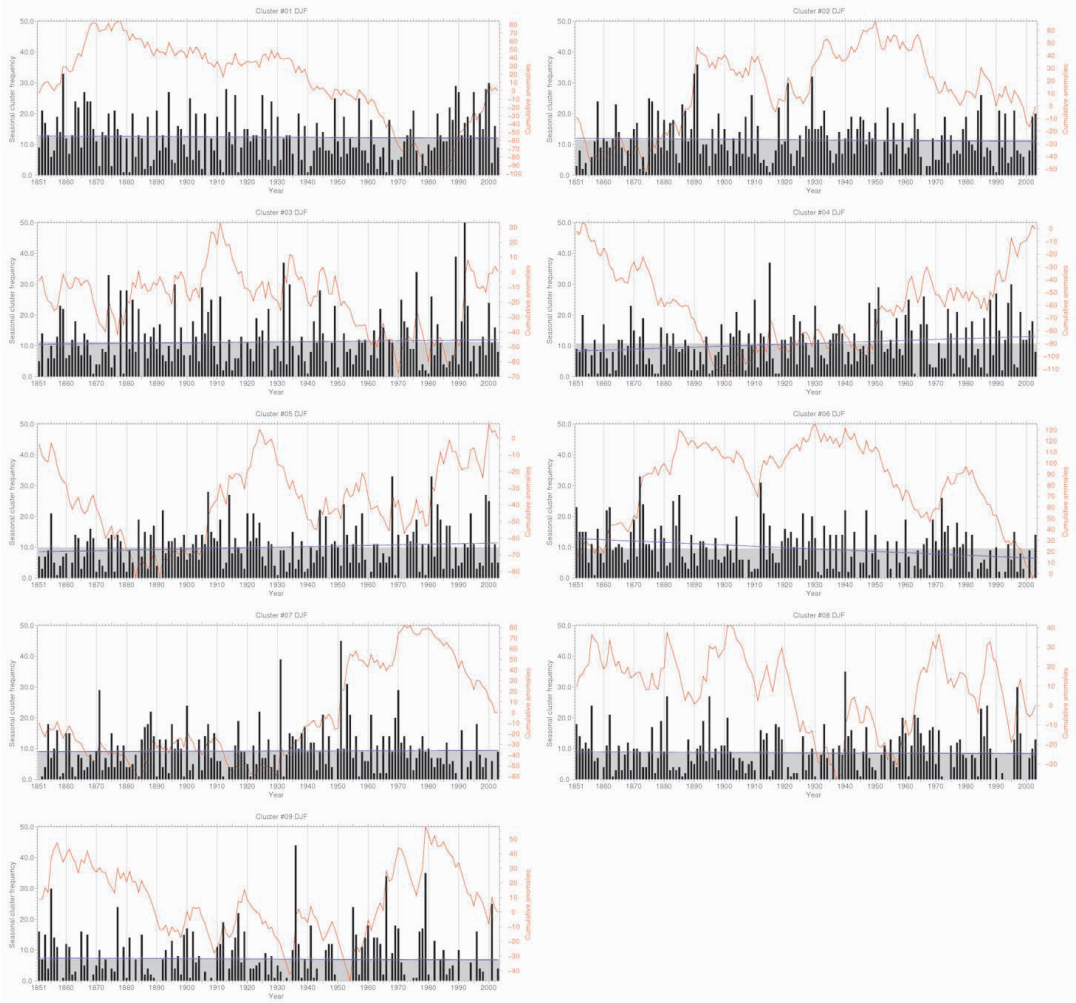

Figure 5. Seasonal cluster frequencies (black bars) of clusters 1 to 9 (see Fig. 4) in winter (DJF) for the period 1851 to 2003. The gray fields indicate the overall long term means, the blue lines the linear trends , and the red lines the cumulative anomalies of cluster frequencies.

4. Application for assessments of European winter temperatures

An example application of the SLP pattern classification is given in figure 6. The information about mean daily temperature conditions associated with each SLP cluster can be used to set up a simple descriptive model for assessing the seasonal mean temperatures from cluster frequencies within each season. For this purpose NCEP/NCAR reanalysis data for the period 1948 to 2003 have been used to calculate for each cluster the average daily temperature anomaly (relative to the monthly mean of the reference period 1961 to 1990) covering the area 5°E to 20°E and 45°N to 55° N. This area covers most of Central Europe and implies convenience because reconstructed and observational monthly mean temperature data exist back to 1851 with the prominent CRUTEM2v dataset from Jones and Moberg (2004). Therefore this region offers the possibility to compare temperatures modeled by SCF against 'observed' data. Past monthly means of temperature were modeled just by summing up the associated mean temperature anomalies for each cluster occurring in that month and dividing this sum by the number of days in this month.

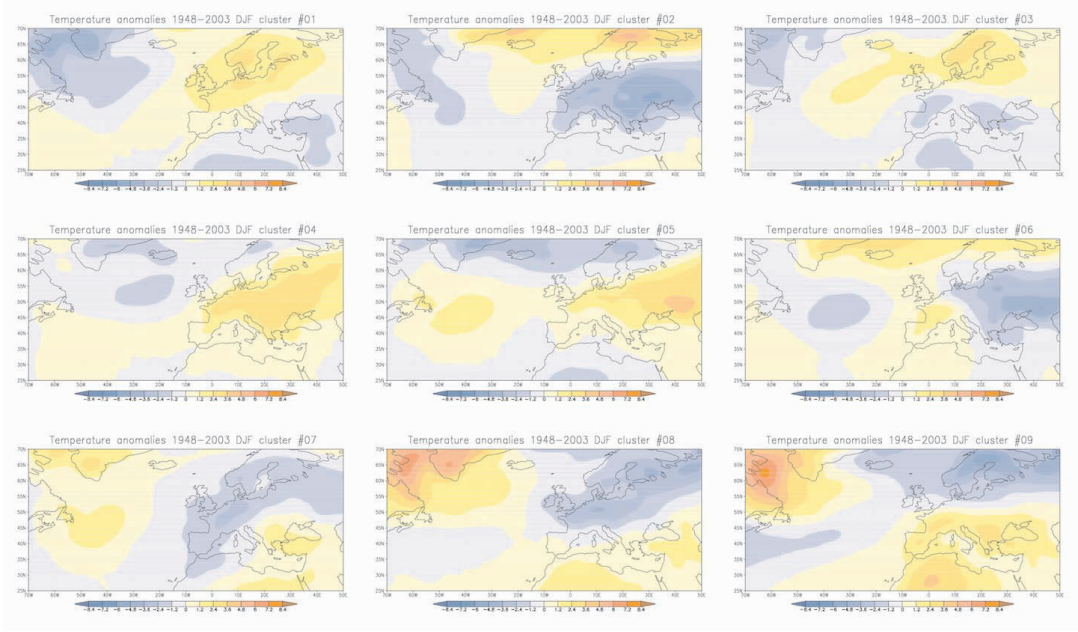

Figure 6. Associated temperature anomaly fields for clusters 1 to 9 (see Fig. 4) in winter (DJF) within the modern reanalysis period 1948 to 2003. Data represent the average anomaly of all days within each cluster related to the monthly long-term mean of the period 1961 to 1990.

The simplicity of this model is obvious: no information about previous history (e.g. persistence of a particular circulation pattern) was introduced into the model which would allow for a more appropriate temperature assessment. However, the only purpose of this simplified model is to describe the varying influence of pressure patterns onto regional temperature. The results can be seen from Fig. 7.

Although of rather low skill, this descriptive model reveals that some parts of temperature variability can be explained by pure SCF data. Remarkably this is also true for low- frequency temperature variability (see the cumulative anomalies in figure 7). This is also true for the recent warming period since about 1985 which is reproduced. However, as the most outstanding exception we find a tendency for overestimation of the temperatures in the very first part of the period (especially between 1852 to 1865) which means that there could have been some other influences than seasonal SLP cluster frequencies which caused the unusual cold conditions.

5. Discussion and Conclusions

Results presented in this report indicate that conventional cluster analysis is limited in finding optimal and stable results for large and complex datasets. Therefore we use the simulated annealing technique to approximate the best solution possible (the global optimum) and to ensure a robust solution of the classification problem. As an example the results for the winter (DJF) season 1851-2003 are presented in terms of SLP cluster centroid patterns, seasonalcluster frequencies and additionally by the associated mean daily temperature fields in the modern reanalysis period. A simple descriptive modelling approach of central European

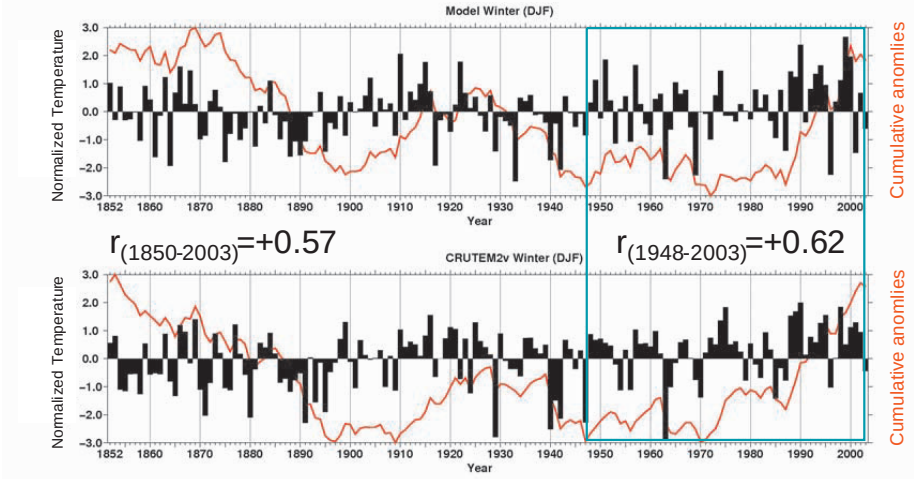

Figure 7. Comparison between Central European seasonal temperature anomalies modeled by SCF (upper panel, for detailed explanation see text) and reconstructed from observations (lower panel, data from Jones and Moberg 2003). The calibration period 1948 to 2003 is boxed by the green frame. Its pearson correlation coefficient is r = 0.62, while the correlation for the whole period is r=0.57. The red lines represent the cumulative anomalies.

temperature based exclusively on circulation cluster frequencies is presented as an example of applying results of this SLP classification. Temperature variations can be explained by SLP cluster frequencies in large parts for most of the period concerning the tendencies of warming and cooling, but not concerning the absolute extend due to the simplicity of the estimation approach. However, during the second half of the 19th century conditions have been colder than it would be expected from the circulation based model. Possible factors relevant for this overestimation of temperatures in the second half of the 19th century – beside random fluctuations - might be decreased solar activity, a weaker thermohaline ocean circulation, or a smaller greenhouse forcing due to lower concentrations of greenhouse gases at this time compared to the modern calibration period. In contrast the recent warming period since the mid 1980s is reflected more or less adequatly by the model, suggesting that it is partly due to circulation changes. This is in good accordance with the increase of the westerly pattern of cluster 1 showing warm conditions for central Europe and the decrease of the continental high of cluster 6 with cold conditions during this period. In order to allow more detailed estimations of the role of circulation pattern frequencies for long-term temperature changes the statistical modelling based on circulation classification should be enhanced in the future.

References

Ansell, T.J., P.D. Jones, R.J. Allan, D. Lister, D.E. Parker, M. Brunet, A. Moberg, J. Jacobeit, P. Brohan, N.A. Rayner, E. Aguilar, H. Alexandersson, M. Barriendos, T. Brandsma, N.J. Cox, P.M. Della-Marta, A. Drebs, D. Founda, F. Gerstengarbe, K. Hickey, T. Jónsson, J. Luterbacher, Ø. Nordli, H. Oesterle, M. Petrakis, A. Philipp, M.J. Rodwell, O. Saladie, J. Sigro, V. Slonosky, L. Srnec, V. Swail, A.M., García-Suárez, H. Tuomenvirta, X. Wang, H. Wanner, P. Werner, D. Wheeler and E. Xoplaki (2005): 'Daily mean sea level pressure reconstructions for the European – North Atlantic region for the period 1850-2003', Journal of Climate (in press).

Jones, P. and A. Moberg (2003): Hemispheric and large-scale surface air temperature variations: an extensive revision and an update to 2001., Journal of Climate, 16, 206–223.

Kalnay, E., M. Kanamitsu, R. Kistler, W. Collins, D. Deaven, L. Gandin, M. Iredell, S. Saha, G. White, J. Woollen, Y. Zhu, M. Chelliah, W. Ebisuzaki, W. Higgins, J. Janowiak, K. Mo, C. Ropelewski, J. Wang, A. Leetmaa, R. Reynolds, R. Jenne and D. Joseph (1996): The ncep/ncar 40-year reanalysis project, Bulletin of the American Meteorological Society 77(3), 437–471.

Kaplan, A., Y. Kushnir and M.A. Cane (2000): Reduced space optimal interpolation of historical marine sea level pressure: 1854-1992', J. Climate, 13, 2987-3002.

Kistler, R., E. Kalnay, W. Collins, S. Saha, G. White, J. Woollen, M. Chelliah, W. Ebisuzaki, M. Kanamitsu, V. Kousky, H. van den Dool, R. Jenne and M. Fiorino (2001): The ncep-ncar 50-year reanalysis: Monthly means cd-rom and documentation, Bulletin of the American Meteorological Society, 82(2), 247–267.

Philipp, A., P.M. Della-Marta, J. Jacobeit, D.R. Fereday. P.D. Jones, A. Moberg, H. Wanner (2006): Long term variability of North Atlantic-European pressure patterns since 1850 classified by simulated annealing clustering. Journal of Climate. Submitted.

The spatial Distribution of Precipitation in Germany for different Weather Types

Peter Bissolli, Gerhard Müller-Westermeier

German Meteorological Service, Dep. Climate Monitoring, Offenbach, Germany
Email: peter.bissolli@dwd.de

Abstract

In this contribution the dependency of the spatial distribution of precipitation in Germany on synoptical circulation patterns is analysed. For this purpose, maps of monthly long-term mean precipitation sums (period 1980-2004) for different circulation types have been produced. The circulation types are described by the objective weather types classification of the German Meteorological Service. This classification consists of 40 types, based on 3 criteria: wind direction in 700 hPa, cyclonality in 950 and 500 hPa, and the tropospheric humidity.

For generating the maps, long-term mean precipitation sums have been computed for each precipitation station of the German Meteorological Service, for each month and each circulation type, averaged over all days when a certain type has occurred (if the number of days is not too small). These averages have been interpolated into a 1km grid over Germany, taking the altitude above sea level for each grid point into account.

The results show in many cases large differences between the maps of different circulation types, dependent on the circulation criteria, the topography in Germany and the season.

1. Introduction

It is evident that the spatial distribution of climate elements such as air temperature, precipitation, sunshine duration etc. is dependent on atmospheric circulation patterns on all scales. The advection of warm/cold and dry/moist air masses determines the large-scale air mass properties and thus the variability of climate elements. These air mass impacts are modified by local topographic features, e.g. luff/lee effects near mountains. Cyclonic or anticyclonic conditions imply dynamical circulation processes, in particular lifting or subsidence of air masses which is essential e.g. for precipitation. Special properties of air masses, such as humidity also influence the daily weather, e.g. by formation of clouds or fog.

The spatial distribution of climate elements is very often displayed by climate maps which are published in climate atlases, climate monitoring publications or via the web. These maps are usually the result of a spatial interpolation of climate mean values over a defined area, e.g. one country, continent or the whole globe. Various interpolation techniques (inverse distance, kriging and others) are used, assuming some relation between a climate value at each gridpoint within the defined area and the climate means of the surrounding observing stations or pixels. To improve the interpolation, additional data of the topography are often considered as a further condition.

However, using climate averages implies just an average over all the various synoptic situations which appear during the averaging period. For one single situation, e.g. a zonal west weather type with moving cyclonic systems the dependency of gridpoint data on surrounding stations and topography could be very different compared to another synoptic situation, e.g. an anticyclonic condition with temperature inversions which would cause a completely different relation between temperature and altitude. Therefore, it appears to be useful to distinguish between various weather types when constructing climate maps.

To consider weather types for climate analysis, these weather types have to be transformed into an appropriate data set which can be used to combine these weather type data with the analysed climate data. For this purpose a huge number of weather types classifications is available, covering various scales, classification areas and criteria. Thus, it is necessary to select an appropriate weather types classification which summarises similar weather situations with similar spatial distributions of climate elements.

This paper describes the application of one special weather types classification, the objective classification of the German Meteorological Service, to the construction of climate precipitation maps for Germany. It describes in particular the approach itself, the weather types classification criteria and the spatial interpolation method used here. The results are maps based on different weather types showing differences of spatial distribution of precipitation which can be attributed to influences of atmospheric circulation and air mass properties.

2. Constructing maps using a weather types classification

The general approach how to use weather types classifications for constructing maps is the following:

a. It is assumed that weather types classification data as well as climate station data are available on a daily basis for the whole climate period (a small number of gaps would not affect the result considerably).
b. For all stations averages of daily climate data with the same weather type over the whole period are computed for each weather type.
c. For each weather type the averaged climate data are interpolated into a grid field.
d. To find a climate average over all the types, a weighted mean of all the interpolated grid fields can be computed. The weights refer to the number of days for each weather type.
e. Plotting a map based on the gridpoint data.

3. The objective weather types classification of the German Meteorological Service

The German Meteorological Service operationally provides data of an objective weather types classification on a daily basis. Details of this classification are described by Bissolli and Dittmann (2001). Here, only a brief overview is given.

The data basis for this classification is the current operational numerical large-scale forecast model of the German Meteorological Service. Presently, the model GME (Global Model extended) is used. It has a horizontal resolution of about 40 km.
The classification criteria are the following:

- Advection of air masses, described by the horizontal wind components in 700 hPa,

- Cyclonality, described by the second derivation of the geopotential in two levels (950 and 500 hPa),
- Humidity, described by the precipitable water, derived from temperature and humidity fields in 5 levels within the troposphere.

The classification area comprises Germany and some adjacent regions (Fig. 1). Thus, the classification refers to the synoptical scale, which means the air masses are subject of the classification.

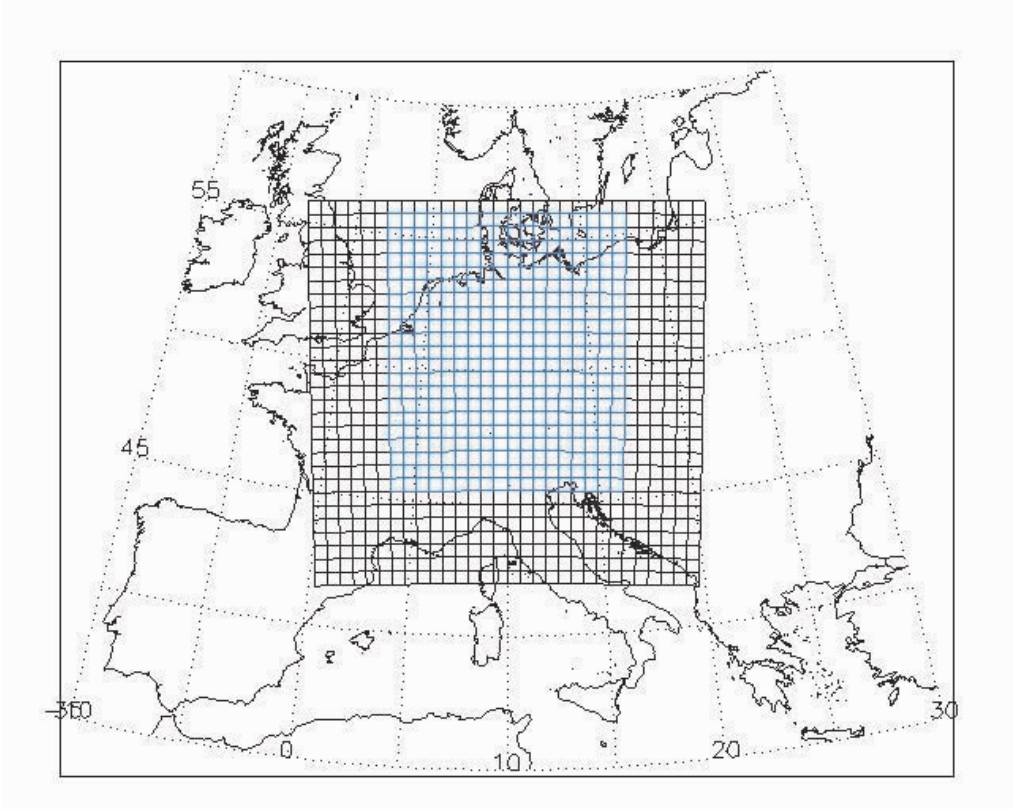

Figure 1: Classification area (blue area) of the objective weather types classification of the German Meteorological Service. (The grid points of the black area are available, but currently not used for the classification.)

The classification result yields the following classes (types):

- 5 classes of advection: northeast (NE), southeast (SE), southwest (SW), northwest (NW), no prevailing direction (XX). XX is given when none of the overlapping 90° wind direction sectors 0-90°, 10-100°, 20-110°, ... , 350-80° contains at least 2/3 of all gridpoints.
- 2 classes of cyclonality in each level (950 and 500 hPa): cyclonic (C; $\nabla^2\Phi>=0$) or anticyclonic (A; $\nabla^2\Phi<0$).
- 2 classes of humidity: dry (D; precipitable water amount is lower than the monthly climate mean 1981-2000), wet (W; precipitable water amount is equal to or higher than the monthly climate mean 1981-2000).

All together these are 40 types which are labelled by a 5-letter abbreviation. The first two letters indicate the direction of the advection, the third and fourth letter the cyclonality in 950 and 500 hPa, respectively, and the 5th letter the humidity. For example, NWACD means: northwest, anticyclonic in 950 hPa, cyclonic in 500 hPa, dry.

The classification is carried out once a day for the numerical 12 UTC analysis of the GME model, and also for the forecast fields (forecast time up to 7 days). A time series of daily classification data for the 12 UTC analysis is available starting in July 1979, this means it covers 27 years now. In this study the 25-year period 1980-2004 (only 12 UTC analysis) has been used to have 25 complete years (apart from a few small gaps) for this analysis.

4. Precipitation data

Data of daily sums of precipitation for the period 1980-2004 are taken from the data base of the German Meteorological Service, consisting of about 4000 stations within the area of Germany. The data are quality-controlled using the operational procedure of the German Meteorological Service.

5. The spatial interpolation method

The German Meteorological Service operationally provides climate maps based on an inverse distance interpolation procedure and considering the altitude of grid points above sea level.

The steps of gridding are the following:

a. Computing linear regression coefficients between the station data and topography (altitude above mean sea level) for 1°x1° regions.
b. Spatial interpolation of regression coefficients.
c. Reducing station data to mean sea level using the regression functions.
d. Spatial interpolation of the reduced station data into a 1kmx1km grid.
e. Recomputing the interpolated data to the actual altitude at each grid point.

This method is applied to climate averages of daily data with the same weather type, for each of the types (except for some which occur only very rarely), which means that for each type a 1kmx1km grid field has been generated. This procedure has also been applied to seasonal data, defined by using only the days of the particular months of the climatological seasons.

6. Results

On the following pages, a selection of the resulting precipitation maps is presented and discussed.

Fig. 2 shows the maps for the types NEAAD, SWAAD, SWAAW and SWCCW. NEAAD is a northeast anticyclonic dry type. For this type very little precipitation can be found, only in some mountainous areas in the east and in the Alps in the south. This is what we would expect from meteorology, since the dry, in winter cold air mass from the east should not be able to produce much precipitation under anticyclonic subsidence. In contrast, when the advection comes from southwest (SWAAD), the air mass is expected to be warmer in most cases and mainly the east of Germany profits from the dry conditions while the western part is influenced by the south-westerly airflow with a little bit more precipitation. If the air mass is

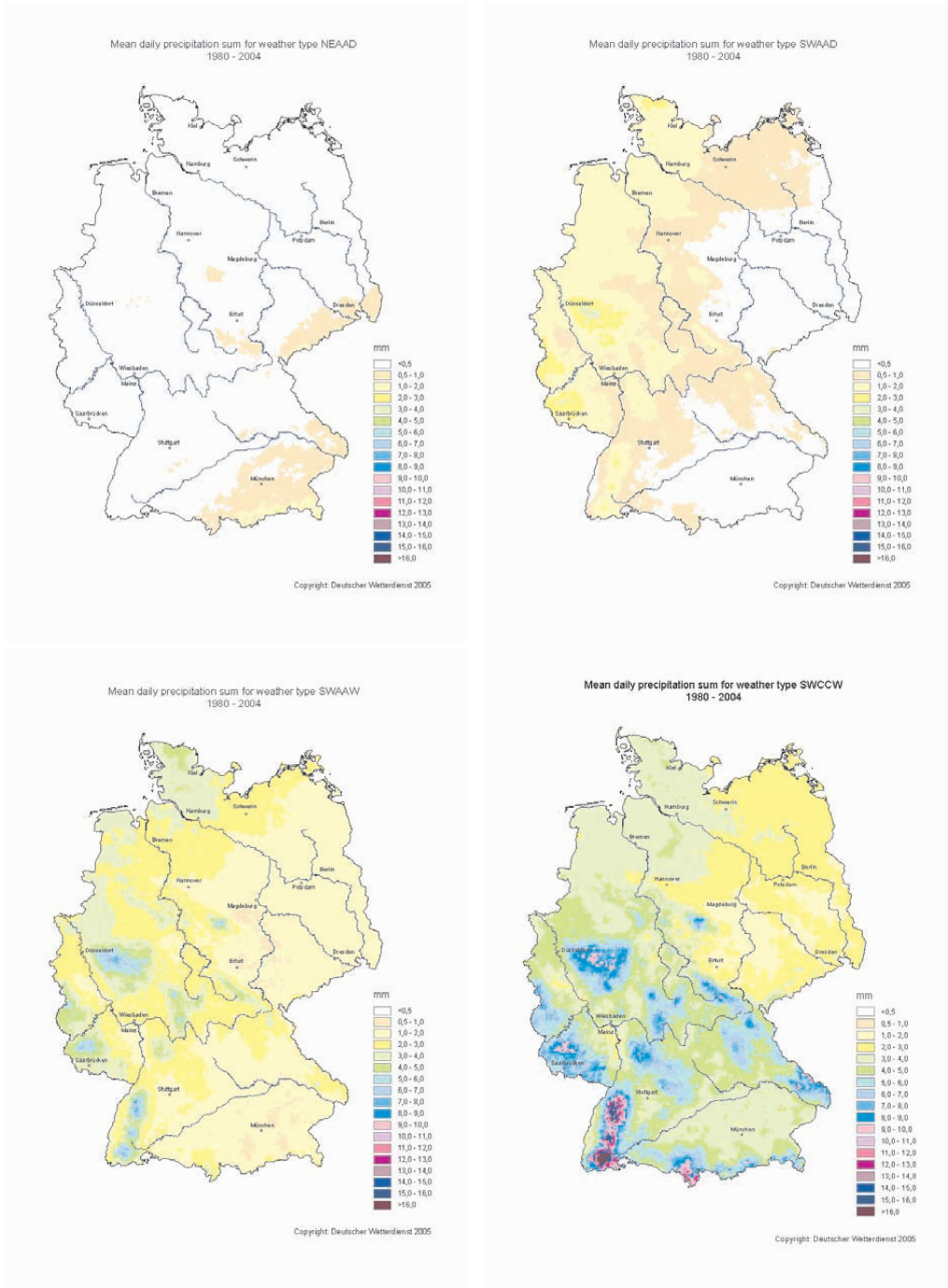

Fig. 2: Mean daily precipitation sum 1980-2004 for the weather types NEAAD (upper left), SWAAD (upper right), SWAAW (lower left), SWCCW (lower right) of the objective weather types classification of the German Meteorological Service.

wet (SWAAW) this southwest type produces more precipitation in spite of the anticyclonic conditions. However, if there are also cyclonic instead of anticyclonic conditions (SWCCW), the increased lifting of air masses causes a considerably higher quantity of precipitation in the whole country, especially in the mountains.

Not only the air mass advection and the cyclonality, but also the humidity (water vapour content) influences the spatial distribution of precipitation. This can be seen from the upper two maps in Fig. 3 in the case of northwest anticyclonic types. The amount of mean precipitation is considerably higher for the wet type NWAAW than for the dry type NWAAD.

Concerning the influence of cyclonality there is also a difference between anticyclonic conditions in 950 hPa / cyclonic conditions in 500 hPa and vice versa. This is illustrated by the lower two maps of Fig. 3 for the case of the southwest humid types SWACW and SWCAW. For cyclonic conditions in the upper air (500hPa, SWACW) the precipitation values are higher in southern Germany in the forelands of the Alps, while for most of the other parts of Germany the precipitation is higher in case of cyclonic conditions near the surface. There are certainly different reasons which contribute to this result. One reason could be that foehn situations near the Alps would occur more likely for SWCAW with upper air anticyclonality and large-scale subsidence over that region while in the case of SWACW an upper air trough would be dominant there which prevents such a foehn situation. In the northern and eastern lowlands on the other hand, surface lows with frontal systems might produce more frequently and more widespread precipitation than upper air trough situations.

Due to the different character of precipitation in the seasons (more convection in summer, more frontal precipitation in winter) it is interesting to generate maps for different seasons. Fig. 4 shows the precipitation maps for the northwest anticyclonic dry type NWAAD for all the four seasons. It can be seen immediately that the summer is the driest season with slight precipitation only in the coastal regions in the northwest of Germany and near the Alps, while in the central parts of the country, the precipitation is almost zero under dry anticyclonic conditions. This is not the same in winter, although the mean precipitation is still low also for this season. However, westerly advection with frontal systems produces some precipitation even for anticyclonic circulation. Spring and autumn appear as transition seasons between summer and winter.

Fig. 5 presents the corresponding seasonal maps for the southwest cyclonic wet type SWCCW. Perhaps it might be surprising that the seasonal differences are not so big at least for spring, autumn and winter, as they all have by far the lowest precipitation for the eastern part of the country, the highest in the Black Forest in the southwest and in some parts of the Alps. In summer however, the precipitation amounts are a little higher in the northern and eastern parts compared to the other seasons, but not in the southwest. On the other hand there are extremely high precipitation amounts in the upper regions of the German alpine area, certainly due to orographically induced convective precipitation.
Some other weather types (not shown) reveal their characteristics in all seasons. The anticyclonic types XXAAD and NEAAD have very little precipitation in general in all seasons. Many effects of advection (e.g. a decrease in precipitation from west to east especially for southwest types), of cyclonality (more precipitation for cyclonic compared to anticyclonic circulation) and of humidity (more precipitation for wet compared to dry types) can be seen for all seasons as well. Differences between seasons within one type occur mostly due to continentality, orographic forcing and different dependency of precipitation on altitude

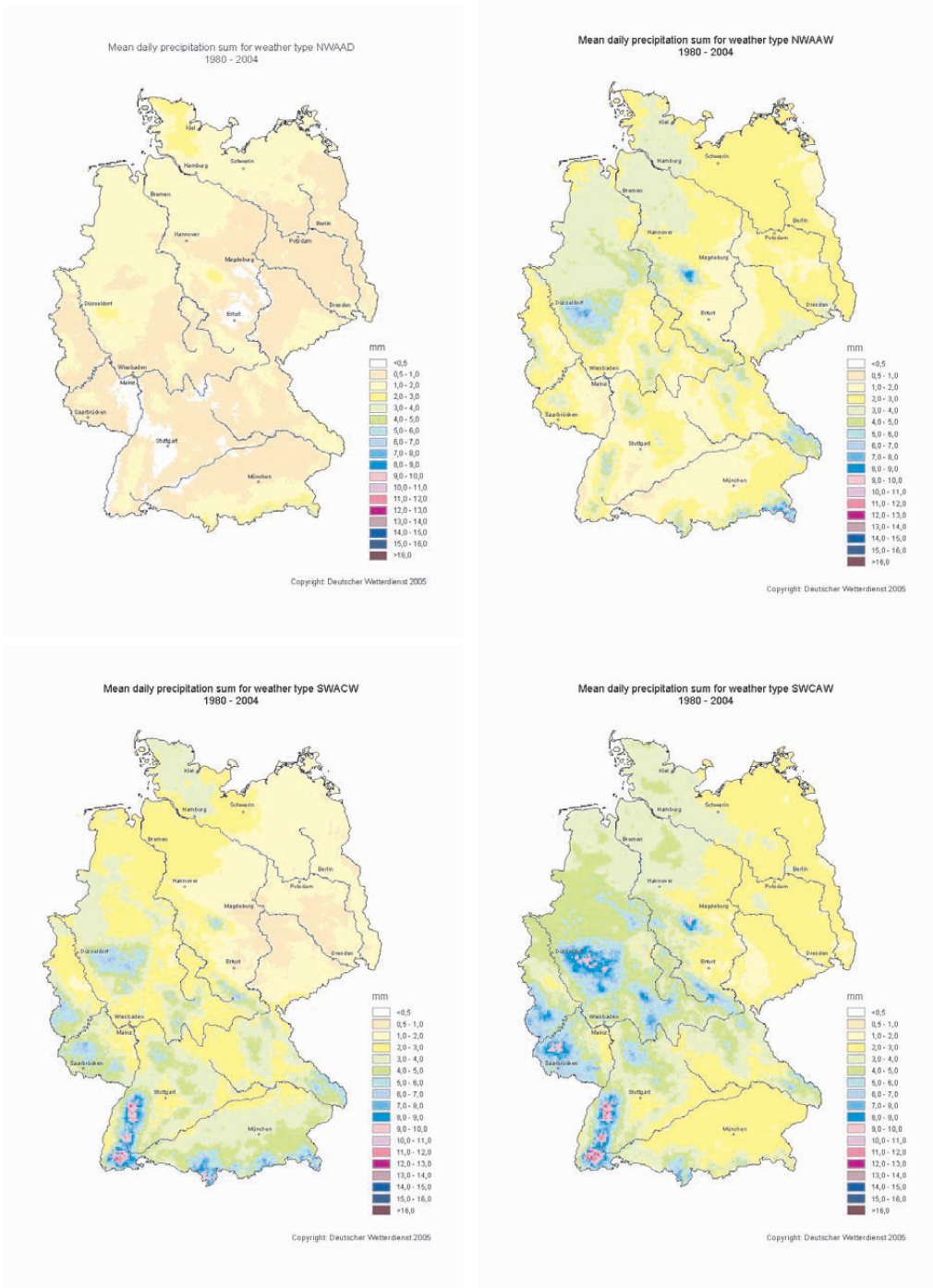

Fig. 3: Mean daily precipitation sum 1980-2004 for the weather types NWAAD (upper left), NWAAW (upper right), SWACW (lower left), SWCAW (lower right) of the objective weather types classification of the German Meteorological Service.

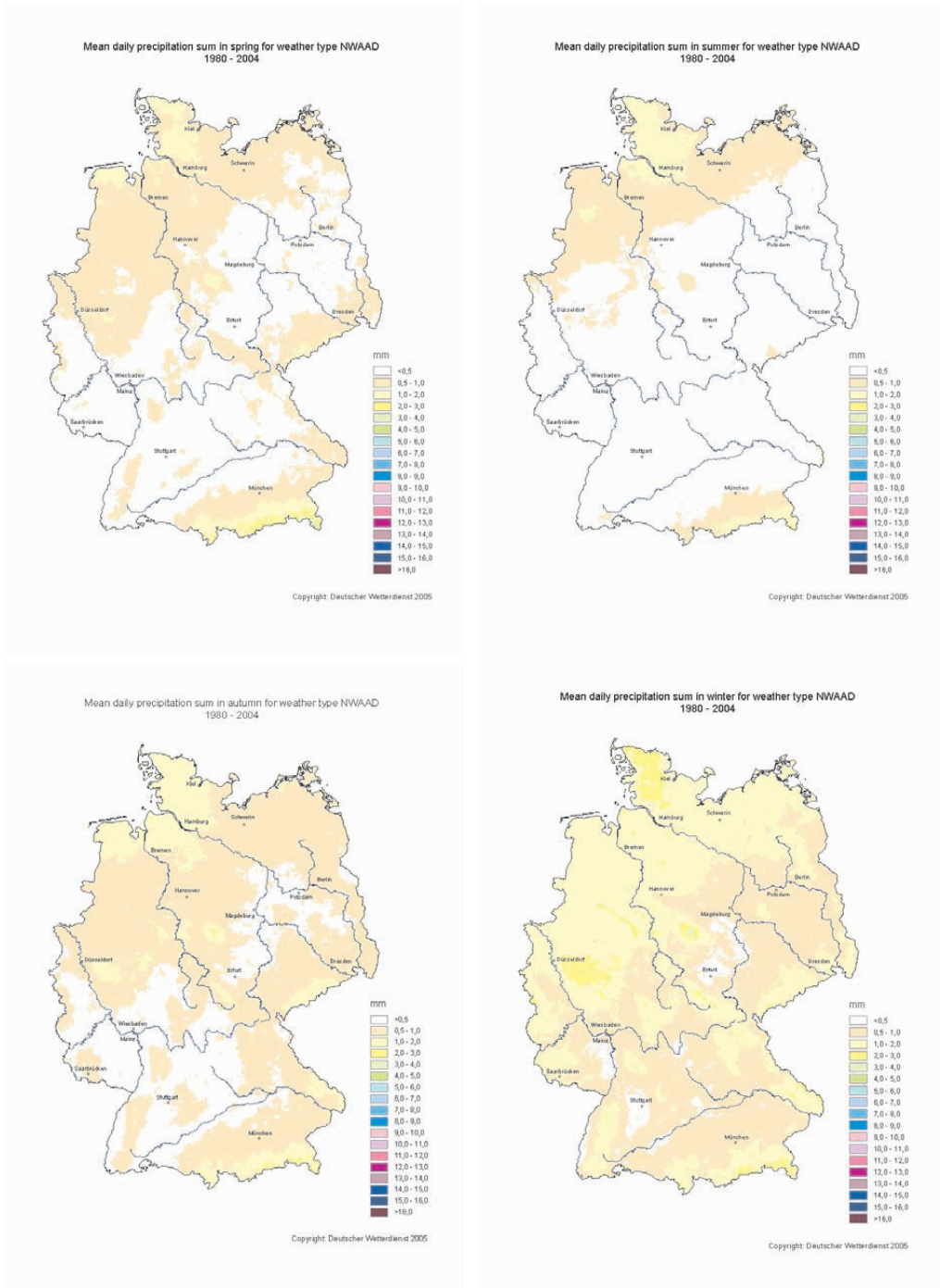

Fig. 4: Mean daily precipitation sum 1980-2004 for the weather type NWAAD in the four seasons spring (upper left), summer (upper right), autumn (lower left), winter (lower right).

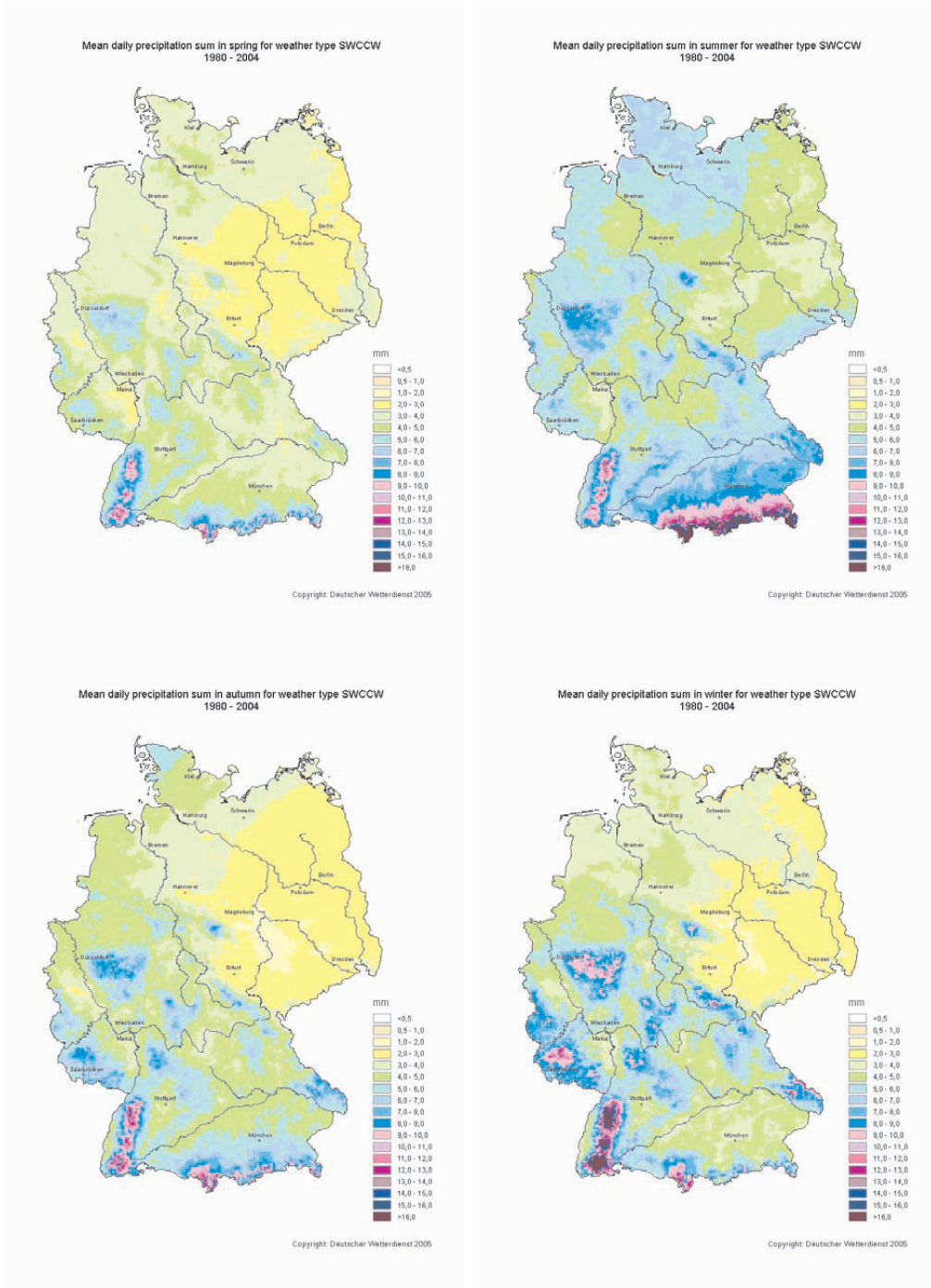

Fig. 5: Mean daily precipitation sum 1980-2004 for the weather type SWCCW in the four seasons spring (upper left), summer (upper right), autumn (lower left), winter (lower right).

in different seasons. However, we have not found any results which are in contradiction to meteorological expectations.

The maps presented here refer to weather types which occur quite frequently throughout the whole period 1980-2004. There are some other types which are very rare and do not occur every year. We left them out of discussion since the corresponding precipitation distributions might be biased as they are based only on some of the years of the period. Nevertheless, each of the type has occurred at least once during the period and is based on a real meteorological situation so even these distributions may be characteristic for those types.

6. Conclusions

Climate maps of precipitation for Germany are now available for various weather types. The objective weather types classification of the German Meteorological Service has been used for distinguishing the weather types, and the resulting maps are reasonable as they are not in contradiction to what we expect from meteorology.

The spatial distribution of precipitation is strongly dependent on weather types, which are described by air mass advection, cyclonality and tropospheric water vapour content. The results reveal that the advection type determines in particular the spatial distribution of precipitation while the cyclonality and the humidity of the troposphere influence mainly the amount of precipitation in general. Various seasonal differences can be detected, mostly due to different continentality in different areas of Germany, a different dependency of precipitation on altitude and due to orographic forcing.

It has to be considered however, that these maps are just a climate mean summarised over similar, but not absolutely identical meteorological situations. Differences are to be expected for example during a transition from one type to another or if the air masses are different in various parts of Germany.

However, it has turned out to be useful to apply weather types classifications to precipitation maps and that the objective weather types classification which is used here is an appropriate tool for it. An earlier study (Bissoli, 2004) has already shown that this classification can be applied to temperature maps as well.

The recently started COST Action 733 “Harmonisation and Applications of Weather Types Classifications for European Regions“ will compile, compare and apply other weather types classifications (see http://www.cost733.org for more details) and will perhaps generate a new one which can be used for any climatological application, in particular for climate monitoring via generating climate maps. This will lead to more and new results concerning the dependency of climate variability on circulation and weather types.

Acknowledgements

We thank our colleagues Ms. S. Kosa, Ms. A. Jaeger and Mr. V. Zins for helping us in data processing, generating the maps, and preparing the layout of this paper.

References

Bissolli, P., Dittmann, E. (2001): The objective weather types classification of the German Weather Service and its possibilities of application to environmental and meteorological investigations. Met. Zeitschr. Vol. 10, No. 4, 253-260.

Bissolli, P. (2004): Using weather types classifications for climate maps. Submitted for proceedings of the Conference "Spatial Interpolation Techniques in the Climatology and Meteorology", Oct. 2004, Budapest.

Analysis of the European cyclone tracks, the corresponding frontal activity, and changes in MCP frequency distribution

Judit Bartholy, Rita Pongrácz, Margit Pattantyús-Ábrahám, Zsolt Pátkai

Department of Meteorology, Eötvös Loránd University, Budapest, Hungary

Abstract

Variability and trend of the large-scale circulation characteristics over the North-Atlantic-European region are analyzed for the 20th century. First, changes in decadal frequency of Hess-Brezowsky macrocirculation patterns (MCP) are evaluated between 1881 and 2000. Frequency of several MCP types increased or decreased considerably during these 120 years, which may be explained by large scale changes in circulation characteristics, e.g., by cyclone activity changes in different regions. Then, cyclone center identification and cyclone tracks and intensity analysis are accomplished on the base of the European Centre for Medium-range Weather Forecast (ECMWF) reanalysis datasets (ERA-40) on a 2.5° horizontal resolution grid for the 45 year period between 1957 and 2002. Time series of the four main geopotential height fields (i.e., AT 500 hPa, AT 700 hPa, AT 850 hPa, and AT 1000 hPa) are used together with the sea level pressure fields. Decadal scale variability and trends are analyzed and compared for all levels. Results suggest that both the number of midlatitude cyclones and the cyclone activity increased considerably in the North-Atlantic-European region, especially, in the northwestern part of the domain. Finally, significant frontal events (e.g., frontal precipitation and temperature changes) are also analyzed, i.e., how often and how intense they occurred in the last few decades, whether or not any trend may be detected in the Carpathian Basin.

1. Introduction

Extratropical cyclones are responsible for a large portion of the heat and moisture transports between the tropics and the polar regions. Therefore, any changes in frequency or intensity of these cyclones may affect significantly the regional climate of the midlatitudes. Several methodological approaches are available and have been applied to these analyses. One of these possible approaches is to analyze the long-term frequency change of macrocirculation patterns (MCPs) (i) defined for Europe by Hess and Brezowsky (1977), or (ii) defined for the region of the British Isles by Lamb (1972). Another method can also be used, namely, to extract and analyze the extratropical cyclones and their tracks. In earlier studies, midlatitude cyclones were subjectively identified by van Bebber (1891) and Klein (1957). Then, objective identification was used by Lambert (1988) and Hodges (1994). Zhang et al. (2004) composed the climatology of cyclone activity in the arctic regions for the 1948-2002, while Alpert et al. (1990) analyzed monthly cyclone frequencies and cyclone tracks based on 5-year-long (1982-1987) seven geopotential level fields for the Mediterranean region. Both analyses used data with 2.5° horizontal resolution. Key and Chan (1999) analyzed seasonal and annual trends of cyclone frequencies using time series of 1000 hPa and 500 hPa geopotential fields for 1958-1997 (with a latitude-longitude grid resolution of 2.5°×5°). Statistically significant increasing trends (at 0.05 level) were found in all seasons at 1000 hPa for the Arctic region.

In this paper, first, significant changes in the frequency of different Western/Central-European MCPs are presented for the 20th century (Section 2). Then, in Section 3 cyclone tracks and intensity analysis is accomplished for the North-Atlantic-European region on the base of the European Centre for Medium-range Weather Forecast (ECMWF) reanalysis datasets (ERA-40) with 2.5° horizontal resolution. Changes of frontal activity in the Carpathian Basin are also analyzed.

2. Observed tendency of frequency of macrocirculation patterns

Phenomenological circulation statistics are analyzed using the Hess-Brezowsky (1977) macrocirculation types. Overview of the regional circulation structures of the Atlantic-European region can be found in Table 1. The MCPs are classified into 29 types based on the dominant direction of air mass movements and the presence of cyclones or anticyclones in different regions. The available dataset consists of daily MCP codes from 1881 to 2000 and is published monthly in the journal "Die Grosswetterlagen Europas" of the German Meteorological Service.

Figure 1 presents the decadal frequency distribution of Hess-Brezowsky MCP types using Box-Whisker plot diagrams, and the significance of the detected trends. Large differences between the upper and the lower quartile values (appearing as large boxes in the figure) may indicate considerable changes in frequency of the given MCP type during the 120 years. Furthermore, the entire range between the maximum and minimum values of the decadal frequency also indicates the variability of MCP type frequency. The signs of the detected trends are presented in small boxes below the x-axis. In case of significant trend sign, the corresponding box is shaded by grey. According to the results, frequency of several MCP types changed significantly.

Figures 2 and 3 illustrate the increasing and decreasing tendency of occurrences, respectively. Frequencies of Southwest cyclonic (SWz), Central European ridge (BM), and Western European Trough (TrW) MCP types increased considerably during the 20th century.

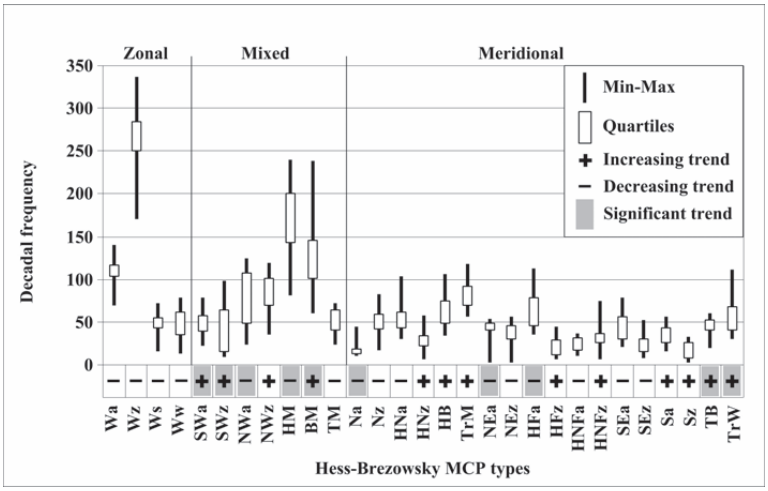

Figure 1. Decadal frequency distribution of Hess-Brezowsky types, 1881-2000. Short description of the MCP types are listed in Table 1.

Frequencies of Northwest anticyclonic (NWa), Central European high (HM), and Fennoscandian high, anticyclonic (HFa) MCP types decreased in the last 120 years, all of them represent anticyclonically dominated circulation features over the European continent. At the lower panels of the figures, the typical sea level pressure patterns of the corresponding MCP types are provided.

Since these Hess-Brezowsky MCP types, as well, as the classification method include many subjective elements, the results presented in this section also involve a lot of uncertainty. In order to reduce this, objective algorithms are used in the next section for cyclone track identification.

Table 1. Macrocirculation types defined in the Hess-Brezowsky classification system.

Circulation type	Main flow direction	Macrosynoptic type (notation)
Zonal	West (W)	West anticyclonic (Wa)
		West cyclonic (Wz)
		Southern West (Ws)
		Angleformed West (Ww)
Half-Meridional	Southwest (SW)	Southwest anticyclonic (SWa)
		Southwest cyclonic (SWz)
	Northwest (NW)	Northwest anticyclonic (NWa)
		Northwest cyclonic (NWz)
	Central European high (HM)	Central European high (HM)
		Central European ridge (BM)
	Central European low (TM)	Central European low (TM)
Meridional	North (N)	North anticyclonic (Na)
		North cyclonic (Nz)
		North, Iceland high, anticyclonic (HNa)
		North, Iceland high, cyclonic (HNz)
		British Islands high (HB)
		Central European Trough (TRM)
	Northeast (NE)	Northeast anticyclonic (NEa)
		Northeast cyclonic (NEz)
	East (E)	Fennoscandian high, anticyclonic (HFa)
		Fennoscandian high, cyclonic (HFz)
		Norwegian Sea – Fennoscandian high, anticyclonic (HNFa)
		Norwegian Sea – Fennoscandian high, cyclonic (HNFz)
	Southeast (SE)	Southeast anticyclonic (SEa)
		Southeast cyclonic (SEz)
	South (S)	South anticyclonic (Sa)
		South cyclonic (Sz)
		British Islands low (TB)
		Western European Trough (TRW)

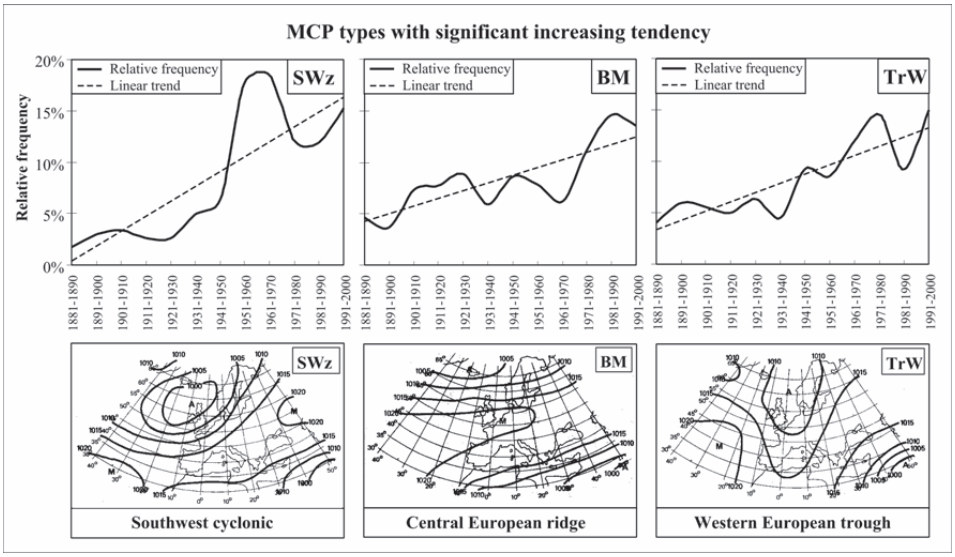

Figure 2. Selected Hess-Brezowsky MCP types with increasing decadal frequency distribution (1881-2000). The linear trend is fitted using the least square method. The description of these MCP types are listed in Table 1. Maps represent the typical sea level pressure patterns.

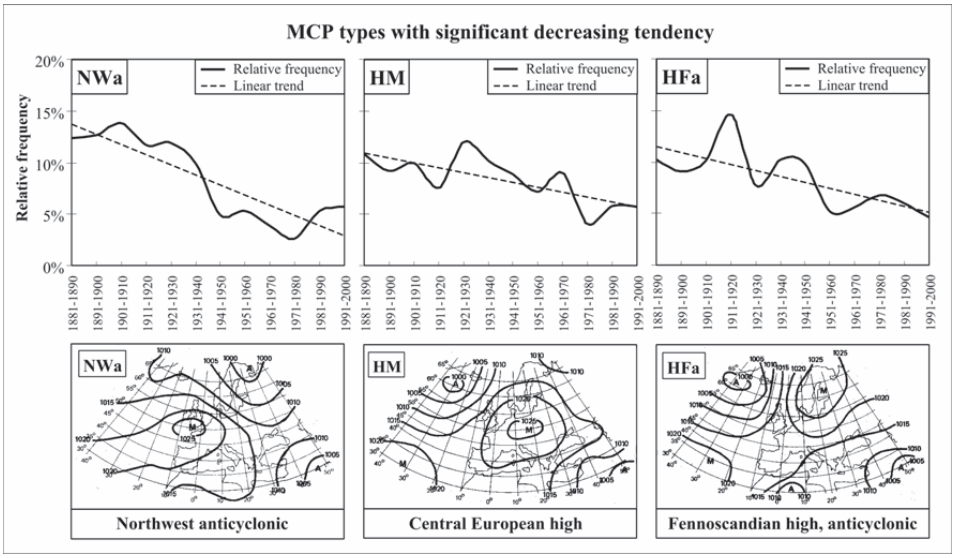

Figure 3. Selected Hess-Brezowsky MCP types with decreasing decadal frequency distribution (1881-2000). The linear trend is fitted using the least square method. The description of these MCP types are listed in Table 1. Maps represent the typical sea level pressure patterns.

3. Identification and analysis of European cyclone tracks

In the Northern hemisphere, midlatitude cyclones with their associated frontal systems influence significantly the local weather in Europe, as well as in most parts of North-America. For instance, more than two-thirds of the winter precipitation amount of the European continent originates from the frontal systems of less than 15 cyclones (Fraedrich et al., 1986), which also highlights the importance of cyclone track and cyclone intensity analysis.

3.1. Data

In the present analysis the ECMWF ERA-40 reanalysis datasets (http://www.ecmwf.int/research/era) are used. ERA-40 has been compiled from both in-situ and remotely-sensed measurements made over the period since mid-1957 until 2002 (Kallberg et al., 2004). ERA-40 datasets provide all meteorological variables at 60 vertical levels between the surface and a height of about 65 km with 6-hour temporal resolution.

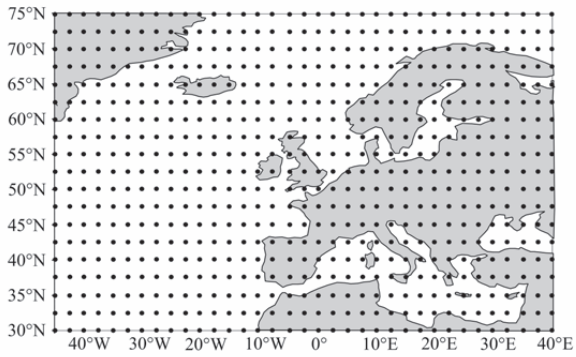

Figure 4. The selected domain and the grid points of the North-Atlantic-European region.

Originally, ERA-40 has a spectral representation based on a triangular truncation at wave number 156 or 1.125° horizontal resolution using a Gaussian grid (Gibson et al., 1997). The spatial resolution of the four main geopotential height fields (or Absolute Topography - AT) used in this analysis (i.e., AT 500 hPa, AT 700 hPa, AT 850 hPa, and AT 1000 hPa) is 2.5°×2.5°, which can be downloaded via Internet. The entire domain of the North-Atlantic-European region used in this paper, covers the area between 30°-75°N and 45°W-40°E (Figure 4), and it consists of 665 (=19×35) grid points.

3.2. Trend analysis of geopotential height fields

In order to explore the structural changes in geopotential height fields, statistical descriptive parameters are analyzed for the last 45 years. Figure 5 presents the standard deviation of the four main geopotential height fields (AT-500 hPa, AT-700 hPa, AT-850 hPa, AT-1000 hPa) of the troposphere. Large standard deviation values, indicating high variability of the geopotential height level, can be observed in the northern part of the selected domain, namely, around Iceland. In general, the North-Atlantic-European region can be characterized by zonal distribution of the standard deviation values. Two disturbances can be identified, namely, (i) in the northwestern part of the selected domain where the large variance may partly be explained by frequent cyclogenesis, (ii) in the Ligurian and the Tyrrhenian Sea with smaller standard deviation values where the so-called Genoa cyclones are often forming.

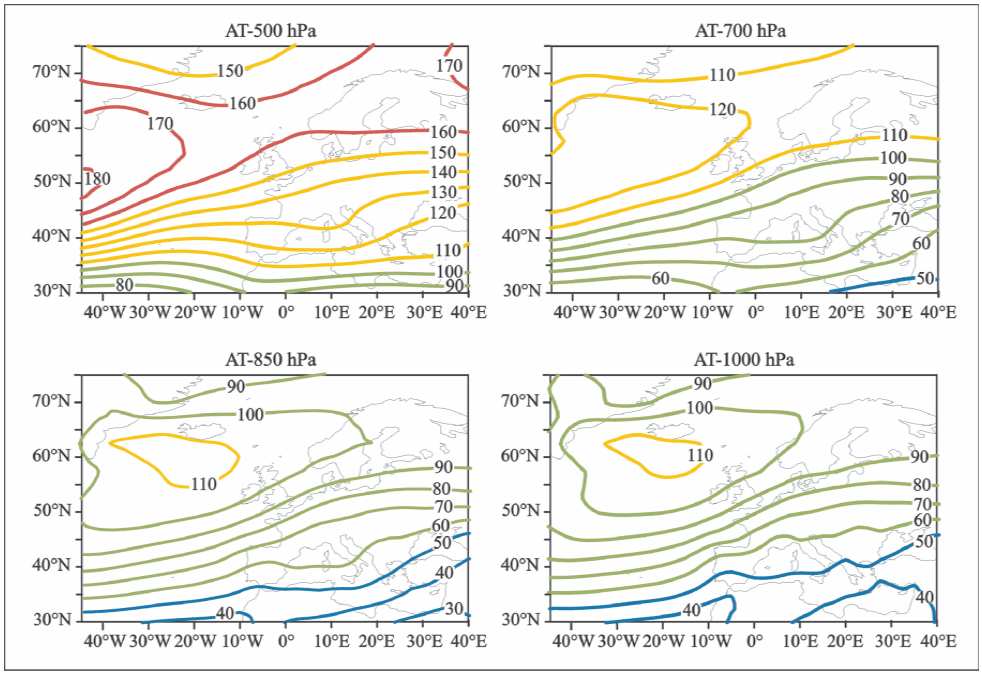

Figure 5. *Standard deviation of the four main geopotential height fields for the North-Atlantic-European region, 1957-2002.*

Linear trend analysis is accomplished for all the grid points of the North-Atlantic-European domain. Decadal trend values are presented on the maps of Figures 6 and 7 for the middle and the lower tropospheric levels, respectively. Similar spatial structures can be seen on these maps representing different geopotential height levels. Special zonal patterns may be recognized with the largest negative trend coefficients in the Greenland/Iceland region, while positive trend coefficients dominate the southern area, where two centers can be identified: (1) in the Mediterranean, and (2) in the Atlantic regions. On the maps, white asterisks represent the northern and the southern central regions. Graphs, shown above the maps of Figures 6 and 7, present the decreasing tendency of the annual mean geopotential height values for the grid point located in the Atlantic Ocean between southern Greenland and Iceland at 65°N latitude, 35°W longitude. Graphs, shown below the maps, illustrate the increasing tendency of the annual mean geopotential height values for the grid point located in the Mediterranean Sea at 42.5°N latitude, 7.5°E longitude. Except the AT 1000 hPa level, all of the presented linear trends for these two selected grid points are significant at 0.05 level using the t-test.

After the evaluation of the annual trend maps, the seasonal trend coefficients are mapped for the four main geopotential height fields. Figure 8 illustrates the detected trend fields for the AT 500 hPa level. No significant trend can be found in summer (coefficients are below 1 gpm/decade in absolute value), while the largest trend coefficients are detected in winter. The structure of the winter trends is similar to the annual trend fields. However, the absolute values of the winter trend coefficients at the two centers (the northwestern part of the selected domain around Greenland/Iceland, and the Mediterranean region in southwestern Europe and the Ligurian/Tyrrhenian Sea) are larger than the annual trend coefficients.

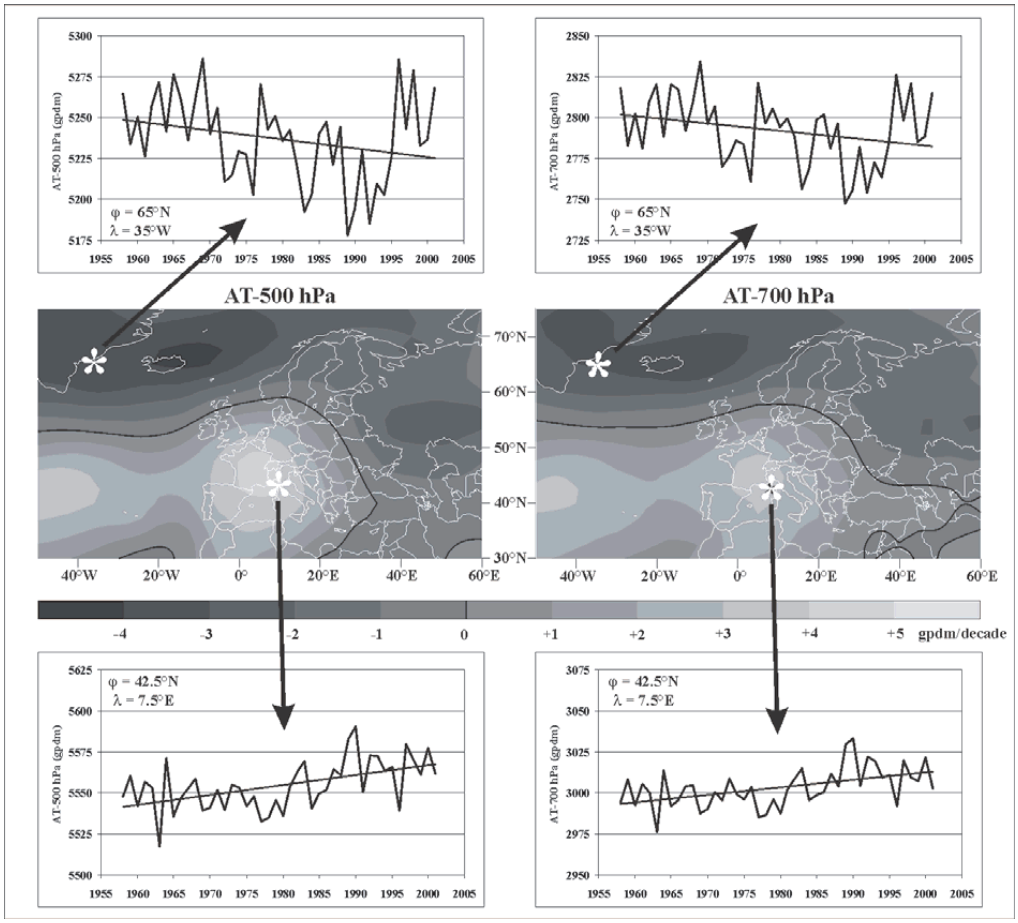

Figure 6. *Tendency analysis of AT-500 hPa (left) and AT-700 hPa (right) geopotential height levels. Detailed linear trends are shown for two selected gridpoints (65°N 35°W and 42.5°N 7.5°E) above and below the map of the trend coefficients, respectively. The fitted linear trends are significant at 0.05 level using the t-test.*

3.3. Cyclone track analysis

One of the main advantages of compiled global reanalysis datasets is to open the possibility for the identification of cyclone centers and cyclone tracks using objective methodology. After obtaining the location of identified midlatitude cyclones, frequency and intensity analysis can be accomplished. Several authors attempted to identify extratropical cyclones using different algorithms, but probably the most often cited method was developed by Serreze (1995) and Serreze et al. (1997). They studied arctic cyclones occurring in spring and winter, 1973-1992, based on sea level pressure data with 2.5° horizontal resolution. Their results suggest that frequency of cyclones increased, while their lifetime decreased. The method applied by Serreze et al. (1997) derives cyclones using pressure gradient, and it is able to detect strong high-latitude cyclones.

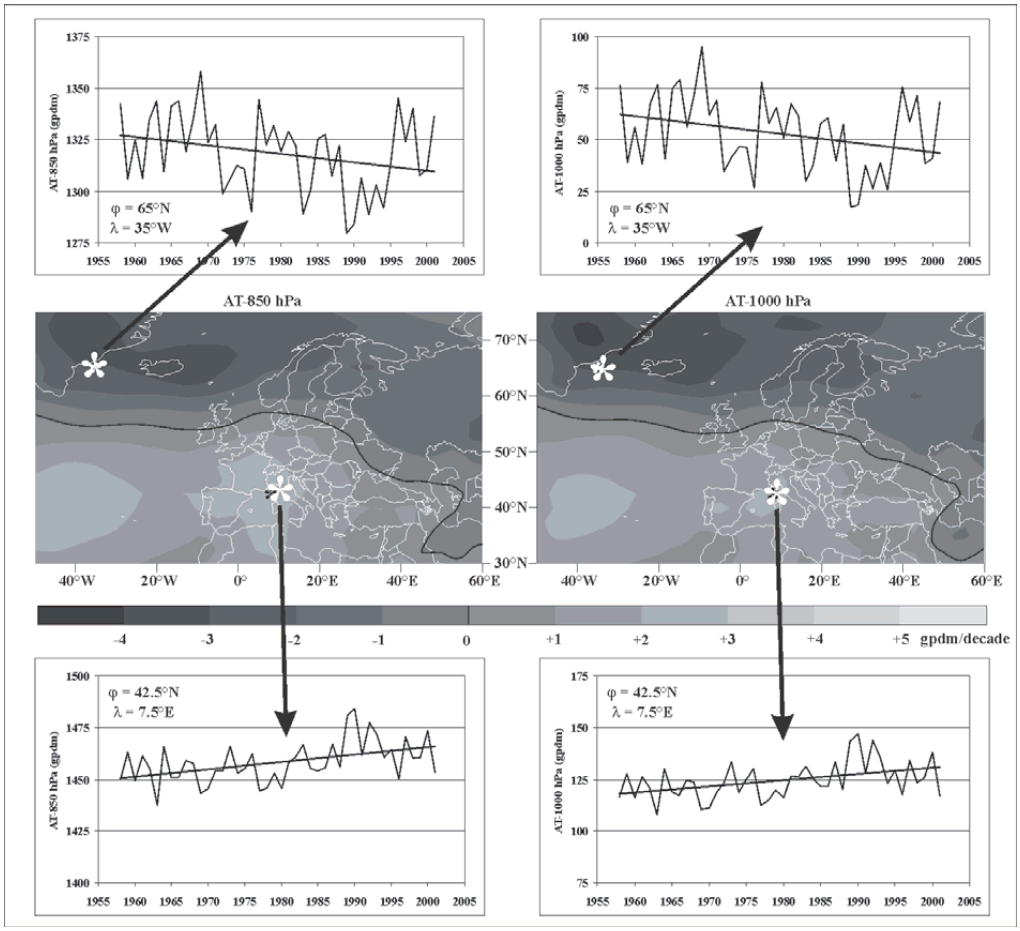

Figure 7. *Tendency analysis of AT-850 hPa (left) and AT-1000 hPa (right) geopotential height levels. Detailed linear trends are shown for two selected gridpoints (65°N 35°W and 42.5°N 7.5°E) above and below the map of the trend coefficients, respectively. The fitted linear trends are significant at 0.05 level using the t-test only in case of AT-850 hPa.*

In this paper, potential midlatitude cyclone centers are defined on the grid points with depression of air pressure where the following main criteria are fulfilled: (1) the sea level pressure is less than 1012 hPa, and (2) the pressure gradient is greater than 0.07 hPa/100 km for all directions. Geographical latitude and longitude, sea level pressure, and minimum of the pressure gradient values of the potential cyclone centers are stored at every time step (i.e., 6 hours). Then, cyclone tracks are determined by special sequences of stored potential cyclone centers. According to the algorithm used in this paper, two subsequent potential cyclone centers may belong to the same cyclone track if (1) their geographical distance is less than 900 km, and (2) their sea level pressure difference is less than 5 hPa in absolute value. Finally, the stored cyclone tracks contain data on (i) the time of the first detection of the cyclone center, (ii) the number of time steps until the last detection, (iii) the minimum pressure gradient during the entire lifetime of the cyclone, (iv) the geographical latitude/longitude coordinates of the cyclone center and (v) the sea level pressure in each time step. In order to verify the obtained cyclone tracks, synoptic charts of the North-Atlantic-

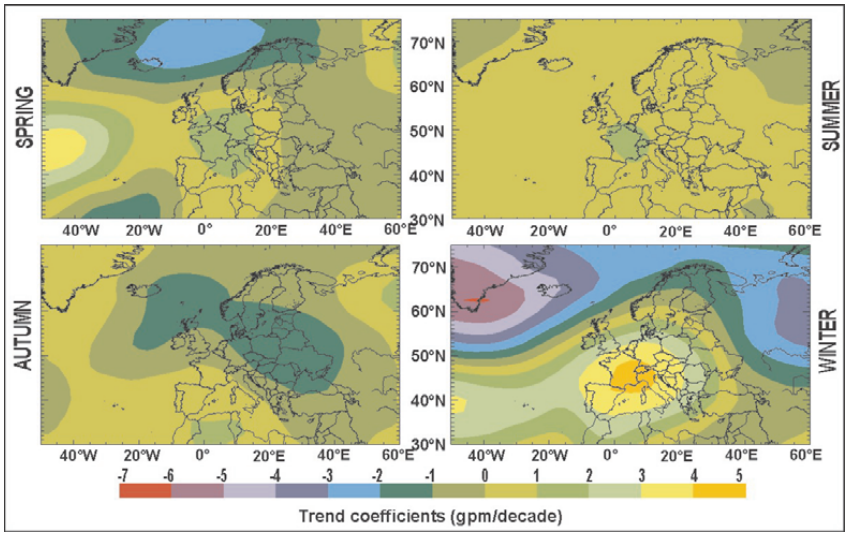

Figure 8. *Seasonal trend analysis of AT-500 hPa geopotential height level, 1957-2002.*

European region have been used for June 2002 (one example is shown in Figure 9). Although slight shifts (a few degrees) in the location of cyclone centers occurred, no false cyclone track has been determined during the verification period.

The starting positions of the identified midlatitude cyclone tracks indicate the geographical locations of cyclogenesis. Figure 10 shows the spatial frequency distribution of these cyclogenesis centers for the entire 45 years (1957-2002). The two largest frequency values can be found in the northwestern part of the selected domain around Greenland/Iceland, and in the Mediterranean region in southwestern Europe and the Ligurian/Tyrrhenian Sea – where the largest trend coefficients occurred (shown in Figures 6, 7, and 8).

Figure 11 summarizes seasonal cyclones center frequency in the North-Atlantic-European region for five equal 9-year-long periods. Maps on the left and the right panels represent smoothed grid point values in winter and summer, respectively. In general, less midlatitude cyclones can be detected in summer than in winter. Furthermore, cyclone tracks shift to the North in summer since they are located mainly north to the 50-55°N latitude zone, while in winter cyclone activity is present in the Mediterranean region too. The results also suggest that the number of cyclones increased considerably in the northwestern part of the domain in the last 45 year in both seasons.

In order to characterize the intensity of midlatitude cyclones, a complex parameter, namely, the Cyclone Activity Index (CAI) was defined by Zhang et al. (2004), which summarizes the differences between the sea level pressure of cyclone centers and the monthly mean pressure of the corresponding grid point for each time step and for all cyclones detected in a given month. For the North-Atlantic-European region, seasonal CAI values are mapped in Figure 12. In order to detect the possible changes in cyclone activity, the entire 45-year-long period is separated into five equal long subsets, similarly to the previous analysis. In general, the Icelandic cyclogenesis region is the most intense activity center on the maps. Genoa cyclone area is much weaker than the Icelandic low. Furthermore, cyclone activity in winter is larger than in summer. The results suggest that a considerable intensification can be detected in

cyclone activity in winter, especially, in the northwestern part of the domain. Further analysis of selected subregions would require different CAI-scale, and dataset with finer spatial resolution.

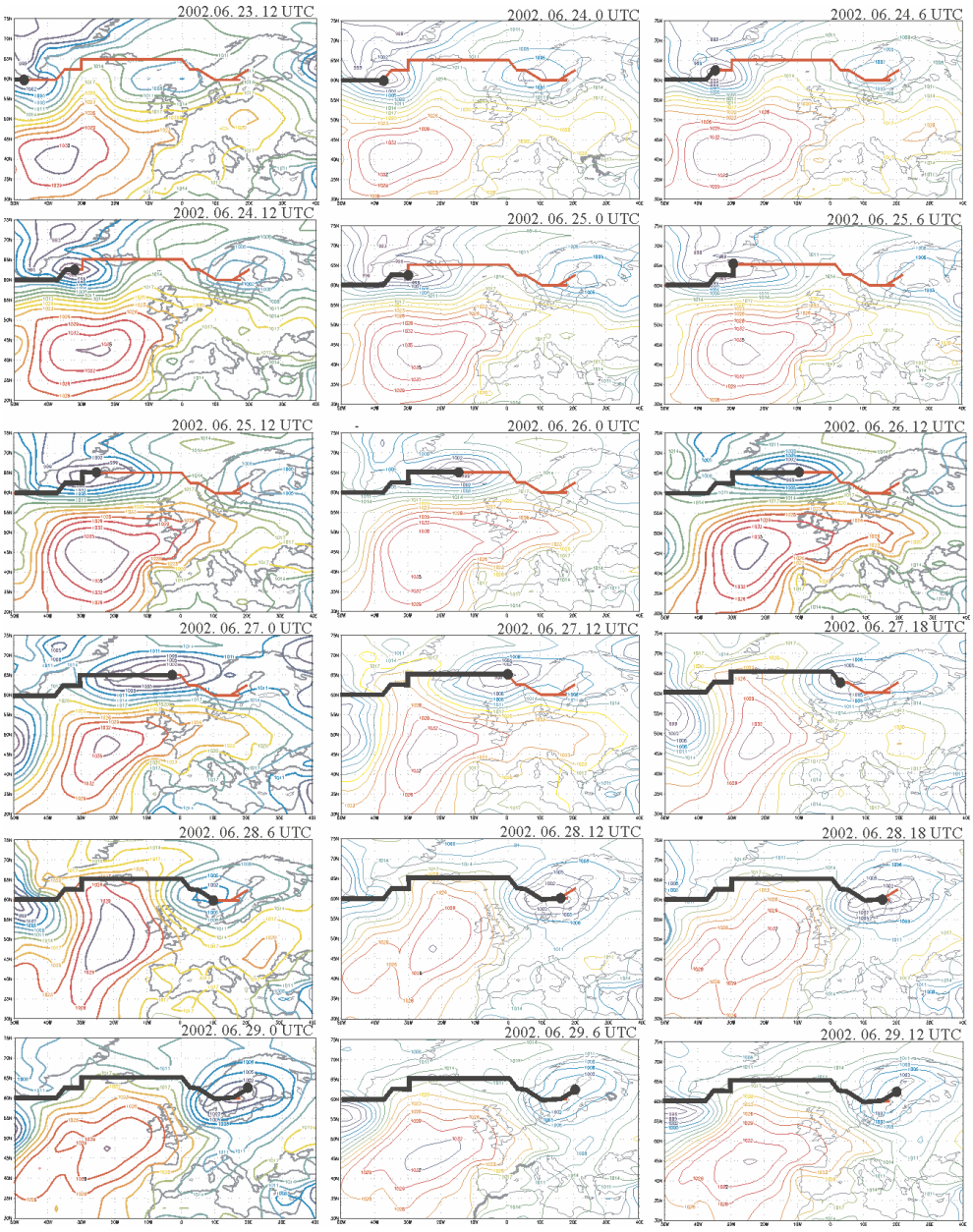

Figure 9. *Midlatitude cyclone track reconstruction, 23-29 June 2002.*

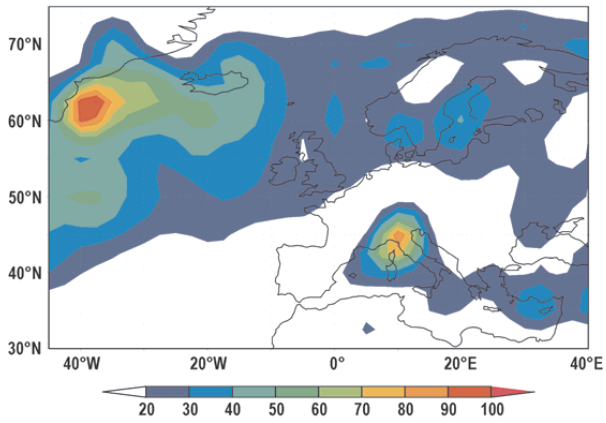

Figure 10. *Frequency of cyclogenesis, 1957-2002.*

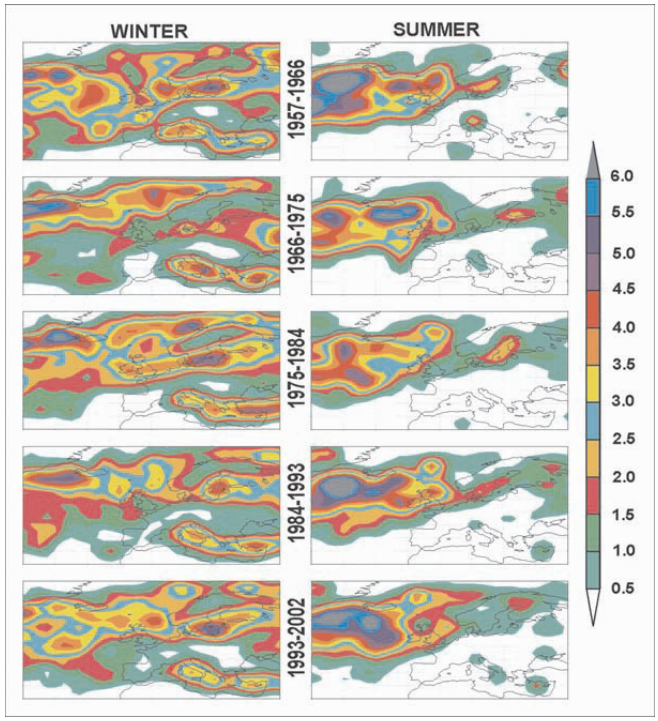

Figure 11. *Changes of seasonal cyclone center frequency (per decade) distribution in the North-Atlantic-European region in winter (December-January-February) and summer (June-July-August).*

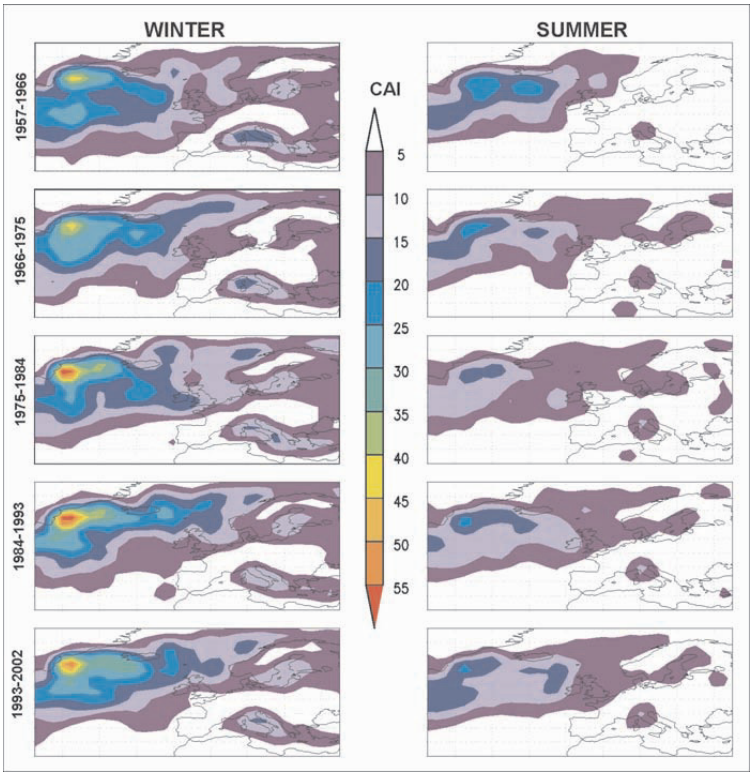

Figure 12. *Decadal changes of seasonal CAI values in the North-Atlantic-European region in winter (December-January-February) and summer (June-July-August).*

3.4. Analysis of frontal activity over the Carpathian Basin

As part of the cyclone activity, frontal systems are investigated in the last part of the paper. We are focusing on the cold and warm fronts passing over the Carpathian Basin. In our analysis, fronts are defined using the temperature values of 850 hPa geopotential height of the ERA-40 database (Kallberg et al., 2004). On the base of the synoptic practical guides, we assume that if the temperature change during 12 hours is more than 3°C it can be considered as a front by definition. Figure 13 presents the frequency distribution of the frontal systems. The total number of cold and warm fronts during the entire 45 year period is 2202 (58%) and 1580 (42%), respectively. According to the results, not only the number of the cold fronts occurred in the region is larger than the number of warm fronts, but the corresponding temperature change is also significantly larger in case of the cold fronts.

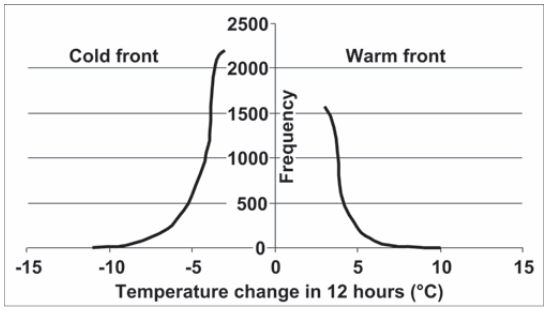

Figure 13. *Frequency distribution of temperature changes in case of cold and warm frontal systems, 1957-2002.*

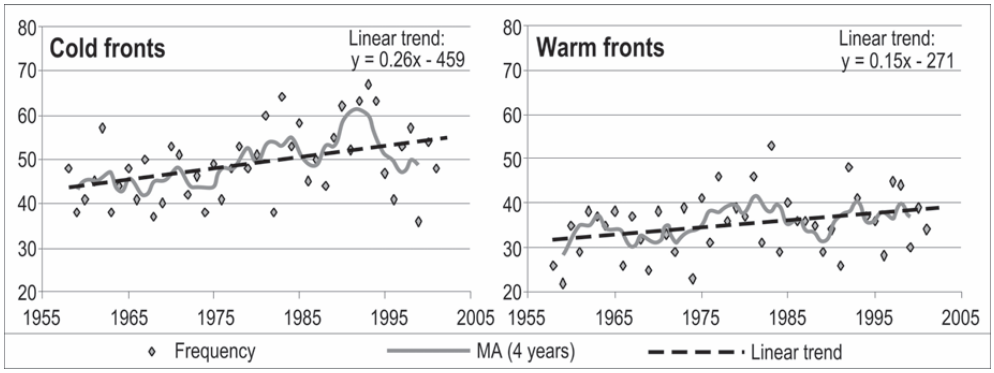

Figure 14. *Annual tendency of cold and warm fronts (using criterion ΔT>3°C), 1957-2002. Linear trend coefficients are significant at 0.05 level.*

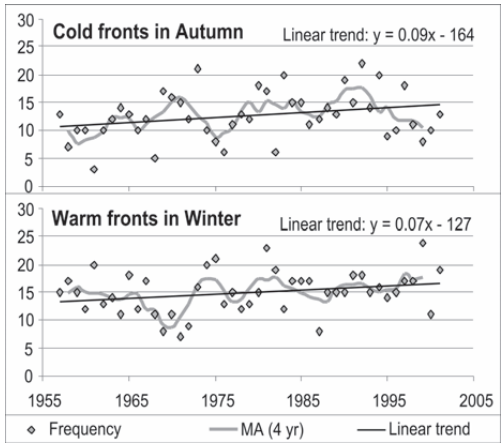

Figure 15*. Seasonal tendency of cold fronts (in autumn) and warm fronts (in winter) using criterion ΔT>3°C, 1957-2002. Linear trend coefficients are significant at 0.05 level.*

Annual, seasonal, and monthly trends of the number of cold and warm fronts are determined. Figure 14 shows the annual tendency analysis of the cold and warm frontal systems in the left and the right panel, respectively. Four-year moving average (MA) and the fitted linear trend using the least squares method are presented in the graphs. The annual number of cold fronts

between 1957 and 2002 increased more than the number of warm fronts. The linear trend coefficients significantly differ from zero at 0.05 level of significance using the statistical t-test. Seasonal trend analysis is illustrated in Figure 15, where the significant positive tendencies of the cold fronts in autumn and the warm fronts in winter are presented.

Precipitation events associated with the frontal systems strongly affect the regional climate, therefore, at the end of the paper we present the results of the frontal precipitation analysis. Several thresholds (i.e., 0 mm, 1 mm, 5 mm, 10 mm) are defined, and then, the annual and the seasonal numbers of cold and warm frontal precipitation events exceeding these thresholds are determined during the 1957-2002 period. Left and right panels of Figure 16 present the annual trend analysis of the cold and warm frontal precipitation events, respectively. Annual number of cold frontal precipitation events increased in the last 45 years (the positive trend is significant in case of 0 mm, 1 mm, 5 mm thresholds at 0.05 level). The largest seasonal trend coefficients can be detected in spring and autumn. Annual number of warm frontal precipitation events decreased between 1957 and 2002 (the negative trend is significant in case of 1 mm, 5 mm, 10 mm thresholds at 0.05 level). The largest seasonal trend coefficients (in absolute value) can be detected in winter.

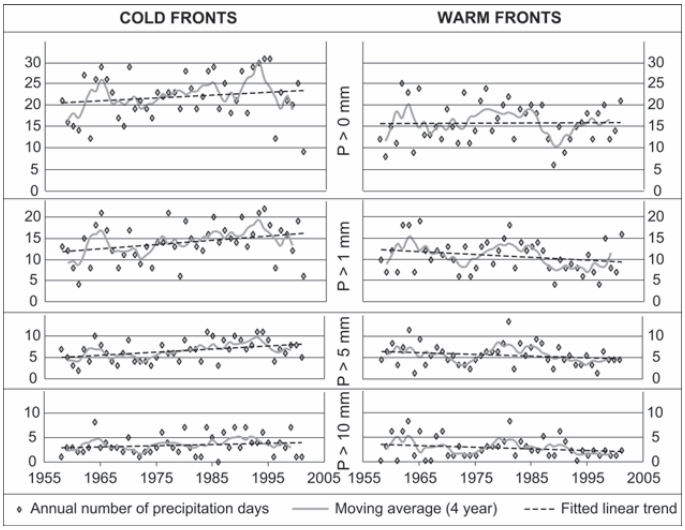

Figure 16. *Annual tendency of cold (left) and warm (right) frontal precipitation using criterion ΔT>3°C, 1957-2002. Linear trend coefficients are significant at 0.05 level except using the 10 mm and 0 mm threshold in case of cold and warm fronts, respectively.*

4. Conclusions

Changes in large-scale circulation have been analyzed for the North-Atlantic-European region for the 20th century. In order to accomplish this task, time series of MCP types (1881-2000) and height fields of four geopotential levels of the ERA-40 database (1957-2002, with 2.5° horizontal resolution) have been used. Based on the presented results, the following conclusions can be drawn:

1. Frequency of many anticyclonic Hess-Brezowsky MCP types decreased significantly in the last 120 years. Several other Hess-Brezowsky MCP types performed considerable increase between 1881 and 2000.
2. Decreasing tendency of the annual mean geopotential height values was detected in the Greenland/Iceland region between 1957 and 2002, while positive trend coefficients dominate the southern area of the North-Atlantic-European region with two centers, one in the Mediterranean subregion and the other one in the Atlantic subregion. The largest seasonal trends can be detected in case of winter with similar spatial structure.
3. Less midlatitude cyclones occurred and cyclone tracks shifted more to the North in summer than in winter in the last 45 years. Furthermore, the number of cyclones increased considerably in the northwestern part of the domain in both seasons.
4. The Icelandic cyclogenesis region is the most intense cyclone activity center in the North-Atlantic-European region. Furthermore, considerable intensification was detected in cyclone activity between 1957 and 2002. CAI values in winter are larger than in summer.
5. Annual number of both cold and warm frontal systems in the Carpathian Basin increased significantly during the 1957-2002 period.
6. Cold frontal precipitation events increased in the region during the 45 years, especially in spring and autumn, while warm frontal precipitation events decreased, especially in winter.

Acknowledgements. The authors thank ECMWF for producing and making available the ERA-40 reanalysis data. This paper is the written version of the presentation at the special session of ECAM-2005 conference organized in the frame of COST Action 733. Research leading to this paper has been supported by the Hungarian National Science Research Foundation under grants T-034867, T-038423, and T-049824, also by the CHIOTTO project of the European Union Nr. 5 program under grant EVK2-CT-2002/0163, the Hungarian National Research Development Program under grants NKFP-3A/0006/2002, NKFP-3A/082/2004, and NKFP-6/079/2005, the Hungarian Academy of Science and the Hungarian Prime Minister's Office under grant 10.025-MeH-IV/3.1/2006.

References

Alpert P, Neeman BU, Shay-el Y. 1990. Climatological analysis of Mediterranean cyclones using ECMWF data. Tellus 42A: 65-77.

van Bebber WJ. 1891. Die Zugstrassen der barometrischen Minima nach den Bahnenkarten der Deutschen Seewarte für den Zeitraum von 1870-1890. Meteorol. Zeitschrift 8: 361-366.

Fraedrich K, Bach R, Naujokat G. 1986. Single station climatology of Central European fronts: number, time, and precipitation statistics. Contr. Atmos. Phys. 59: 54-65.

Gibson JK, Kallberg P, Uppala S, Nomura A, Hernandez A, Serrano A. 1997. ERA description. ECMWF Reanalysis Project Report Series No. 1., 77p.

Hess P, Brezowsky H. 1977. Katalog der Grosswetterlagen. Berichte Deutscher Wetterdienst Offenbach. 113 Bd 15.

Hodges KI. 1994. A general method for tracking analysis and its application to meteorological data. Mon. Wea. Rev. 122: 2573-2586.

IPCC, 2001: Climate Change 2001: The Scientific Basis. Contribution of Working Group I to the Third Assessment Report of the Intergovernmental Panel on Climate Change. (Houghton

JT, Ding Y, Griggs DJ, Noguer M, van der Linden PJ, Dai X, Maskell K, Johnson CA, eds.) Cambridge University Press: Cambridge, U.K. and New York, NY, USA. 881pp.

Kallberg P, Simmons A, Uppala S, Fuentes M. 2004. The ERA-40 archive. ERA-40 Project Report Series No. 17.

Key JR, Chan ACK. 1999. Multidecadal global and regional trends in 1000 mb and 500 mb cyclone frequencies. Geophys. Res. Lett. 26: 2053-2056.

Klein W. 1957. Principal tracks and mean frequencies of cyclones and anticyclones in the Northern hemisphere. Research Paper No. 40. U.S. Weather Bureau: Washington.

Lamb HH. 1972. British Isles weather types and a register of the daily sequence of circulation patterns, 1861-1971. Geophys. Mem. 116. HMSO: London.

Lambert SJ. 1988. A cyclone climatology of the Canadian Climate Centre general circulation model. J. Climate 1: 109-115.

Serreze MC. 1995. Climatological aspects of cyclone development and decay in the Arctic. Atmosphere-Ocean 33: 1-23.

Serreze MC, Carse F, Barry R. 1997. Icelandic low cyclone activity: Climatological features, linkages with the NAO, and relationships with recent changes in the Northern Hemisphere circulation. J. Climate 10: 453-464.

Zhang X, Walsh JE, Zhang J, Bhatt US, Ikeda M. 2004. Climatology and interannual variability of arctic cyclone activity: 1948-2002. J Climate 17: 2300-2317.

Weather type classification: Approaches in Switzerland

Mark A. Liniger, Christoph Frei
Federal Institute of Meteorology and Climatology (MeteoSwiss), Zürich, Switzerland

1. Introduction

Mountain weather and climate is particularly sensitive to variations in atmospheric circulation. It is therefore natural that the development and application of weather types classifications (WTC) has a long tradition in Switzerland. However the prominent influence of the Alpine mountain ridge on the regional circulation and its peculiar location between the Western European, the Mediterranean and the Continental climates brings along some specific challenges to classification and requires adaptation of conventional classification techniques. Here we briefly introduce the techniques for weather classification developed and operationally implemented in Switzerland.

2. Weather type classification after Schüepp

The most widely known weather type classification developed and maintained in Switzerland is the Alpine Weather Statistics (AWS) from Schüepp (1968). The daily classification is continuously available from 1945 till the time of writing. A detailed description of the method can be found in Schüepp (1968). The subjective classification focuses on the meteorological conditions within an area defined as a circle with a radius of 2 degrees in latitude (approx. 222 km) around the point 46.5° N und 9° E. This point corresponds to the Rheinwaldhorn, close to the St. Gotthard pass. The main criterion or motivation for the classification is the air movement in the horizontal and vertical direction. The classification is made analysing weather parameters at various stations within the area of interest as surface pressure distribution, wind distribution and strength and the position of the 500 hPa level. The daily weather is classified into 40 types. These types can be ordered into three main groups and 10 base types (Table 1).

From the AWS, there exists a continuous time series from 1.1.1945 that is operationally updated. Some analyses of the time series have been undertaken (Salvisberg, 1996; Wanner et al., 1998; Wanner et al., 2000). The frequency of the main groups is not constant over time (Fig. 1). In particular, changes can be identified since the 70ies for all three groups. This time period falls together on the one hand with marked changes in circulation characteristics over Europe (e.g. those related to the NAO, Hurrell 1995), but it also coincides with a change in the persons responsible for the classification. The possibility that the AWS is affected by inhomogeneities is a drawback for its application in long-term climate variability studies. (Wanner et al., 1998).

There have been attempts in automating the AWS applying objective criteria to gridded fields (Salvisberg, 1996). The technique is based on four grid points within the mentioned area and evaluates six parameters: surface wind, upper level wind, 500hPa geopotential and baroclinicity. 47% of the days are classified identically in a comparison with the official, manually obtained classification (Fig. 2). However, the matches strongly vary with weather type and season.

Table 1: Grouping of AWS types (adapted from Wanner et al., 2000).

Main groups	Base types	Comments
Convective types	1. high pressure 2. flat pressure 3. low pressure	High, flag and low pressure corresponds to the 500hPa surface
Advective types	4. westerlies 5. northerlies 6. easterlies 7. southerlies	The directions correspond to the wind direction at 500hPa.
Mixed types	8a. vortex types 8b. upper level jet stream 8c. lower level jet stream	

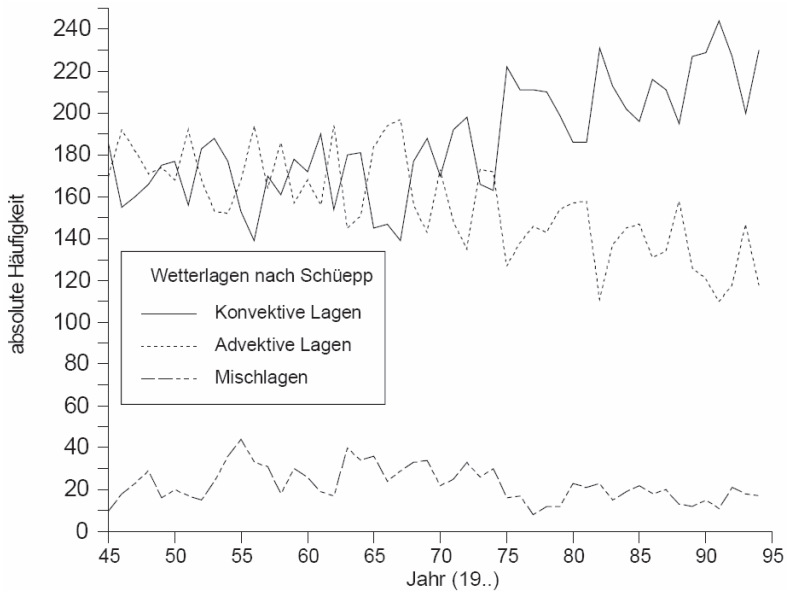

Figure 1: *Number of occurrence of AWS main groups from 1945 till 1994. The main groups consist of convective types (solid), advective types (short dashed) and mixed types (long – short dashed), from Wanner et al. (2000).*

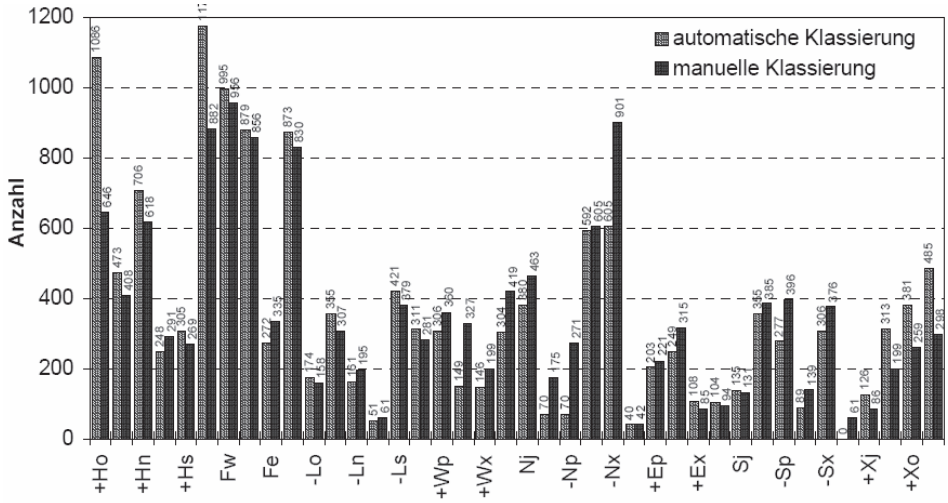

Figure 2*: Number of days classified into individual AWS types from the manual (black columns) and automatic classification (grey columns) from 1946 till 1989 (from Wanner et al., 2000).*

3. Weather type classification after Perret

A second weather type classification maintained in Switzerland has a more synoptic focus (Perret, 1987). After an assessment of the various classifications, Perret adapted the method from Hess and Brezowsky (HB, 1969) to the needs for Switzerland and the Alpine area. The classifications makes use of 31 types: The 27 ones from HB and 3 additional ones to take into account Swiss specific weather. One type of HB has been chosen differently less restrictive. The 31 types are numbered newly. The types can be ordered in 3 main groups (straight currents, anticyclonic and cyclonic or Thalweg). The classification is made manually based on the synoptic charts of surface pressure and 500 hPa geopotential on a daily level. The observed weather in Switzerland is used as guidance. From the Perret-Classification, there exists a continuous time series from 1.1.1955 that is updated on an operational basis.

4. Other, non-operational classifications

There are several additional WTCs valid for the central Alpine region, which, unlike AWS and Perret, have not been operationally continued, either because they were designed for specific research purposes or because of lack of resources. For example, Rickli (1995) has regrouped the traditional Hess and Brezowsky classification into 8 groups merging HB weather types with similar weather characteristics in the Alpine region. Steinacker (1991) has designed a very regional Alpine classification, which, distinct from most classical schemes, uses wind information at the 850 hPa level. In addition, several more recent WTCs have been developed with a focus on the distribution of heavy precipitation in the Alps (Busch and Heimann, 2001; Plaut and Simonnet, 2001; Seibert et al. 2006). These are objective classification schemes intended mostly for statistical or statistical-dynamical downscaling of daily precipitation.

A more methodological contribution to WTC from Switzerland is the Kirchhofer classification. Using pattern correlation as a similarity measure Kirchhofer (1974) introduced

a scheme, which assesses similarity of pairs of pressure maps both for a large region (e.g. the continent) and user-specified sub-regions (see also Blair, 1998). Two patterns are classified as similar if both the Kirchhofer score at the continental scale as well as at the sub-regions are sufficiently strong. This procedure corrects for deficiencies of classical pattern correlation methods, which happen to allow patterns to be grouped together even though some sections are extremely different. The Kirchhofer technique has been used in several downscaling applications (e.g. Saunders and Byrne, 1999; Yarnal et al. 2001). However it was never implemented operationally in the Alpine region.

5. Conclusion

Switzerland has a long tradition in weather type classification, both with respect to methodological developments and the operation and application of Alpine specific classifications. However, currently operational WTCs in Switzerland are all manual and subjective, laborious to execute and likely inhomogeneous in time. An objective and automated WTC that is capable of reproducing Alpine-specific dynamic features and that extends over a long period is an urgent need for reliable applications.

References

Blair, D., 1998: The Kirchhofer technique of synoptic typing revisited. Int. J. Climatol., 18, 1625-1635.

Busch, U. and D. Heimann, 2001: Statistical-dynamical extrapolation of a nested regional climate simulation. Clim. Change, 19, 1-13.

Hess, P. and Brezowsky, H.,1969: Katalog der Grosswetterlagen Europas. Berichte des Deutschen Wetterdienst, 113.

Kirchhofer, W., 1974: Classification of European 500mb patterns. Arbeitsbericht der Schweizerischen Meteorologischen Zentralanstalt, 43. Available from MeteoSchweiz, Krähbühlstr. 58, 8044 Zürich, Switzerland.

Perret, R., 1987: Une classification des situations météorologiques à l'usage de la prévision. Veröffentlichung der Schweiz. Meteorol. Anstalt, 46, 127 pp.

Plaut, G. and E. Simonnet, 2001: Large-scale circulation classification, weather regimes, and local climate over France, the Alps and Western Europe. Climate Res., 17, 303-324.

Rickli R., 1995: Gruppierung Europäischer Grosswetterlagen nach alpin-synoptischen Kriterien. Arbeitsbericht NFP 31, 38 pp.

Salvisberg, E., 1996: Wetterlagenklimatologie- Möglichkeiten und Grenzen ihres Beitrages zur Klimawirkungsforschung im Alpenraum. Dissertation Univ. Bern.

Saunders, I.R. and J.M. Byrne, 1999: Using synoptic surface and geopotential height fields for generating grid-scale precipitation. Int. J. Climatol., 19, 1165-1176.

Seibert, P., A. Frank and H. Formayer, 2006: Synoptic and regional patterns of heavy precipitation in Austria. Theor. Appl. Climatol., DOI 10.1007/s00704-006-0198-8.

Schüepp, M., 1968: Regionale Klimabeschreibungen, 1. Teil. Beiheft z.d. Ann. Schweiz. Meteorol. Zentralanstalt, 2, 245 pp.

Steinacker, R., 1991: Eine Ostalpine Strömungslagenklassifikation, 8 pp. (Available from Institute for Meteorology and Geophysics, University of Vienna. http://www.univie.ac.at/IMG-Wien/weatherregime/)

Wanner, H., E. Salvisberg, R. Rickli and M. Schüepp, 1998: 50 years of Alpine Weather Statistics. Meteorol. Zeitschrift, N.F. 7, 99-111.

Wanner, H., D. Gyalistras, J. Luterbacher, R. Rickli, E. Salvisberg und C. Schmutz, 2000: Klimawandel im Schweizer Alpenraum. Verlag der Fachvereine, Hochschulverlag AG an der ETH Zürich, 296 pp.

Yarnal, B., A.C. Combrie, B. Frakes and D.P. Brown, 2001: Developments and prospects in synoptic climatology. Int. J. Climatol., 21, 1923-1950.

A simple approach to derive objective circulation pattern classifications

F. Kreienkamp (1), W. Enke (1), Th. Deutschländer (2), A. Spekat (1)
(1) Climate & Environment Consulting Potsdam GmbH, Potsdam, Germany
(2) German Meteorological Service (DWD), Offenbach, Germany

Abstract

A method to obtain circulation patterns from fields of atmospheric variables and surface observations is presented. In its course, temperature classes are formed which group the local temperature regime. These are used to build composites of atmospheric fields, grouped by the temperature classes. This way, circulation patterns are derived according to the local temperature values they cause. The selection of optimal predictor fields is achieved by conducting a screening discriminant analysis which is basically analogous to a stepwise screening regression. Statistical parameters to assess the similarity/dissimilarity between individual days and the weather patterns are presented and reference is made to applications of the method.

1. Introduction

A multitude of synoptic classifications exist that can be distinguished by way of the variables used and the classification procedure applied. Circulation pattern classifications typically employ large scale pressure data while others use local weather elements as input variables. Besides, a classification can either be subjective, objective, or hybrid. The choice of the appropriate technique depends on the needs of the research, the skills of the investigator, and the nature of the data (Frakes and Yarnal, 1997). Initial classifications were commonly subjective and their application was mainly limited to medium- (at that time 3 to 5 days) and long-range forecasting (Baur, 1948). Two of the most widely known subjective classifications are the so-called Grosswetterlagen (Baur et al., 1944; Hess and Brezowsky, 1952) and the British Isles Weather Types (Lamb, 1972). Apart from forecasting, these classifications were also found to be a useful tool for climate diagnosis. Brown (2002), for example, found some indication of a progressive warming by analysing the relationships between the Lamb daily weather types and the central England temperatures from 1881 to 2000. Whilst Bárdossy and Caspary (1990) and Gerstengarbe and Werner (1993), carried out their analysis of climate fluctuations by inspecting the frequency distributions of the Großwetterlagen.

An alternative to manual classifications are objective algorithms. Especially during the past decade, increasing computer resources have led to the development of a variety of automated techniques. As a result, not only were the subjective classifications mostly superseded, but the field of application was also extended. Environmental meteorological studies, for example, utilize different approaches to determine or forecast the level of atmospheric air pollution (Eder et al., 1994; Stohl and Scheifinger, 1994). Among the most popular classification procedures are correlation based algorithms (Brinkmann, 1999) and clustering techniques (Huth et al., 1993; Kidson, 1994), to name but a few.

To overcome the inherent shortcomings both types of classifications suffer from, yet another approach has been pursued quite extensively. Hybrid techniques combine elements of

empirical and automated procedures, thereby avoiding being time consuming and enabling the production of easily reproducible and interpretable results (Sheridan, 2002). Such classifications are usually based on subjectively chosen model cases which exhibit the typical characteristics of each group and serve as seeds for objective algorithms (Bárdossy et al., 1995; Kalkstein et al., 1996).

2. Data

There are two kinds of data required to carry out this study: (i) Synoptic scale aerial fields and (ii) surface observations. Source for the aerial data is the reanalysis set of the National Center for Environmental Prediction (NCEP) and the National Center for Atmospheric Research (NCAR), (Kalnay et al., 1996). These data were received in the form of 2.5°x2.5° resolution grids, and were subsequently interpolated to an equally spaced grid of approximately 150 km resolution which comprises a total of 289 (17x17) points centred on 51°N and 10°E (Fig. 1). According to a study executed prior to the actual variable selection, the choice of this window had proven to best represent circulation conditions in the area of central Europe on average. It should be mentioned that results varied slightly according to the geographical location of the specific region of interest.

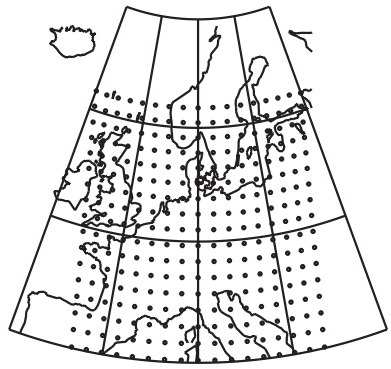

Figure 1: *Position of the 17x17 equidistant gridpoints*

As a source for the surface observations data from climate stations of the German Weather was used.

For this study, the upper level fields of geopotential heights, temperatures and relative humidity were extracted from the reanalyses and the data set was then subdivided into typical 3-month periods MAM, JJA, SON, and DJF, in order to allow for seasonality and also to enable the use of absolute values.

It should be mentioned that, alternatively, the use of ERA40 reanalysis data is possible. Both perform well (and in a comparable way) in areas of good data coverage (Greatbatch and Rong, 2006). However, the NCEP data have the advantage that they are, unlike ERA40, constantly updated.

3.Description of the method

The following steps are describing a hybrid system. For a more detailed description of the method please refer to Enke et al., 2005.

Step 1: Prescription of the number of classes

The first step of the procedure involves a prescription of the number of final classes. The choice of the correct number depends upon the local weather element for which the classification is to be designed.

Two choices are possible:

- using predefined classes like the Grosswetterlagen;
- defining new classes.

A procedure developed by Enke and Spekat (1997) can be used to determine the optimal model complexity - in essence they found that on the order of 10 classes are well sufficient to describe the pattern regime and not be subject of overfitting.

Step 2: Derivation of composites

The next step is to compute composite maps reflecting the large-scale mean atmospheric patterns corresponding to each of the subjective local weather classes (Fig. 2). This is simply done by averaging all observations previously assigned to each specific empirical group separately for all grid points.

Step 3: Screening discriminant analysis

To enable the procedure to recognize future independent cases solely on the basis of synoptic scale data, it is necessary to identify those (aerial) fields that best represent regional conditions. This means the aim is to find the combination of input variables that, when used to assign individual cases, produces minimal mistakes in comparison to the subjective classification. Therefore several different meteorological parameters at various levels were used in addition to the usual geopotential heights. Furthermore, a variety of derivatives from these fields were calculated to account for as many physical processes as possible. However, to avoid overfitting, the number of fields that were subjected to the filtering process we employed had to be limited. A full list of the potential predictor fields that were finally included in this analysis is given in Table 1.

Generally, all derivative fields employed could be easily calculated. The relative vorticity, computed in geostrophic approximation, was used, but constants such as the Coriolis parameter f, having no crucial influence within statistical models, were neglected (also see Table 1). The situation described above is analogous to the starting point of a screening regression analysis. For this reason we employ an algorithm similar to a procedure known as forward selection or stepwise regression which yields a nearly optimal discrimination.

The screening discriminant analysis is begun by calculating the distances D between the individual daily observations and the composite maps pertaining to the different classes. This is done separately for each potential predictor field. Each case is then assigned to that composite map, i.e. group, the distance measure D is minimal for that particular day and potential predictor field. This yields as many new classifications as there are potential predictor fields. Finally, the candidate predictor field minimizing the RMSE between forecasts (from the pertaining classification) and observations of the local variable of interest is selected first. At the next stage the procedure is repeated for all remaining potential predictor fields. However, the predictor already selected is included when calculating the distances D. This is realized by simply adding the distances of the new candidates to the

Table 1: Potential predictors used in this study

Nr.	Feld	Kürzel
1	Geopotential Height 1000 hPa	GP 1000
2	Geopotential Height 850 hPa	GP 850
3	Geopotential Height 700 hPa	GP 700
4	Geopotential Height 500 hPa	GP 500
5	Temperature 850 hPa	TP 850
6	Temperature 500 hPa	TP 500
7	Relative Humidity 850 hPa	RH 850
8	Relative Humidity 500 hPa	RH 500
9	horizontal Difference N-S 850 hPa	HD1 850
10	horizontal Difference W-O 850 hPa	HD2 850
11	horizontal Difference N-S 500 hPa	HD1 500
12	horizontal Difference W-O 500 hPa	HD2 500
13	Vorticity 1000 hPa	VOR 1000
14	Vorticity 850 hPa	VOR 850
15	Vorticity 700 hPa	VOR 700
16	Vorticity 500 hPa	VOR 500
17	Thickness 1000/850 hPa	RT 1000/850
18	Thickness 1000/700 hPa	RT 1000/700
19	Thickness 1000/500 hPa	RT 1000/500
20	Temperature Difference 850 - 500 hPa	TD 850-500

distance of the previously chosen field. The procedure is terminated when either of the following stopping rules is fulfilled:

1. the number of predictor fields reaches 4,
2. the reduction of the RMSE resulting from the inclusion of another predictor does not exceed a prescribed threshold.

As a distance measure we use *RMSD,* a slightly modified version of the widespread Euclidean distance similar to the the root mean square error (*RMSE*).

$$D = RMSD = \sqrt{\frac{1}{n}\sum_{i=1}^{n} R_i^2}$$

Because the analysis includes variables not measured in the same physical units, which yields arbitrary relative scalings, a normalization was necessary to maintain comparability and allow for the summation of the distances $D_{j,k,l}$ during the screening procedure. Therefore all fields were a priori normalized by

$$o'_{i,j,k} = \frac{o_{i,j,k} - \overline{o}}{S}$$

Here $\overline{o}$ is the overall average of all grid point values $\hat{o}_{i,j}$, and S is the corresponding spread, i.e. both values are characteristics of the entire composite maps. The spread is obtained by simply subtracting the absolute minimum of all $\hat{o}_{i,j}$ from their maximum value. To ensure

statistical stability the complete screening discriminant analysis is carried out in a cross-validation framework. That is, composite maps are calculated using one part of the data batch, while the other part of the data is reserved to assign cases on the basis of synoptic-scale information and to compute the resulting *RMSE* values.

Step 4: Reassignment of cases
The final step of our classification scheme is to reassign all daily observations according to the large-scale atmospheric conditions following the rules determined by the screening procedure.

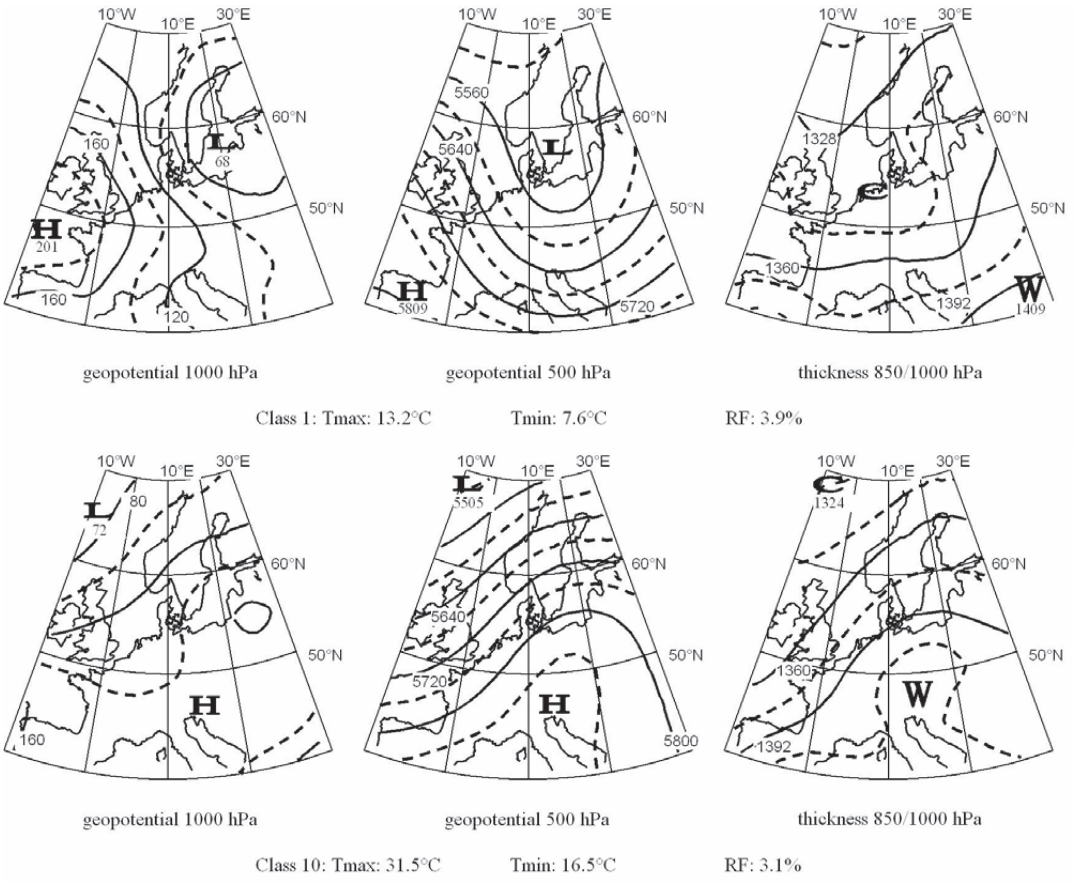

Figure 2: *Composites of GP 1000, GP 500 and RT850/1000 (see Tab. 1) for the coolest (top three panels) and the warmest (bottom three panels) class in summer. It is furthermore indicated what the average maximum and minimum temperature of those days which constitute the class is, as well as the class's relative frequency.*

4. Outlook: Applications

A wide range of applications is possible once the above method has been applied to produce circulation patterns. For example, they can be used to investigate the future circulation regime by applying the method not to reanalysis data but climate model scenario runs. Prescribing a set of patters which is derived from the current climate, shifts in their frequency can be detected. Moreover, the method can be used to investigate if hitherto unknown patters emerge in the future under scenario conditions. Since there are, of course, no observation data from the future time periods that the climate model scenarios describe, a stochastic weather generator is needed to generate ``observations''. These informations can then be used in climate impact studies of all kinds.

References

Bárdossy, A., H.J. Caspary, 1990: Detection of climate change in Europe by analysing European atmospheric circulation patterns from 1881 to 1989, Theor. Appl. Climatol. **42**, 155-167.

Bárdossy, A., L. Duckstein, I. Bogardi, 1995: Fuzzy rule-based classification of atmospheric circulation patterns, Int. J. Climatol. **15**, 1087-1097.

Baur, F., 1948: Einführung in die Großwetterkunde, Dietrich, Wiesbaden, Germany, 165pp.

Baur, F., P. Hess, H. Nagel, 1944: Kalender der Großwetterlagen Europas 1881-1939. - Forschungsinstitut für langfristige Witterungsvorhersage, Bad Homburg v.d.H., Germany.

Brinkmann, W.A.R., 1999: Within-type variability of 700 hPa winter circulation over the Lake Superior Basin, Int. J. Climatol. **19**, 41-58.

Brown, P.R., 2002: Relationships beween the Lamb daily weather types and Central England temperatures from 1881 to 2000, J. Meteorol. **27**, 326-334.

Eder, B.K., J.M. Davis, P. Bloomfield, 1994: An automated classification scheme designed to better elucidate the dependence of ozone on meteorology, J. Appl. Meteorol. **33** 1182--1199.

Enke, W., A. Spekat, 1997: Downscaling climate model outputs into local and regional weather elements by classification and regression, Clim. Res. 8, 195-207.

Enke, W., F. Schneider, Th. Deutschländer, 2005: A novel scheme to derive optimized circulation pattern classifications for downscaling and forecast purposes, Theor. Appl. Climatol. **82**, 51-63, DOI10.1007/s00704-004-0116-x.

Frakes, B., B. Yarnal, 1997: A procedure for blending manual and correlation-based synoptic classifications, Int. J. Climatol. **17**, 1381-1396.

Gerstengarbe, F.-W., P.C. Werner, 1993: Katalog der Großwetterlagen Europas 1881-1998 nach P. Hess und H. Brezowsky. 5. Auflage, Potsdam Institut für Klimafolgenforschung, Potsdam, Germany, 138pp.

Greatbatch, R.J., P.-P. Rong, 2006: Discrepancies Between Different Northern Hemisphere Summer Atmospheric Data Products, J. Clim., **19**, 1261-1273

Hess, P., H. Brezowsky, 1952: Katalog der Großwetterlagen Europas. - Berichte des Deutschen Wetterdienstes US Zone **33**, Selbstverlag des Deutschen Wetterdienstes, Bad Kissingen, Germany, 39pp.

Huth, R., I. Nemesová, N. Klimperová, 1993: Weather categorization based on the average linkage clustering technique. An Application to European mid-latitudes, Int. J. Climatol. **13**, 817-835.

Kalkstein, L.S., M.C. Nichols, C.D. Barthel, J.S. Greene, 1996: A new spatial synoptic classification. Applications to airmass analysis, Int. J. Climatol. **16**, 983-1004.

Kalnay, E., M. Kanamitsu, R. Kistler, W. Collins, D. Deaven, L. Gandin, M. Iredell, S. Saha, G. White, J. Woollen, Y. Zhu, M. Chelliah, W. Ebisuzaki, W. Higgins, J. Janowiak, K.C. Mo, C. Ropelewski, J. Wang, A. Leetma, R. Reynolds, R. Jenne, D. Joseph, 1996: The NCEP/NCAR 40-year reanalysis project, Bull. Amer. Met. Soc. **77**, 437-471.

Kidson, J.W., 1994: An automated procedure for the identification of synoptic types applied to the New Zealand region, Int. J. Climatol. **14**, 711-722.

Lamb, H.H., 1972: British Isles weather types and a register of the daily sequence of circulation patterns 1861-1971, Geophys. Memoirs **116**, Her Majestys Stationery Office, London, U.K., 85pp.

Stohl, A., H. Scheifinger, 1994: A weather pattern classificaton by trajectory clustering, Meteorol. Z. **3**, 333-336.

Spatial and temporal variance of cyclones in the Baltic Sea region

P. Link, P. Post
University of Tartu, Ülikooli Str 18, 50090 Tartu, Estonia

1. Introduction

Northern Europe is an area of high cyclonic activity. The dominant westerly flow of the atmospheric circulation brings warm and moist air from the Atlantic far inland. It makes the climate of Northern Europe warmer and milder than that experienced at equivalent latitudes in Asia and America. Cyclones propagate eastwards with the westerly flow.

The temporal variability of European weather and climate is largely affected by the North Atlantic Oscillation (NAO). An interrelation between the strength of the winters in Scandinavia and Greenland has been already known since the 18th century and qualitatively described by van Loon and Rodgers (1978) as a 'seesaw in winter temperatures'. Attempts have been made to relate climate change in Europe to changes in NAO (Hurrell, 1995; Hurrell and van Loon, 1997; Jaagus, 2006). More than the expected number of positive phases of NAO have been noticed in last decade (Hurrell, 1995). This has lead to stronger westerly flow and a more maritime climate in the Northern Europe. While cyclogenesis is strongly correlated with westerly flow, it can be speculated that there has been changes in cyclonic activity as well. To quantify the spatial and temporal variability of cyclones in the Baltic Sea region, 53 years (1948-2000) of cyclonic activity have been analyzed.

Chen (2000), Linderson (2001) and Post et al. (2003) have classified atmospheric circulation over Northern Europe using the Jenkinson and Collison (1977) synoptic classification. Their conclusions about the dominating weather type are dissimilar – whether it is cyclonic (Chen, 2000) or anticyclonic (Post et al., 2003; Linderson, 2001). One possible reason for this is that cyclones and anticyclones distribute so unevenly in the region, that the exact location chosen for the classification causes the difference. This possibility has motivated this investigation of the spatial distribution of cyclone properties within the Baltic Sea region.

2. Data and methods

A database of cyclones for the Northern Hemisphere (Gulev et al., 2001) has been used. It is based on NCEP/NCAR reanalysis data with spatial resolution of 2.5°×2.5°. Special feature tracking software (Grigoriev et al., 2000) has been used to identifying cyclones. A cyclone is detected from air pressure field if closed isobars occur. The Gulev et al. (2001) cyclone database contains the following cyclone characteristics with 6 h time-step: coordinates of cyclone center, pressure in the cyclone center, deepening rate for 6 h, cyclone velocity as a vector etc. Only cyclones, for which the minimum pressure dips at least once below 1000 hPa are analyzed.

The mapping process can underestimate the number of cyclones by 20% for a 5°×5° grid size and 6h or 12h temporal resolution (Zolina and Gulev, 2002). This is because fast-moving cyclones skip grid boxes. Smaller spatial and larger temporal resolutions result in higher uncertainties of cyclone frequencies. The use of a circular grid decreases the uncertainties. Both a 5°×5° grid and mapping in circular sub-areas are applied in this analysis.

Cyclone frequencies and life cycle characteristics have been computed in diverse spatial levels: Atlantic-European (A-E) sector (30° W – 45° E and 35° – 75° N) and in five circles with a radius of 1000 km in the Baltic Sea region. The centers of three of the circles (Figure 2b circles 1 - 3) were chosen to match the locations of existing atmospheric circulation classifications (Linderson, 2001; Chen, 2000; and Post et al., 2003). The remaining two centers were taken so, that the whole Baltic Sea area was covered. The radius of 1000 km from a certain center point was used because this is the average scale of influence of cyclones.

3. Annual mean cyclone frequencies

During the period 1948 - 2000 the mean annual number of cyclone frequencies in the Atlantic-European sector was 297. There was a significant ($P<0.05$) increasing trend until the 1970s and a insignificant decreasing trend thereafter (Fig. 1a). Cyclone frequencies in the Baltic Sea sub-areas had overall positive trend till the 1970s as well, but afterwards there have been increasing tendencies in northerly areas and decreasing ones in the most southerly area. In average 94 cyclone centers occurred in the radius of 1000 km – less in the southern area and more in the northern area of the Baltic Sea.

As Fig. 1b shows, cyclones are most frequent in winter (December and January), especially in the northerly sub-area and the most southerly area of the Baltic region. The fewest cyclones occur in May and July in northerly areas and in July in the most southerly area. Only the easternmost area (4) remains without any notable differences between the seasons, exclusively the minimum of cyclones in February can be outlined there. Annual amplitude of cyclones occurrences is larger in northerly areas.

For the 5°×5° grid, annual cyclone frequencies (Fig. 2 a, b) as well as annual cyclone generation frequencies (Fig. 2c, d) have been computed. A number of very intense cyclone generation areas can be outlined: one in the Atlantic close to Iceland and several northwestward from Scandinavia. More cyclones are present near the intense cyclone generation areas.

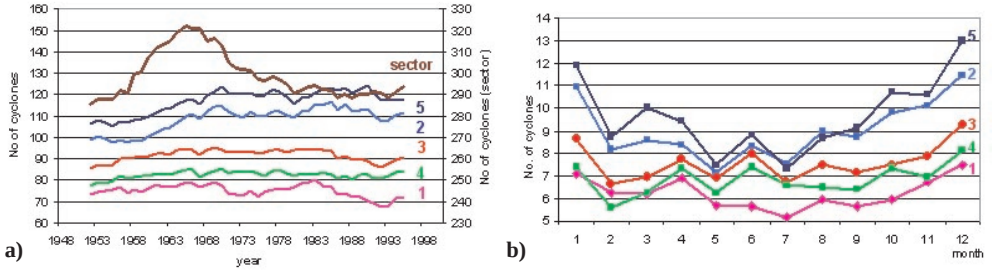

Figure 1. *a) Ten-years moving average of cyclone numbers in the Atlantic-European sector and in 5 chosen Baltic sub-areas. b) Annual cycle of number of cyclones in the Baltic sub-areas. The locations of the sub-areas can be seen in Fig. 2b.*

4. Cyclones life cycle characteristics

The characteristics of cyclone lifetime, propagation and pressure are compared between the 5 chosen sub regions and the Atlantic-European sector. A cyclone lifetime is defined as the time a cyclone exists in the database with its temporal resolution of 6 h.

Cyclones counted in the region of the Baltic Sea are characterized by longer lifetimes and higher velocities than those in the whole Atlantic-European sector (Table 1). The mean

lifetime in the Atlantic-European sector was 106 h = 4.4 days. The average lifetime in the Baltic Sea region was 114–120 h = 4.7–5.0 days. The average difference is about 10 hours. Here no correlation with latitude can be found. The longest mean lifetime exemplifies the cyclones around center points 3 and 5, i.e. those in the middle of the Baltic Sea region.

Comparing Fig. 1a and 3a shows that while the number of cyclones was increasing - cyclones lifetime was decreasing up to the 1970s. A wavy trend can be seen in the lifetime time series. Seasonally, cyclones live longer in winter. Nearly half of cyclones last 2-5 days (fig 3b). About 20% of cyclones are long lasting – they last more than 7 days. In sub-areas 1, 2 and 5 percentage of 2-day cyclones is relatively higher than in Figure 3b that represents sub-area 3. Longer lifetimes in central part of the Baltic region may be due to the relatively warm Baltic Sea supplying moisture and energy to support the cyclones.

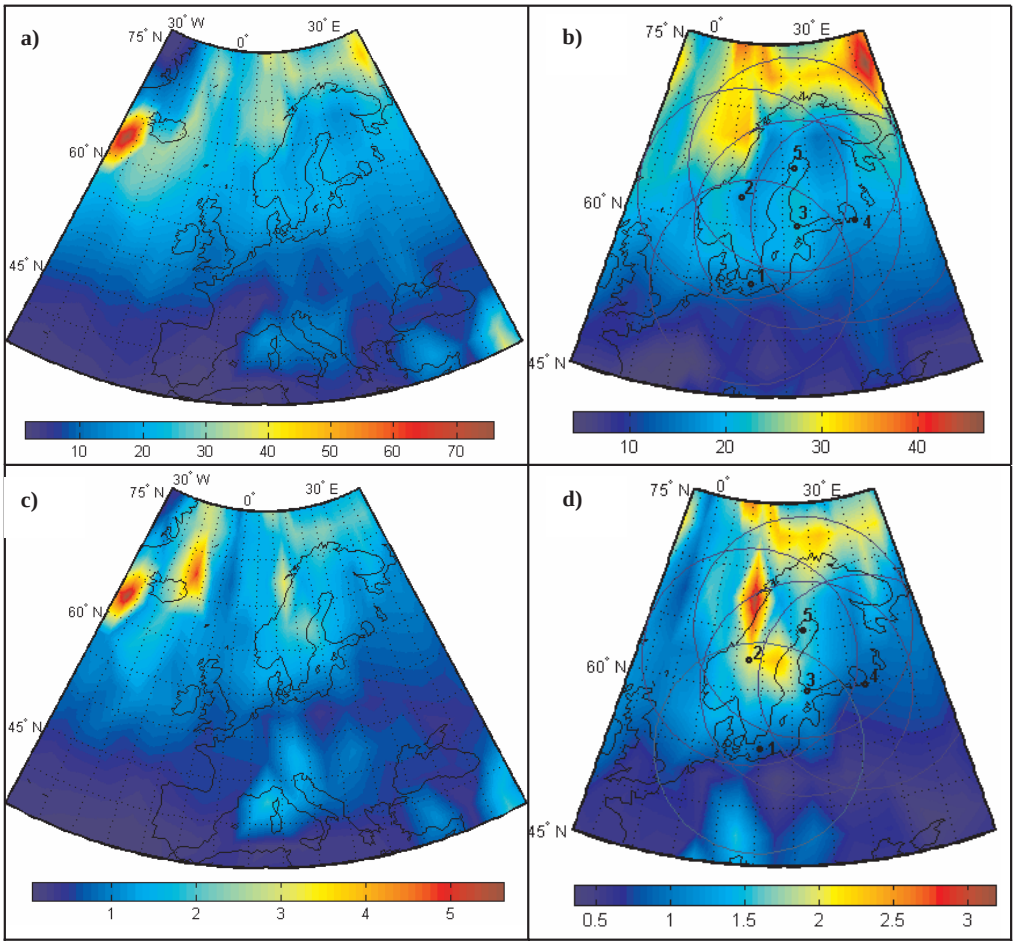

Figure 2. Annual frequency of cyclone centers that occur in 5°×5° grid boxes (a, b) and cyclone generation frequencies (c, d). Cyclone numbers are normalized for 100 000 km2 areas. The central points of 5 sub-areas in the Baltic Sea region are indicated with numbers (b and d).

Table 1. Annual mean lifetime of cyclones.

No of sub-area	1	2	3	4	5	A-E sector
Hours	117	115	117	114	120	106
Days	4.9	4.8	4.8	4.7	5.0	4.4

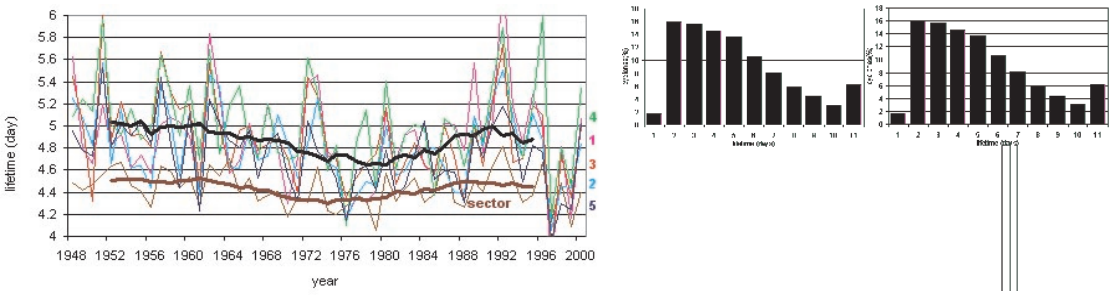

a) b)

Figure 3. *a) Ten-years moving average of cyclone lifetimes in the A-E sector and in the Baltic Sea region. b) Histogram of cyclones lifetimes in sub-area 3.*

The minimum pressure of each cyclone center was one argument in the database that we used to define a cyclone – it had to drop below 1000 hPa at least once in its lifetime. Eliminating very weak cyclones makes the analysis more reliable.

The mean annual minimum pressure in the Atlantic-European sector was 985 hPa. For the Baltic sub-areas it varied from 984 to 987 hPa, having lower values in northern areas. The number of deep cyclones increased with latitude. There were no significant differences between the annual averages for the A-E sector and the Baltic Sea region. Dissimilarities between seasons were more marked. In Figure 4a annual mean and average distribution for winter and summer season are shown. Average minimum pressure in winter was 980.5 hPa, while in summer it was 992.0 hPa – more than 10 hPa higher. In wintertime there were more deep cyclones and in warm seasons there were more cyclones with higher central pressures.
In Figure 4a cyclones with minimum central pressure above 1000 hPa are included to show the proportion of these cyclones. In any other part of our investigation those are excluded to increase the reliability of the analyses. The percentage of very weak cyclones increases inversely with latitude. Deepest cyclones appear near central points 2 and 5. The maximum of weak cyclones is in summer, in sub-area 1, for example, 40% of all cyclones are very weak in summer. Those weak cyclones have shorter lifetimes and smaller propagation velocities than cyclones analyzed in this article.

a) b)

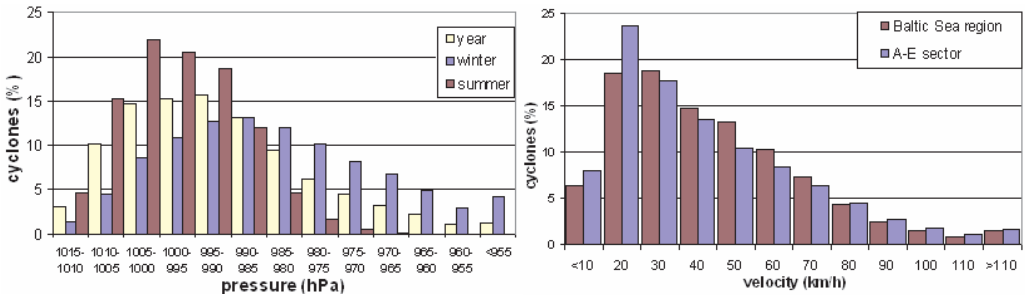

Figure 4. *a) Distribution of minimum pressure of cyclones in the whole Baltic Sea region. b) Distribution of cyclones velocity in the Baltic Sea region compared to A-E sector.*

The velocity of cyclone propagation for every 6h was given in the source dataset. We defined the average velocity within each particular region as the average of the propagation velocities for each cyclone at its nearest approach to the chosen central point. In Atlantic-European sector mean cyclone velocity was 34.1 km/h. In the Baltic Sea region average velocity was 39.0 km/h – it varied from 38.2 to 40.7 km/h in different areas of the region. The majority of cyclones had velocities in the range 10 - 20 km/h. Cyclones with velocities faster than 70 km/h constitute a 10 % of all cyclones. In the Atlantic-European sector there are both more very fast and more very slowly moving cyclones (Fig. 4 b).

When comparing different seasons – the velocity is higher in cold season: winter or autumn (Table 2).

Table 2. Mean velocity of cyclones propagation (in km/h) in the Baltic Sea region.

Area No	Winter	Spring	Summer	Autumn	Year
1	41.6	38.7	34.8	40.8	39.3
2	40.6	39.3	31.9	39.8	38.2
3	39.8	39.4	33.7	41.5	38.7
4	38.8	39.6	32.9	39.9	38.1
5	41.7	43.1	34.6	43.1	40.7

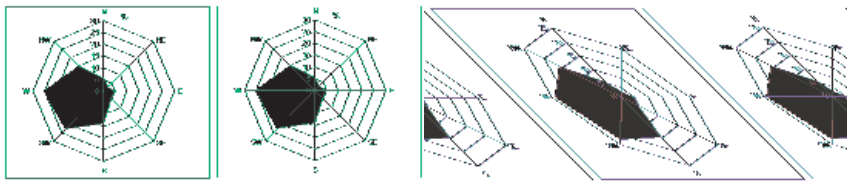

a) b)

Figure 5*. a) Distribution of direction of cylones origin for central point 3. b) Distribution of direction of cyclones moving in sub area 3.*

The direction of cyclones origin has been computed as a vector from the place cyclone was formed to the chosen central point. Nearly 50% of cyclones are formed southwestward from the chosen central point (Fig. 5a). Distribution is irrespective of which central point is used. There is a remarkable number of cyclones that are formed inside the Baltic Sea region (Table 3). Look Figure 2 c and d for geographical distribution of cyclone generation. In average 40 % of all cyclones are of local origin. Main reason is that the area involves also Norwegian Sea, which is one clearly notable cyclone generation area.

Table 3 Cyclones formed inside the Baltic Sea region.

Area No	1	2	3	4	5
No of cyclones	30.7	46.3	36.5	29.8	49.6
% of all cyclones	40.9	42.9	40.1	36.4	42.7

The direction of cyclones propagation shows the direction from where the cyclone approaches to the closest point to the sub-area central point. It describes which directions cyclones prefer when moving over chosen sub-area. An example of distribution is shown in Fig. 5b. Differences between sub-areas of the Baltic Sea region are very small.

5. Discussion

The aim of this work was to investigate the variability of cyclones properties inside the region of the Baltic Sea. The hypothesis was made that the prevailing weather type of the classification could be influenced by choice of exact location: that the cyclones prefer to pass the sub-area 2, that Chen (2000) has chosen, not the areas 1 or 3. When comparing cyclone frequencies, cyclone lifetimes, cyclone velocities, cyclone minimum pressures in chosen Baltic sub-areas no remarkable differences were detected. There were some small dissimilarities in number of cyclones and the trends weren't exactly the same for all the sub-areas as well as there were minor differences in minimum pressure, lifetime and velocity of cyclones. But these differences were not large enough to cause diverse results of weather type classifications.

Very similar results inside the Baltic Sea can be caused by the wrong choice of the radius of the ring used for describing sub-area. Using the radius smaller than 1000 km causes significantly more varying results. For a closer study of differences in cyclone propagation, a Langrangian analysis of cyclone trajectories must be done.

An alternative hypothesis to explain the diverse conclusions about the prevailing weather type may be that the contradictory findings result from the use of different temporal averaging. Chen (2000) has used in his analysis monthly mean pressure fields while Post et al. (2003) and Linderson (2002) used daily ones. In future this can be controlled by using monthly mean pressure fields for atmospheric circulation classification in center points 1 and 3.

6. Conclusion

Cyclone frequencies and life cycle characteristics in the Baltic Sea region in comparision with whole Atlantic-European sector have been investigated.

On average 94 cyclone centers occurred in the radius of 1000 km in the area of the Baltic Sea – less in the southern regions and more in the northern ones. There has been a positive trend

in the frequency of cyclone occurrences in northern areas and negative trend in the most southerly as it has been during the 53 years of analysing.

Cyclones passing through the region of the Baltic Sea are characterized by longer lifetime (114 to 120 hours) and higher velocity (39.0 km/h) than those in the whole Atlantic-European sector (106 h and 34.1 km/h respectively). While the number of cyclones was increasing - cyclones lifetime was decreasing up to the 1970s.

Minimum pressures in cyclone centers in the Baltic Sea region are on average 984 hPa –987 hPa, against 985 hPa in Atlantic-European sector, the pressures in northerly areas of the Baltic Sea region are especially low.

The region of Baltic Sea is also an important area of cyclone generation. 40 % of cyclones that appear in the region are formed inside (main reason is that the area involves also Norwegian Sea). Those cyclones that come outside the region are mostly formed south-westward.
In wintertime cyclones have lower pressures, higher velocities and longer lifetimes than in any other season. Cyclones are most frequent in winter. The annual amplitude of cyclones frequencies is larger in northerly areas.

Results of our investigation do not explain diverse results of classifications of the dominant weather type of the atmospheric circulation: the differences of cyclone frequencies and properties inside the Baltic Sea region are not large enough.

Acknowledgements
We express our gratitude to Olga Zolina (University of Bonn) for making available the Northern Hemisphere cyclones database. The study was funded by the Estonian Science Foundation grant 5786. Presentation of this study at EMS 5th Annual Meeting 2005 was supported by the EMS.

References
Chen, D. 2000. A monthly circulation climatology for Sweden and its application to a winter temperature case study. *Int. J. of Climatol.,* 20: 1067-1076.

Grigoriev, S., Gulev, S.K. and Zolina, O. (2000) Innovative software facilitates cyclone tracking and analysis. *EOS,* 81:170.

Gulev, S.K., Zolina, O., Grigoriev, S. 2001. Extratropical cyclone variability in the Northern Hemisphere winter from the NCEP/NCAR reanalysis data. *Clim. Dyn.* 17: 795-809.

Hurrell, J. W., 1995. Decadal Trends in the North Atlantic Oscillation: Regional Temperatures and Precipitation. *Science*, 269: 676-679.

Hurrell, J. W., van Loon H., 1997. Decadal variations in climate associated with the North Atlantic Oscillation. *Clim. Change*, 36: 301-326.

Jaagus, J., 2006. Climatic changes in Estonia during the second half of the 20th century in relationship with changes in large-scale atmospheric circulation. *Theor. Appl. Clim.,* 83: 77-88.

Jenkinson, A.F., Collison, F.P., 1977. An initial climatology of gales over the North Sea. *Synoptic Climatology Branch Memorandum*, Meteorological Office, Bracknell, 62.

Linderson, M.L. 2001. Objective classification of atmospheric circulation over Southern Scandinavia. *Int. J. Climatol.,* 21: 155-169.Post, P., Truija V., Tuulik J. 2002. Circulation weather types and their influence on the temperature and precipitation in Estonia. *Boreal Env. Res.,* 7*:* 281-289**.**

Van Loon, H., Rodgers, J.C., 1978. The seesaw in winter temperatures between Greenland and Northern Europe. Part I: General description. *Mon. Wea. Rev.,* 106: 296-310.

Zolina, O., Gulev, S.K., 2002. Improving the Accuracy of Mapping Cyclone Numbers and Frequencies. *Mon. Wea. Rev.*, 130: 748-759.

Stochastic Contrasts for Rainfall Variability over Continental Portugal. Persistent Oscillation Weather Patterns.

P. S. Lucio, F. C. Conde, A. M. Ramos
Centre of Geophysics of Évora (CGE) – University of Évora
Apartado 94, 7000-554 Évora – Portugal
pslucio@uevora.pt; fabconde@uevora.pt; andreara@uevora.pt

Corresponding author : Paulo Sérgio Lucio INMET - Instituto Nacional de Meteorologia Eixo Monumental Via S1 Sudoeste 70680-900 Brasília-DF - Brazil

Abstract

The complex interaction of coupled ocean-atmosphere processes is still far from being completely understood, and documented. Rainfall over the Western part of the Iberian Peninsula is known to be related to the large scale sea level pressure field and thus to advection of humidity into this area. The strong wintertime connection between several climate variables over Europe and the North Atlantic Oscillation (NAO) is now widely recognized. The winter precipitation anomalies in Portugal have been analysed over the period 1901-2000 based on the NAO and on the El Niño Southern Oscillation (ENSO) states. The winters of 1991/1992, 1999/2000 (dry) and 1989/1990, 1995/1996 (wet) were marked by strikingly different weather conditions over the North Atlantic Ocean and adjacent continents. Furthermore, during 1991/1992 and 1999/2000 sea level pressures over the North Atlantic ocean were unusually low and Portugal experienced an unusually dry winter. By contrast, during 89/90 and 95/96 sea level pressures over the North Atlantic Ocean were unusually high and Portugal experienced a rainy winter. The period 1989-2000 was also marked by a major cycle of the ENSO with the positive phase (*El Niño*) peaking in the winter of 97/98 and the negative phase (*La Niña*) peaking in the winter of 98/99. We use a state-of-the-art to investigate the hypothesis that the anomalous conditions in the North Atlantic sector during these winters were related to the ENSO cycle.

1. Introduction

There is a variety of widely-used statistical methods for analyzing fields of data which vary in both space and time. These tools can help us systematically parse through data fields. They can be used to characterize typical spatial modes of variability, their time evolution, and the relationships between the various observables. The choice of a statistical method is always subjective and depends on the particular question that one wants to address. Therefore, the results of statistical analysis should be interpreted with caution. A useful concept in extracting a physical phenomenon from the data using statistical tools is to consider the superposition of independent statistical approaches and interprets the results as a clearly defined common property.

The “Principal Component Analysis” (PCA) is a method widely used to find a spatial pattern which explains the maximal variance of the data field. However, PCAs may combine independent but non-orthogonal spatial patterns of variability. Because higher PCAs are forced to be orthogonal to their predecessors, they may not be physically realizable. PCAs are affected by sampling biases in the covariance matrix. A good practical check on robustness is

to separately apply PCA to the first and second half of the observed times and then examine the similarity of the two PCAs.

The "Principal Oscillation Pattern" (POP) analysis fits a field of data to an AR (1) process. This is an idealized model of a damped linear response to stochastic forcing. The associated eigenvalues should all have magnitudes less than one and the corresponding eigenvectors (or POPs) describe the modes of variability of the system. The complex eigenvalues indicate damped oscillations and the complex eigenvectors describe the oscillations in the spatial structure of the response. Considering the methods discussed above, only compositing is a nonlinear method. There are more advanced nonlinear methods, one of which is "Cluster Analysis" (CL). In CL the field is usually filtered first using one of the linear methods to reduce the number of spatial degrees of freedom (weather regime partition). Then, in the phase space of the amplitudes of the leading spatial patterns, the region where the system spends most of its time, are determined. These regions are called clusters.

The "Compositing" (C) technique involves constructing an index which correlates with the variability of the phenomenon of interest. Regressing the index onto the data or binning the data according to the ranges of the index, yields composite spatial patterns of variability. It is extremely flexible, able to capture both localized and moving features and to quantify nonlinearities in the behaviour (by comparing opposite phases of the extreme events). However, the choice of the index is highly subjective and there is no set way to determine the most sensible index. Compositing (C) all the events from such a region give the corresponding spatial pattern and some additional temporal information can be obtained by observing the temporal character on the occurrence of events. Changes in large-scale atmospheric flow have an important impact on rainfall variability over Portugal, mostly explained by the North Atlantic Oscillation (NAO) and slighted (intriguing) associated with the Pacific Decadal Oscillation (PDO).

The increasing of economic losses, coupled with a raise in deaths due to extreme events, has focused attention on the possibility that these events are increasing in frequency. Short-duration episodes of extreme heat or cold are often responsible for the major impacts on society. Conversely, the location, timing, and magnitude of local and regional changes remain unknown because of uncertainties on future changes in the frequency and intensity of meteorological systems that cause extreme weather and climate events. It is likely that anthropogenic forcing will eventually cause global increases in extreme precipitation, primarily because of probable increases in atmospheric water vapour content and destabilization of the atmosphere.

2. Experimental Dataset

This work is based on monthly total precipitation time series taken from 7 meteorological stations in Portugal (Figure 1), covering the period 1901-2000. Herein, the stations of Porto, Montalegre and Guarda represent the conditions over northern Portugal, Lisbon, Évora and Beja represent the conditions over centre-southern and Faro over southern Portugal. Time series of rainfall at these stations provide a good representation of Portuguese precipitation. The variability of precipitation in Portugal is characterized by a strong annual cycle (Figure 1). The maximum rainfall occurs in winter (DJF), with additional significant contributions coming from late autumn (ON) and early spring (M). The total precipitations recorded at each station are highly correlated (≥99%). All the coefficients are statistically significant at the 1% significance level, which is also a clear proof of the dominance of the large-scale forcing of

.

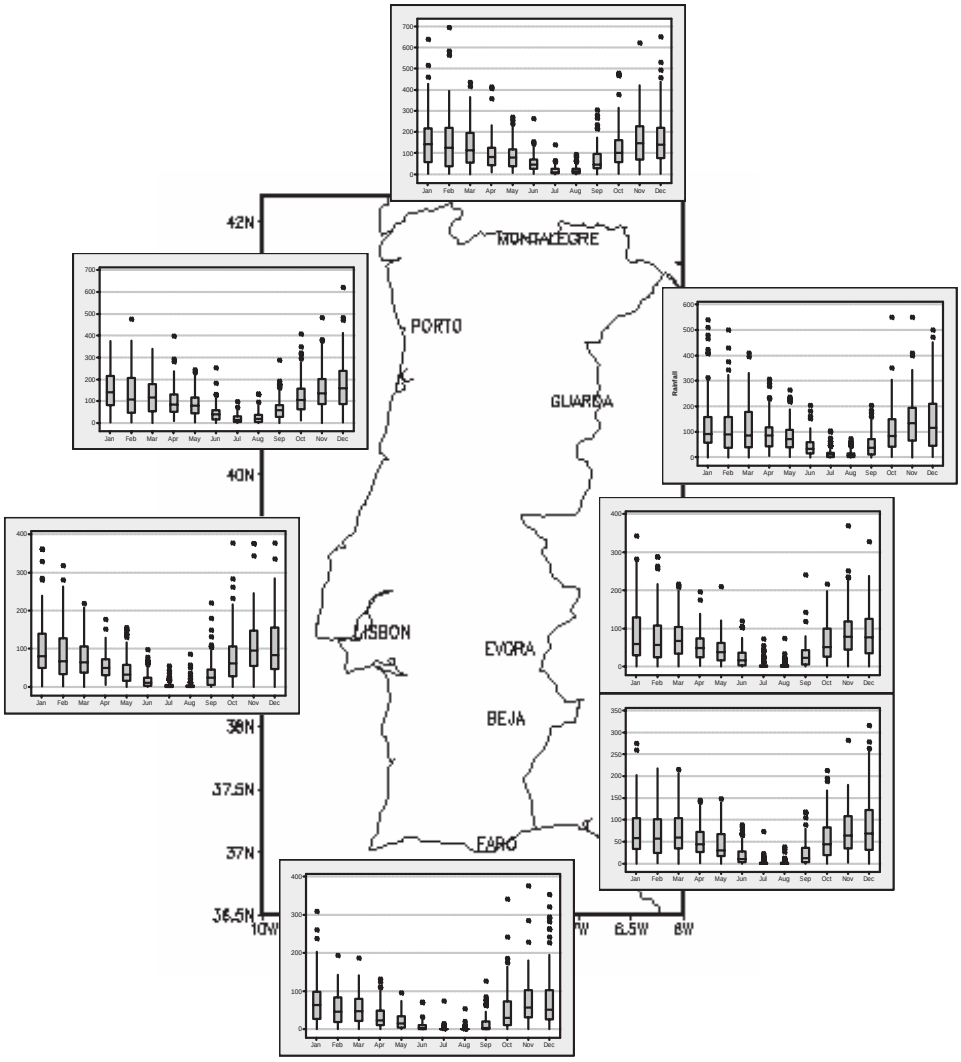

Figure 1. *Map with the geographical locations of the rain-gauge stations (Porto, Montalegre, Guarda, Évora, Beja, Faro and Lisbon) and the monthly (seasonal) regimes, covering the period 1901-2000.*

winter (ONDJFM) precipitation throughout the country; the local and regional processes are not strong enough to weaken these correlations

3. Teleconnections over the West Europe and Oriental North Atlantic Ocean

The Southern Oscillation Index (SOI) is based on the standardized pressure difference between Tahiti and Darwin. The El Niño Southern Oscillation (ENSO) phenomenon is the major cause of year-to-year variations in climate over lower latitudes and one of the most significant causes of global climate change on this timescale. The ENSO is associated with disruption to tropical climates in many regions. The Trans-Niño Index (TNI), which is given by the difference in normalised (1950-79) anomalies of SST between Niño1+2 and Niño4

regions, is used as an optimal description of the character and evolution of El Niño or La Niña. The Pacific Decadal Oscillation (PDO) is a leading index associated to the ENSO phenomenon by taking into account the monthly Sea Surface Temperature (SST) anomalies in the North Pacific Ocean. In effect, to characterize the nature of the ENSO, SST anomalies in different regions of the Pacific is used (Niño1+2: 0-10°S, 90-80°W; Niño3: 5°N-5°S, 150-90°W; Niño4: 5°N-5°S, 160E-150°W; Niño3+4: 5°N-5°S, 170-120°W).

The North Atlantic Oscillation (NAO) is a major disturbance of the atmospheric circulation and climate of the North Atlantic region, linked to a waxing and waning of the dominant middle-latitude westerly wind flow during winter. The NAO index is based on the pressure difference between the Iceland (north) and Azores (south) of the mid-latitude westerly flow. It is, therefore, a measure of the strength of these winds. Strictly, it should only be used for the north hemisphere winter period (DJFM). The NAO exerts a strong influence on year-to-year climate variability and there is evidence of longer-term trends in this phenomenon. It is related to the shorter-term shift between zonal and meridional circulation types that occurs on a day-to-day time scale and is know as the index-cycle.

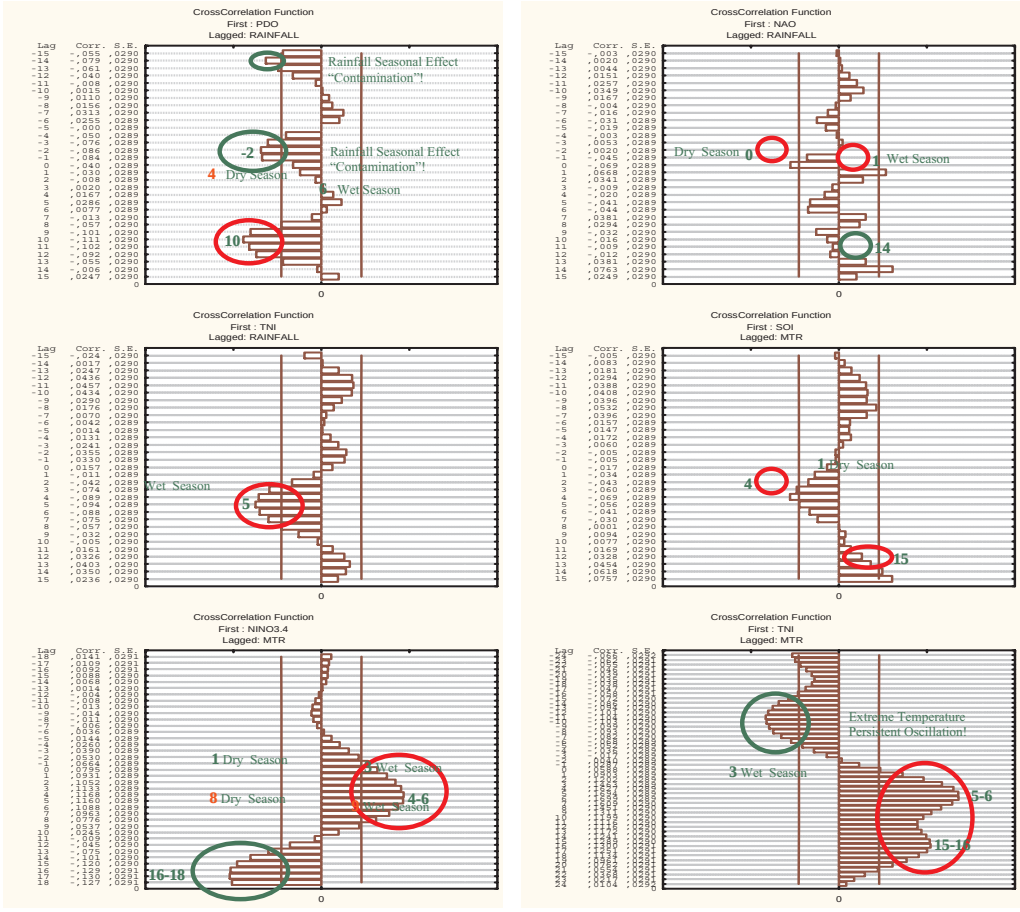

Figure 2. The crosscorrelation diagrams: PDO, NAO, TNI and SOI with the Rainfall over Portugal; Nino3+4 and TNI with the Monthly Range Temperatures (MTR) on the period from Jan/1901 to Dec/2000.

Figure 2 shows the cross-correlation diagrams of PDO, NAO, TNI and SOI with the Rainfall over Portugal; Nino3+4 and TNI with the Monthly Range Temperatures (MTR) on the period from Jan/1901 to Dec/2000.

4. Stochastic Approach

The role of statistics (data analysis) is not so much to summarise what has already happened, but to infer the characteristics of randomness in the process that generated the data set regarding the sequence of its realisations. A useful concept in extracting a physical phenomenon from the data using statistical tools is to consider the superposition of independent statistical approaches and interprets the results as a clearly defined common property.

Simply speaking clustering is an algorithm to classify or to group N objects based on attributes/features into K number of group. The grouping is done by minimizing the "*distances*" between data and the corresponding cluster centroid. Thus the purpose of clustering is to classify the data. There are a lot of applications of the clustering, range from unsupervised learning of neural network, pattern recognitions, classification analysis, artificial intelligent, image processing, machine vision, *etc*. In principle, we have several objects and each object have several attributes and you want to classify the objects based on the attributes, then we can apply this algorithm. The principle of application of clustering to machine learning or data mining: Each object represented by one attribute point is an example to the algorithm and it is assigned automatically to one of the cluster – the "*unsupervised learning*" because the algorithm classifies the object automatically only based on the criteria of minimum distance to the centroid.

The Embedded Compositing method (CL & C) for Clustering and Fuzzy Clustering are different than Hierarchical Clustering and Diversity Selection in that the number of clusters, K, needs to be determined at the onset. The goal is to divide the objects into K clusters such that some metric relative to the centroids of the clusters is minimized. The metric to minimize and the choice of a distance measure will determine the shape of the optimum clusters (global optimization method). Cluster analyses are used to analyze micro array time-course data for pattern recognition. However, in general, these methods do not take advantage of the fact that time is a continuous variable, and existing clustering methods often group weather pattern together.

We propose a CL & C method for identification and classification of weather based on their temporal expression profiles for cyclic time-course micro array data (Figure 3). This method treats time as a continuous variable, therefore preserves actual time information. We applied this method to a micro array time-course study of rainfall expression at time intervals. Six regression patterns have been identified and shown to fit climatological expression profiles better than cluster analysis. CL & C analysis identified over-represented functional groups in each regression pattern and each cluster, which further demonstrated that the regression method provided more climatologically meaningful classifications of weather expression profiles than the clustering method. Consistency study indicates that regression patterns have the highest reliabilities. Our results demonstrate that the proposed CL & C regression method improves pattern recognition for cyclic time-course micro array data.

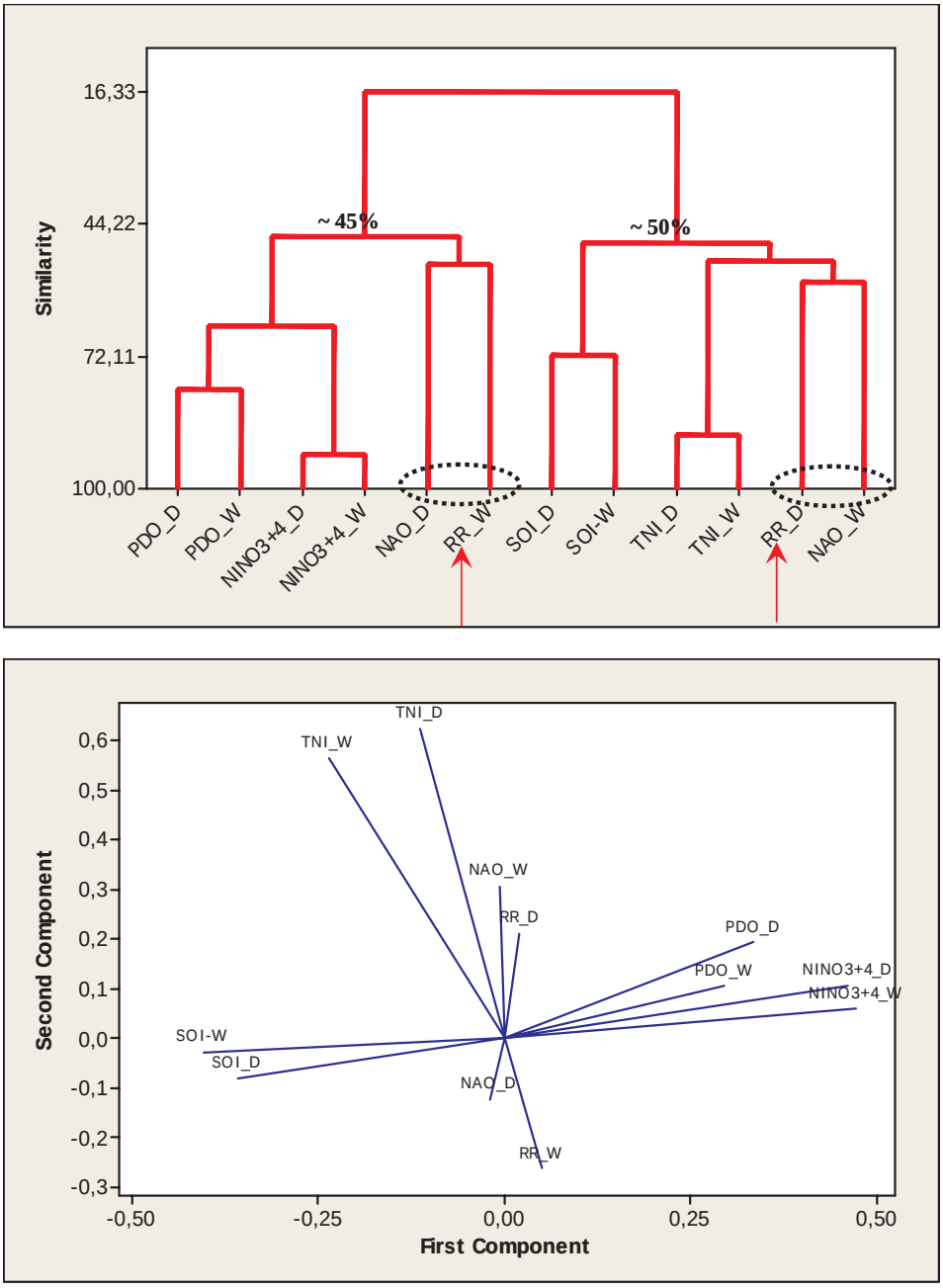

Figure 3. Portuguese Extreme (Seasonal Climate Clustering) Weather Characterization

5. Summary

Our results confirm the importance of the North Atlantic Oscillation (NAO) and the El Nino-Southern Oscillation (ENSO) states; for the variability of Portuguese rainfall, a fact which is imposed by the NAO`s close relationship with humidity advection, cyclone occurrence, and upper air variability. Changes in large-scale atmospheric flow have an important impact on rainfall variability over Portugal, mostly explained by the North Atlantic Oscillation (NAO) and slighted (intriguing) associated with the Pacific Decadal Oscillation (PDO). Then, the *Embedded Compositing Method* seems powerful in the empirical prediction of circulation pattern recognition based on four-to-six fundamental weather systems (Illustration 1 and Illustration 2).

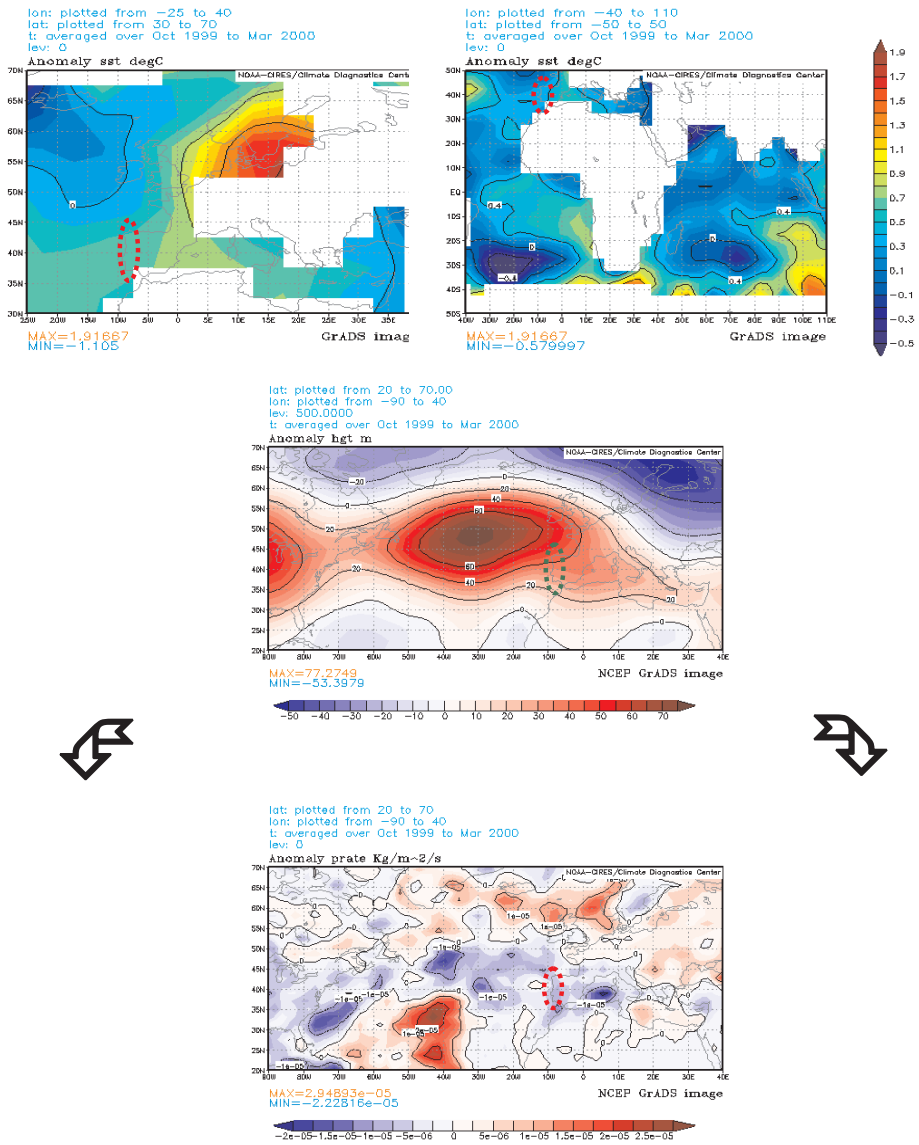

Illustration 1: Dry Rainy Season (1999/2000).

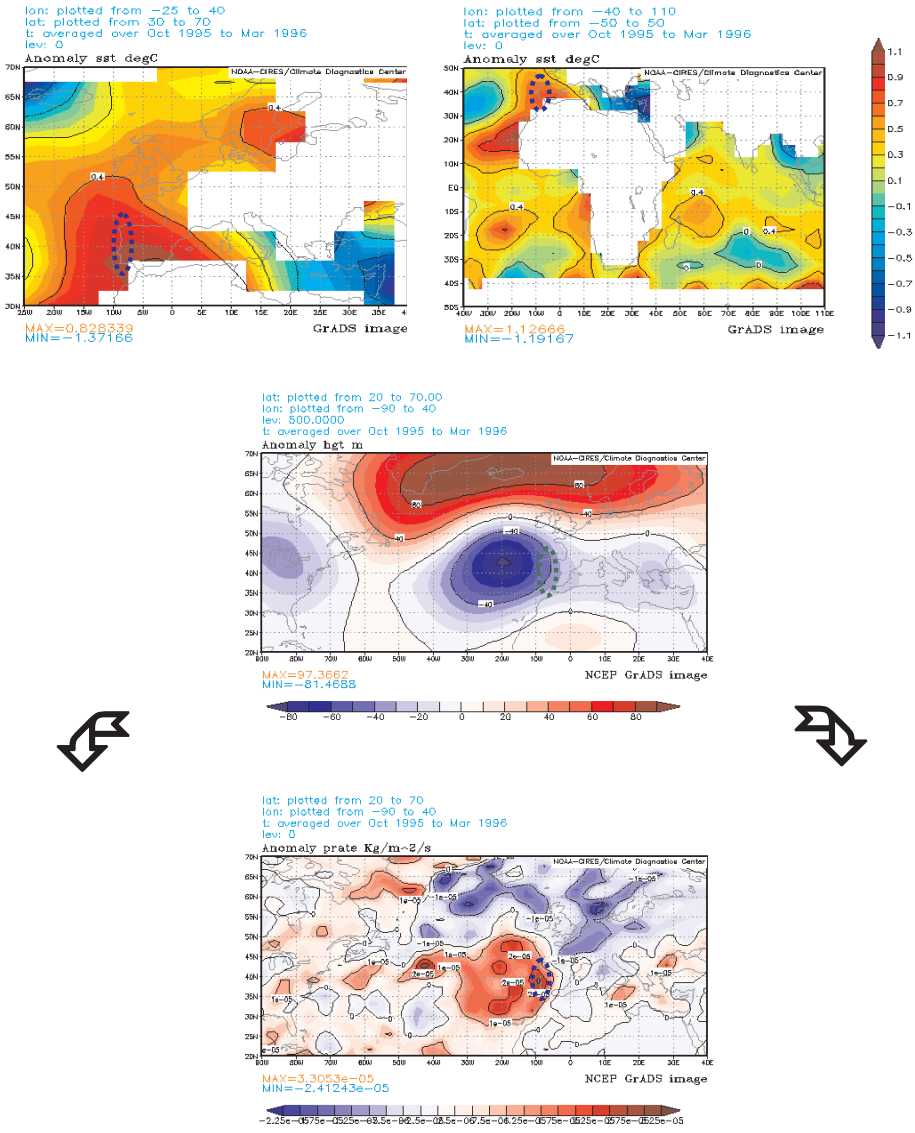

Illustration 2: Wet Rainy Season (1995/1996).

Owing to the strong connection between winter rainfall over Portugal and the large-scale circulation patterns, a keying of the days into a set of non-overlapping large-scale rainfall regimes is particularly meaningful. An information measure was computed so that a maximum discrimination of the rainfall amounts amongst the weather regimes could be achieved. From four-to-six weather regimes were isolated in this manner, and both their statistical and dynamical properties enabled a validation of the clustering strategy. This study also revealed that the frequencies of occurrence of some particular regimes are skilful

predictors of winter rainfall over Portugal. Considering basically the Classification and Discriminant principles, the Embedded Compositing method (CL & C) seems powerful in the empirical prediction of circulation pattern recognition based on four-to-six (4-6, where the maximum discrimination of the rainfall amounts amongst the weather regimes is achieved) fundamental weather systems. Outstanding the strong connection with large circulation system patterns the winter rainfall over Portugal is particular significant. Moreover, the frequency and occurrence of particular regimes are considerable (statistical significant) predictors of winter rainfall over Portugal – maybe a high-quality strategy for the assessment of rainfall scenarios.

References

Barnston, A., Smith, T. M., 1996. Specification and prediction of global surface temperature and precipitation from global SST using CCA. *J. Climate*, 9: 2660–2697.

Bishop, C. M., 1995. *Neural Networks for Pattern Recognition*. Oxford: Oxford University Press.

Briggs, W. M., Wilks, D. S., 1996. Estimating monthly and seasonal distributions of temperature and precipitation using the new CPC long-range forecasts. *J. Climat*e, 9: 818–839.

Fraedrich, K., Muller, K., 1992. Climate anomalies in Europe associated with ENSO extremes. *Int. J. Climatology*, 12: 25–31.

Goodess, C. M., Jones, P. D., 2002. Links between circulation and changes in the characteristics of the Iberian rainfall. *Int. J. Climatology*, 22: 1593–1615.

Hastenrath, S., Greischar, L., 1995. Prediction of the summer rainfall over South Africa. *J. Climate*, 8: 1511–1518.

Hulme M., 1992. A 1951–80 global land precipitation climatology for the evaluation of general circulation models. *Climate Dynamics*, 7: 57–72.

Hulme, M., 1995. Estimating global changes in precipitation. *Weathe*r, 50: 34–42.

Hurrell, J. W., van Loon, H., 1995. Decadal trends in the North Atlantic Oscillation and relationships to regional temperature and precipitation. *6th International Meeting on Statistical Climatolog*y, *Uni*s*ersity Colleg*e, *Galwa*y.185–188.

Hurrell J. W., 1996. Influence of variations in extratropical wintertime teleconnections on Northern Hemisphere temperatures. *Geophysical Research Letters*, 23: 665–668.

Hurrell J. W., van Loon, H., 1997. Decadal variations in climate associated with the North Atlantic oscillation. *Climate Change*, 36: 301–326.

Hurrell JW, Kushnir Y, Visbeck M. 2001. The North Atlantic oscillation. *Science*, 291: 603–605.

Knippertz, P., 2004. A simple identification scheme for upper-level troughs and its application to winter precipitation variability in northwest Africa. *J. Climate*, 17: 1411–1418.

Knippertz, P., Christoph, M., Speth, P., 2003. Long-term precipitation variability in Morocco and the link to the large-scale circulation in recent and future climates. *Meteorology and Atmospheric Physics*, 83: 67–88.

Kutiel, H., Maheras, P. and Guika, S., 1996. Circulation and extreme rainfall conditions in the eastern Mediterranean during the last century. *Int. J. Climatology*, 16: 73–92.

Michelangeli, P., Vautard, R., Legras, B., 1995. Weather regimes: recurrence and quasi-stationarity. *Journal of the Atmospheric Sciences*, 52: 1237–1256.

Muñoz-Dyaz, D., Rodrigo, F. S., 2003. Effects of the North Atlantic oscillation on the probability for climatic categories of local monthly rainfall in southern Spain. *Int. J. Climatology*, 23: 381–397.

Murphy, J., 1999. An evaluation of statistical and dynamical techniques for downscaling local climate. *Int. J. Climatology*, 12: 2256–2284.

Peterson, T., Easterling, D. R., 1994. Creation of homogeneous composite climatological reference series. *Int. J. Climatology*, 14: 671–679.

Osborn, T. J., Briffa, K. R., Tett, S. F. B., Jones, P.D., Trigo, R. M., 1999. Evaluation of the North Atlantic oscillation as simulated by a coupled climate model. *Climate Dynamics*. 15: 685–702.

Pozo-Vázquez, D., Esteban-Parra, M. J., Rodrigo F. S., Castro-Dyez, Y., 2001. A study of NAO variability and its possible non-linear influences on European surface temperature. *Climate Dynamics*, 17: 701–715.

Rasmusson, E. M., Arkin, P. A., 1993. A global view of large-scale precipitation variability. *J. Climat*e, 6: 149–522.

Rocha, A., 1999. Low-frequency variability of seasonal rainfall over Iberian Peninsula and ENSO. *Int. J. Climatology*, 19: 889–901.

Rodo, X., Baert, E., Comin, F., A., 1997. Variations in seasonal rainfall in Southern Europe during the present century: relationships with the North Atlantic Oscillation and the El Niño–Southern Oscillation. *Climate Dy*n., 13: 275–284.

Rodriguez, C., Hernandez, A., Fidalgo, M. R., Garmendia, J., 1992. Statistical method of precipitation prediction. *Atmo*s. *Re*s., 28: 299–309.

Rodriguez-Puebla C., Encinas, A. H., Nieto, S., Garmendia, J., 1998. Spatial and temporal patterns of annual precipitation variability over the Iberian Peninsula. *Int. J. Climatology*, 18: 299–316.

Rogers, J. C., 1997. North Atlantic storm track variability and its association to the North Atlantic oscillation and climate variability of northern Europe. *J. Climate*, 10: 1635–1647.

Romero, R., Sumner, G., Ramis, C., Genovés, A., 1999. A classification of the atmospheric circulation in patterns producing significant daily rainfall in the Spanish Mediterranean area. *Int. J. Climatology*, 19: 765–785.

von Storch, H., 1995. Spatial patterns: EOFs and CCA. *In*: *Analysis of Climate Variability* , Springer-Verlag, Berlin, 227–257.

von Storch, H, Zwiers, F., 1999. *Statistical Analysis in Climate Researc*h. Cambridge University Press: Cambridge.

Sumner G. N., Romero, R., Homar, V., Ramis, C., Alonso, S., Zorita, E., 2003. An estimate of the effects of climate change on the rainfall of Mediterranean Spain by the late twenty first century. *Climate Dynamics*, 20: 789–805.

Trenberth, K. E., Hoar, T. J.: 1996. The 1990–1995 El Niño–Southern Oscillation Event: Longest on Record. *Geophys. Res. Lett.*, 23: 57–60.

Trigo, R. M., da Câmara, C. C., 2000. Circulation weather types and their influence on the precipitation regime in Portugal. *Int. J. Climatology*, 20: 1559–1581.

Ulbrich, U., Cristoph, M., Pinto, J. G., Corte-Real, J., 1999. Dependence of winter precipitation over Portugal on NAO and baroclinic wave activity. *Int. J. Climatology*, 19: 379–390.

Wibig, J., 1999. Precipitation in Europe in relation to circulation patterns at the 500 hPa level. *Int. J. Climatology*, 19: 253–269.

Wilks, D. S., 1996. Statistical significance of long-range optimal climate normal temperature and precipitation forecasts. *J. Climate*, 9: 827–839.

Zorita, E., Kharin, V., von Storch, H., 1992. The atmospheric circulation and sea surface temperature in the North Atlantic area in winter: their interaction and relevance for Iberian precipitation. *J. Climate*, 5: 1097–1108.

Zorita, E., Hughes, J. P., Lettemaier, D. P., von Storch, H., 1995. Stochastic characterization of regional circulation patterns for climate model diagnosis and estimation of local precipitation. *J. Climate*, 8: 1023–1042.

Weather types according to the wind direction in Sfax (Middle East of Tunisia)

S. Dahech. and G. Beltrando
University of Paris VII (Denis Diderot, France. UMR PRODIG du CNRS
salem.dahech@paris7.jussieu.fr, beltrando@paris7.jussieu.fr

Abstract

This paper describes a climatologically study, useful for local forecasting, based on meteorological data of Sfax (middle-east of Tunisia). The weather of each day is characterized by using the daily direction of the vector mean wind. The average of many meteorological parameters is given by wind direction for each season which are identified using clustering methods.

1. Introduction

The majority of weather parameters vary with the wind direction. The sailor as well as the farmer, who live in contact with nature, usually begins their day by looking at the wind direction. Sfax is a coastal city located in Middle-eastern Tunisia (Fig. 1). This agglomeration is characterized by an important industrial activities and high urban density (500 000 habitants). The Mediterranean Sea has a significant impact on the weather and on the climate in this coastal plain. The wind direction (coming from the continent or from the sea) influences other weather parameters like the temperature, the relative humidity and rainfall. The purpose of this paper is to identify daily weather characteristics using the direction of vector mean wind. The averages of some meteorological parameters are given by wind direction for each season. This climatological study can be useful for meteorological forecasting.

2. Data and methods

To define the direction of flows, we use mainly the direction of vector mean wind for the 8 wind diurnal observations. The direction of vector mean wind characterizes the air mass: its temperature, its humidity and its vertical stability. For each direction, the weather parameters are specified. To obtain significant results, the seasonal analysis is necessary for the simple reason: the wind blowing from the west (from the continent) brings heat back in summer but cold in winter. It is important also to study the wind direction stability during the day. The wind directions whose frequency is less than 1% (like the NW in summer) are eliminated from initial data. This study extends over 33 years going from 1970 to 2002 because of the annual variability of the seasonal weather types. The studied parameters are: wind directions frequency in %, average wind velocity in m/s, rainfall (mm), temperatures (°C), relative humidity (%), insolation in hour, average pressure (hPa) and visibility (dm). For each season, we know the characteristics of the air masses brought by each flow and their frequency. Studying the weather parameters variability according to the diurnal wind direction for all the season and during 33 years is relatively long. Thus, we select 4 months, each one represents a season. To identify these months, a season classification according to minimal and maximum temperatures for the periods studied is adopted. Every month is divided into 5-consecutive day period (6 days for the last period of the 31's day-month and 3 or 4 days for that of February). Each year is then divided into 72 periods of 5 days. The maximum and minimal average temperature of each one of these periods is calculated per year and for the 33 years studied. The Agglomerative Hierarchical Clustering (AHC) is the statistical method used for this classification.

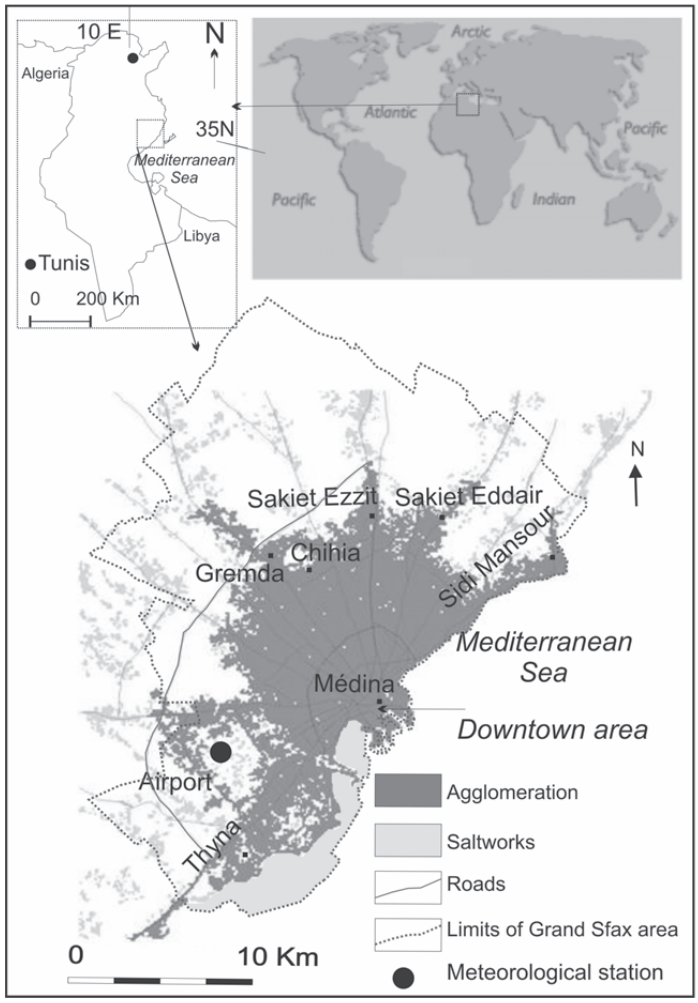

Figure 1: Localisation of Sfax

3. Seasons classification

To classify the seasons, we use the technique of Agglomerative Hierarchical Clustering. The index of similarity used is Euclidean distance and aggregation criterion selected is ward's method. The *Center/Reduce* options were selected to avoid having group creation influenced by scaling effects. Classification results are presented by the dendogram (Fig. 2). It represents how the algorithm works. The dotted line represents the automatic truncation, leading to three groups. The first group is the largest one, it contains the days included between the 1st June and the 15th October and represents the hot season with maximum and minimal temperature respectively between 27.2 and 33.2°C and 17.8 and 22°C. The second group extends over two periods, the first lies between the 16th October (16.2°C, 26°C) and the 20th November (10.7°C, 21.2°C), the second between the 21st March (9.3°C, 20.9°C) and 31st May (15.9°C, 26.15°C). Obviously, between these two periods, we find the third group characterized by an apparently strong homogeneity. It's the cold season where the maximum and minimal temperatures recline between 19.2 and 19.3 °C and between 8.3 and 8°C.

The seasons classification varies from one year to other according to the temperatures (maximum and minimal). Thus, the summer can be longer and in certain cases the winter comes earlier as it is shown in the two following figures presenting the same type of classification for the years 1970 and 1994.

According to the dendrograms below which show the seasons division and the fluctuation in Sfax, we can distinguish 4 months each one represents one season, October for the autumn, January for the winter, July for the summer, and April for spring. The daily weather characteristics using the direction of victor mean wind will be studied only during these months.

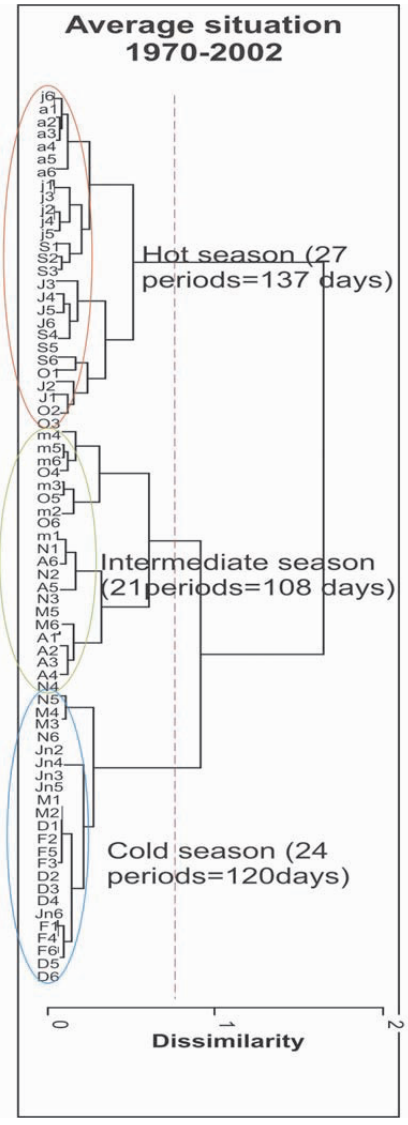

Figure 2: Agglomerative Hierarchical Clustering of seasons between, 1970 and 2002. (Jn1=The First five days of January; F2= the second five days of February…)

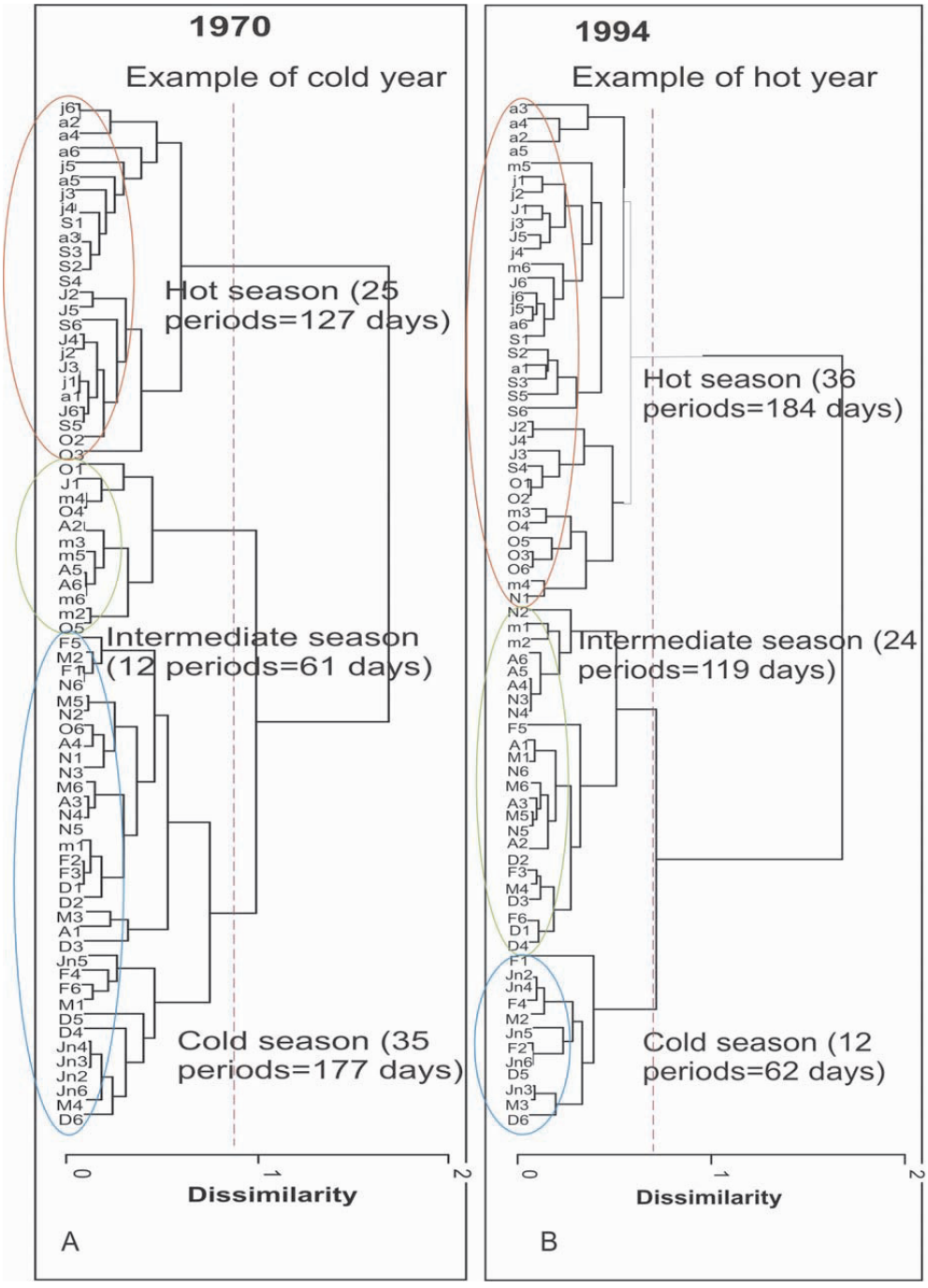

Figure 3: Agglomerative Hierarchical Clustering of seasons in 1970 (A) and in 1994 (B)(Jn1=The First five days of January; F2= the second five days of February…)

4. Weather types according to the wind direction

The results obtained are assembled in table showing the weather parameters distribution per month and by wind direction (Tab. 1). As it is seen below, each line corresponds to a wind direction. For every parameter and for each month we find on a column the daily averages by wind direction. The table shows the general climatological characters in Sfax, for example in winter (January), by western flow, the minimal temperature average is the weakest (4.5°C), the same parameter reaches its maximum (23.2) in July by a SSW flow.

This table is converted in wind roses and every seasonal value is materialized by a polygon. This type of chart is well adapted to visualize a great number of values (Wisdorff et al 1999).

4.1 Wind direction frequency

Figure 4 shows that during July, the flows coming from the sea (eastern sectors) dominate. However, during January, flows coming from the land are most frequent (western sectors). In summer sea breeze dominates (80% in July, Dahech 2005), but in winter the North Westerns wind dominates according to the general circulation in middle latitudes. During April and october, the situation is transitional, we find the eastern and the western flows but the former are still more considerable.

Table 1: Distribution of the principal weather parameters per season and wind direction in Sfax (1970-2002)[v: average wind speed (m/s); a: amplitude, t: minimal temperature (°C), T: maximal temperature (°C); h: minimal relative humidity (%); H: maximal relative humidity(%); f:wind directions frequency in %;p: pressure (hPa); I: insolation in hour; v: minimal visibility (dm); r: rainfall (mm); ts: Ground temperature (°C)].

October	v	at	ah	i	ats	p	v	r	h	t	H	T	f
N	3,7	7,5	39,3	6,7	14,3	1011,1	666,7	2,7	51,2	16,2	90,5	23,7	11,1
NNE	3,6	9,3	46,3	7,1	14,6	1013,3	680,0	1,3	41,0	17,3	87,3	26,6	7,8
NE	3,5	8,1	35,8	10,3	11,9	1014,9	675,0	7.4	50,8	18,6	86,5	26,7	5,8
ENE	3,1	7,4	42,5	7,8	14,4	1014,0	694,4	23.8	47,2	16,8	89,7	24,2	4,9
E	3,3	8,1	33,5	6,6	14,4	1014,6	587,5	1,6	55,8	19,9	89,3	28,0	11,2
ESE	3,0	8,0	31,2	8,1	14,1	1013,7	686,1	0,1	57,5	19,4	88,7	27,4	5,7
SE	2,7	9,1	39,0	8,4	13,8	1014,8	479,4	2,7	53,3	18,7	92,3	27,8	6,0
SSE	2,4	10,0	38,0	8,8	12,4	1013,9	626,7	0,1	52,8	17,8	90,8	27,8	5,9
S	2,8	11,1	49,8	8,9	14,3	1014,9	563,9	1,4	39,8	18,7	89,7	29,8	4,7
SSW	2,9	12,9	59,4	10,3	15,0	1014,4	613,9	0,0	30,6	17,0	90,0	29,9	4,3
SW	3,0	13,4	62,2	11,2	15,1	1010,1	725,0	0,0	31,8	17,8	94,0	31,2	3,4
WSW	3,6	14,8	61,2	6,7	18,5	1009,4	550,0	2,7	18,8	17,2	80,0	31,9	3,8
W	2,3	13,7	53,0	5,8	18,9	1012,6	750,0	0,0	26,7	13,2	79,7	26,8	6,2
WNW	3,1	9,6	42,3	7,4	17,3	1012,5	780,0	0,9	42,3	15,9	84,5	25,5	4,5
NW	3,9	9,9	49,0	6,6	14,6	1009,3	691,7	0,0	39,3	16,1	88,3	25,9	7,0
NNW	3,1	9,7	46,2	9,9	16,2	1010,6	608,3	1,1	42,2	15,7	88,3	25,3	8,0

Table 1 continued…..

July	v	at	ah	i	ats	p	v	r	h	t	H	T	f
N	4,0	12,9	40,0	12,2	25,1	1014,5	900,0	0,0	34,0	19.2	74,0	29,7	7,4
NNE	5,8	11,0	44,9	9,5	17,5	1008,2	800,0	0,0	39,5	21,0	84,4	32,0	9,4
NE	5,3	10,7	42,3	9,4	15,7	1011.1	905,9	0,0	33,0	21,7	75,3	32,5	7,0
ENE	5,3	9,8	43,5	10,7	19,6	1010,6	860,0	0,0	33,5	22,2	77,0	32,0	7,0
E	4,1	10,2	46,8	10,0	16,9	1012,2	940,0	0,5	33,0	21,5	79,8	31,8	19,6
ESE	3,1	11,0	47,9	11,6	17,0	1012,2	855,0	0,0	35,5	20,9	83,4	32,0	12,4
SE	2,9	12,0	43,6	11,7	21,1	1013,5	920,8	0,0	38,0	20,4	81,6	32,4	11,0
SSE	2,7	11,8	33,5	10,6	18,9	1012,0	910,0	0,0	46,5	20,4	80,0	32,1	10,6
S	2,8	14,3	52,3	11,8	20,1	1011,8	950,0	0,0	26,5	22,5	78,8	36,8	5,2
SSW	3,5	13,9	57,3	11,3	19,8	1011,1	890,0	0,0	21,0	23,2	78,3	37,1	1,6
SW													0,6
WSW													0,5
W													1,0
WNW													1,2
NW	3,8	10,0	53,3	11,2	18,8	1012,1	890,0	0,1	25,0	22,0	78,3	32,0	2,1
NNW	3,9	9,9	52,4	11,1	19,0	1012,2	900,0	0,2	26,0	22,3	78,4	32,2	3,2
April	**v**	**at**	**ah**	**i**	**ats**	**p**	**v**	**r**	**h**	**t**	**H**	**T**	**f**
N	4,8	9,3	50,5	8,4	16,8	1009,1	834,0	0,7	33,8	10,8	84,3	20,0	11,2
NNE	5,0	9,5	48,0	10,2	19,6	1014,0	933,3	0,2	32,5	11,7	80,5	21,2	7,2
NE	4,0	8,7	41,3	6,7	14,7	1010,4	686,3	4,6	48,2	12,9	89,5	21,6	6,8
ENE	3,9	10,1	50,7	9,5	18,0	1010,3	836,1	0,0	37,8	12,7	88,5	22,8	6,2
E	3,1	9,8	46,8	8,3	17,9	1010,2	655,1	9,5	43,0	11,8	89,8	21,6	13,8
ESE	3,0	10,3	46,2	9,3	16,2	1010,6	654,0	1,0	43,8	11,1	90,0	21,4	6,5
SE	3,3	10,0	46,2	9,5	18,9	1011,7	620,0	0,0	42,0	9,7	88,2	21,2	5,9
SSE	2,8	11,9	49,0	8,9	19,3	1014,3	577,5	0,1	41,0	9,6	90,0	21,5	7,4
S	3,2	13,7	62,0	9,6	20,8	1012,1	637,6	0,1	28,7	11.3	90,7	25,0	5,8
SSW	3,1	13,0	59,3	9,9	21,4	1009,4	902,3	1,0	26,3	11,1	85,7	24,0	2,9
SW	3,6	15,4	67,0	11,3	25,4	1010,3	900,0	0,0	23,5	11,5	90,5	26,9	2,4
WSW	4,6	17,9	74,4	9,3	18,0	1008,2	436,7	0,1	15,6	11,6	90,0	29,5	2,1
W	3,5	10,6	59,3	8,1	20,6	1009,8	675,0	1,2	31,0	11,1	90,3	21,8	5,6
WNW	4,4	10,6	51,8	6,9	21,5	1008,5	907,6	0,0	28,4	9,3	80,2	19,9	4,3
NW	4,9	12,6	56,7	7,6	21,9	1009,8	661,5	1,4	27,2	8,4	83,8	21,0	5,7
NNW	4,3	10,5	44,2	8,7	20,6	1009,2	708,0	2,6	33,4	10,1	77,6	20,7	6,3
January	**v**	**at**	**ah**	**i**	**ats**	**p**	**v**	**r**	**h**	**t**	**H**	**T**	**f**
N	3,4	8,4	38,3	5,7	12,5	1020,0	558,4	18,2	54,3	7,0	92,6	15,4	8,5
NNE	2,7	8,3	38,1	4,3	16,3	1022,9	722,2	2,3	55,3	7,3	93,4	15,6	3,5
NE	3,0	8,9	38,8	6,2	14,9	1021,3	630,0	3,7	54,5	6,8	93,3	15,6	1,6
ENE	5,0	7,7	29,3	1,9	7,7	1024,6	500,0	14,3	57	7,7	94,0	15,4	1,5
E	3,3	10,6	34,4	4,9	16,0	1021,9	351,7	2,7	58,6	5,6	93,0	16,2	2,5
ESE	2,4	10,6	40,8	6,1	15,8	1019,5	533,8	1,1	50,9	5,7	91,7	16,3	1,5
SE	3,4	7,3	44,7	5,7	14,7	1021,5	424,0	0,0	49	9,7	92,7	17,0	1,4
SSE	2,5	8,3	44,5	5,4	15,9	1017,2	367,5	0,6	45,3	8,4	89,8	16,7	2,1
S	1,8	13,2	50,3	7,6	21,6	1022,8	463,0	0,0	40,0	5,7	90,3	18,9	4,0
SSW	2,8	11,1	45,7	5,5	16,4	1018,8	586,3	0,3	44,8	5,6	90,5	16,7	7,8
SW	3,0	12,4	45,4	7,1	17,1	1019,1	642,9	0,4	37,8	6,3	83,1	18,7	10,2
WSW	2,8	13,7	49,8	7,2	19,3	1018,9	601,4	0,0	32,8	4,5	82,6	18,2	11,0
W	4,0	12,0	43,5	7,9	16,1	1015,9	692,4	0,7	41,8	6,0	85,3	18,0	16,4
WNW	3,7	10,6	44,6	7,5	16,8	1017,0	777,2	0,8	76,9	5,6	85,3	16,2	8,1
NW	4,2	9,2	47,0	6,0	19,3	1018,1	589,5	0,8	37,7	5,9	84,7	15,1	11,1
NNW	4,0	9,3	45,3	6,1	15,6	1019,3	655,7	0,2	42,9	6,5	88,3	15,8	8,8

4.2. Wind speed

The strongest winds come from the NNE and the NE in July, from the N and the W in January, April and October (synoptic wind). The winds coming from the sectors ranging between east and the south are usually weak, its average velocity does not exceed 3.5m/s, it represents the sea breeze situation. We notice that the wind speed is stronger in April than in October for all directions (Fig. 5).

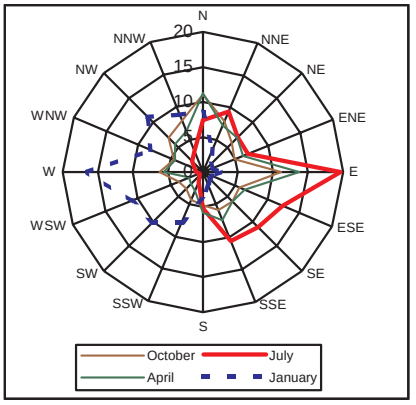

Figure 4. Frequency of the situations observed for each class of wind direction (%) in Sfax (1970-2002)

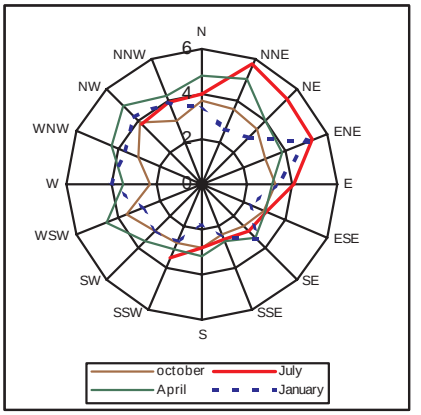

Figure 5. the wind average velocity (m/s) according to the wind direction, each polygon corresponds to a month representinga season. Sfax (1970-2002)

4.3. Temperature according to the wind direction

The highest maximum temperatures are observed when the wind comes from the Southern sectors (from Sahara) for the four months, particularly in summer (37°C). But, the northern winds are the less warm ones (Fig. 6 A). The highest minimal temperatures are observed when the wind blows from the sea (NNE → SSW) (Fig. 6 B). Consequently the great thermals amplitudes are observed by land wind. October is hotter than April but the later is characterized by more important thermal amplitudes, during this month the sky is most limpid (Fig. 6 C).

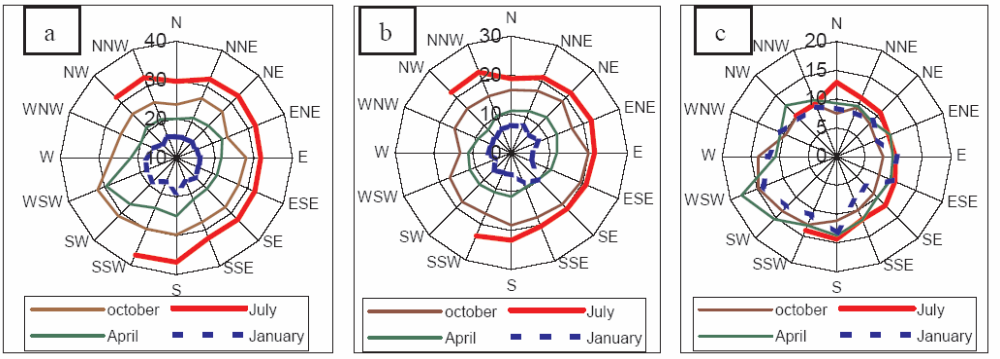

Figure 6. The maximal, minimal temperatures (a and b) and thermal amplitude (c) according to the wind direction, each polygon corresponds to a month representing a season. Sfax (1970-2002)

4.4. Relative humidity according to the wind direction

The winds blowing from the sea are the wettest. The highest relative humidity rates are recorded in January and October by a wind coming from the eastern sectors (90%) (Fig. 7 A). Since the temperatures and humidity "evolve contrarily", it is reliable that the two thermal and hygrometric amplitude roses having the same form. Thus we observe maximum humidity amplitude by a land wind in the spring (70% by WSW wind) (fig.7 C).

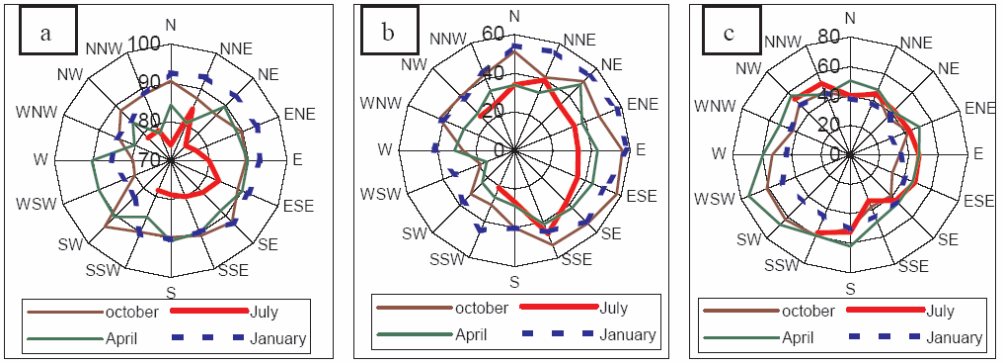

Figure 7 : The maximal, minimal humidity (a et b) and hygrometric amplitude (c) according to the wind direction, each polygon corresponds to a month representing a season. Sfax (1970-2002)

4.5. Rainfall according to the wind direction

The Figure 8 shows that the most abundant rainfalls occur in October by ENE wind, it is the same fact in April and January. These precipitations are related to "return from east situations". For instance, these weather situations caused, in October 1982, 233 mm during just two days at Sfax (Hénia et Melki, 2000). We notice some rainfalls in January and in October by N and NW wind; these situations are caused by the polar perturbations. In July, precipitations are exceptional; they do not exceed 1mm on average, because of the domination of the Azores anticyclone on western Mediterranean basin.

4.6. Atmospheric pressure, insolation, and visibility according to the wind direction

The high pressures dominate in January. The lowest pressures are recorded by NW wind. It is by there that the strong winds blow. Generally, in every month, the atmospheric pressure is higher than 1010hPa (Fig.9 a). In July the Atlantic anticyclone dominates, but the Saharian and continental European ones are more frequent in January (Hénia, 1998). The insolation is related to the sunshine duration which decreases from July to October to April to January. The highest values are recorded by wind coming from southern (Fig.9 b) sectors. However the lowest ones are recorded by NW winds, these flows convey more clouds. It is the same fact for the visibility (Fig.9 c).

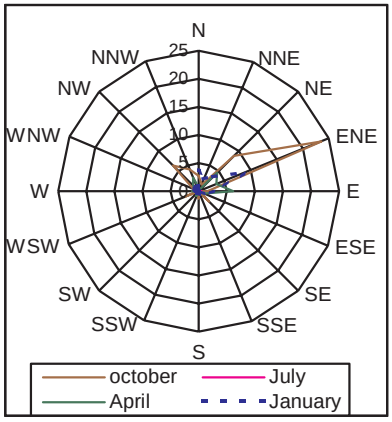

Figure 8. Rainfall according to the wind direction, each polygon corresponds to a month representing a season. Sfax (1970-2002)

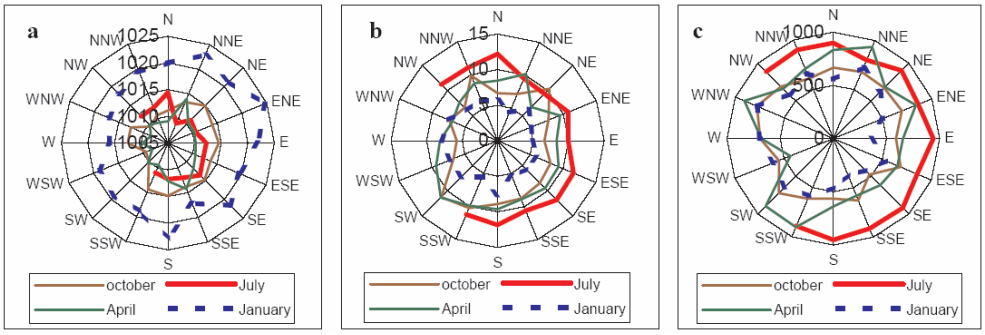

Figure 9. Atmospheric pressure in hPa (a), insolation in hours, and visibility (dm) according to the wind direction, each polygon corresponds to a month representing a season. Sfax (1970-2002)

5. Conclusion

This study permits to understand the general proprieties of Sfax climatology. It gives interesting information for the forecasters. Indeed, knowing what usually occurs for each season and by all the wind direction can contribute to preview the weather type. In particular, flows direction can be identified earlier than one day by the digital models of weather forecasting. It would be interesting to extend the method to the other regions of the country and use other weather parameters.

References

Dahech S. and Beltrando G. 2005: Sea-land breeze circulation and atmospheric pollution in Sfax. *Geophysical Research Abstracts*, Vol. 7, 00085, 2005.

Hénia.L. 1998: Les situations anticycloniques en Tunisie. *Publications de l'Association Internationale de Climatologie*, Vol. 11, 1998. 166-174.

Hénia. L et Melki. T 200 : Circulation de « Retour d'Est » et pluies diluviennes sur la Tunisie orientale. *Publications de l'Association Internationale de Climatologie*, Vol. 13, 2000. 121-127.

Wisdorff. D ; Beucher. F; Salvayre. L; Thoumieux.F et Douerin.j.p. 1999 : Climatologie saisonnière de la Charente- Maritime par classes de direction de vent. *La météorologie* 8ème série-n° 25.29-37.

The CaliM&Ro Project: Calibration of Met&Roll Weather Generator for sites without or with incomplete meteorological observations

Martin Dubrovsky[(1)], Ladislav Metelka[(2)], Daniela Semeradova[(3)], Miroslav Trnka[(3)], Olga Halasova[(2)], Martin Ruzicka[(4)], Ivana Nemesova[(1)], Stanislava Kliegrova[(2)], Zdenek Zalud[(3)]

[(1)] Institute of Atmospheric Physics ASCR, Prague, Czechia (dub@ufa.cas.cz)
[(2)] Czech Hydrometeorological Institute, Hradec Kralove, Czechia
[(3)] Institute of Landscape Ecology MAFU, Brno, Czechia
[(4)] Institute for Hydrodynamics ASCR, Prague, Czechia

Abstract.

The main aim of the 3-year (2005-2007) CaliM&Ro project (www.ufa.cas.cz/dub/calimaro/calimaro.htm) is interpolation of the single-site four-variable stochastic daily weather generator (WG) Met&Roll. The paper gives the sample results obtained during the first year of the project. The experiments are based on daily weather series from 45 Czech stations. WG parameters are interpolated using the nearest neighbours method with accounting for the effect of the altitude. Observed weather series and synthetic weather series produced by site-calibrated and interpolated WGs are (a) analysed in terms of the frequency of heat waves and cold waves, and (b) fed into the WOFOST crop growth model with model crop yields being analysed thereafter. Two validation tests are made: (a) Performance of WG is validated by comparing characteristics (heat and cold wave frequencies and the model crop yields) obtained with the site-calibrated WG with those obtained with observed weather series. (b) Performance of the interpolation method is assessed by comparing characteristics obtained with the interpolated WG with those obtained with the site-calibrated WG.

1. Introduction

Stochastic weather generators (WGs) are used to produce observed-like synthetic weather series, which may serve as an input to various weather-dependent models (e.g. crop models [Dubrovsky et al., 2000; Zalud and Dubrovsky, 2002; Trnka et al., 2004a, 2004b] and rainfall-runoff models [Buchtele et al., 1999]). Typically, WGs are used in assessing sensitivity of the modelled processes to variability and changes in climatic characteristics. CaliM&Ro project (2005−2007) focuses on calibrating a stochastic single-site four-variables daily weather generator Met&Roll for sites with non-existent or incomplete historical daily weather series (these are normally used to determine WG parameters). To calibrate WG for the ungauged location, WG parameters may be interpolated from the surrounding stations. In our project, we test applicability of various interpolation techniques, including common methods implemented in GIS (with a stress put on co-kriging), neural networks and nearest neighbours. The performance of the interpolation techniques is examined in three ways: (A) Assessment of accuracy of interpolation of individual WG parameters (= comparison of the interpolated WG parameters with those derived from the site-specific observed weather series). (B) Comparison of the climatic characteristics derived from synthetic series produced

by the interpolated *vs.* site-calibrated WGs (interpolated WG = WG, whose parameters were interpolated; site-calibrated WG = WG, whose parameters were derived from the site-specific observed weather series). (C) Comparison of outputs from the crop growth models and rainfall-runoff models fed by synthetic series produced by interpolated *vs.* site-calibrated generators. In approach B, the weather series will be compared in terms of various climatic characteristics, including means, variability and extremes. In approach C, several crop growth models (WOFOST, CERES, STICS) and hydrological model SAC-SMA will be used. The experiments should show, what is the effect of the errors involved in WG interpolation process on the climatic characteristics derived from the synthetic weather series and on the output from the impact models fed by these series. In addition, the characteristics obtained using the synthetic weather series will be compared with those obtained with the observed series. Ideally, stochastic structure of observed and synthetic weather series should be the same.

The present paper brings the first results of the project. Nearest neighbours interpolator is used, and its performance is assessed in terms of heat and cold waves and wheat yields simulated by the WOFOST crop growth model.

2. Data and Methodology

Observed weather data

The present analysis is based on 40-year daily weather series from 45 Czech stations (Fig. 1). The series consist of daily temperature extremes (*TMAX* and *TMIN*), daily precipitation amount (*PREC*) and daily sums of global solar radiation (*SRAD*). The former three variables are observed values, *SRAD* values have been estimated from the sunshine duration using the Angstrom-Prescott formula (Trnka et al., 2005).

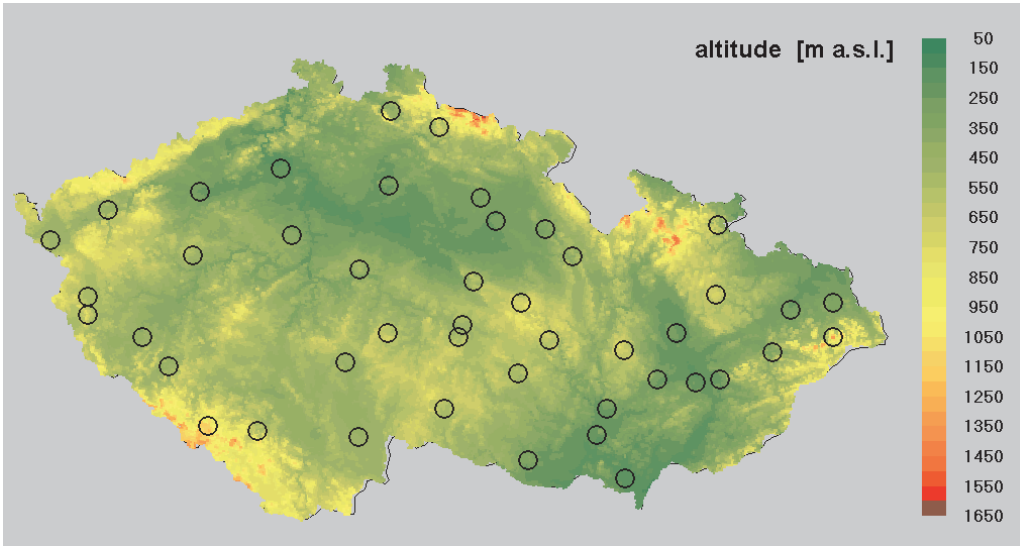

Figure 1 *Topography of Czechia and location of the 45 stations used in the analysis.*

Met&Roll weather generator

Met&Roll is a parametric daily WG (Dubrovsky, 1997; Dubrovsky et al., 2004). It uses Markov chain (order = 1 to 3) to model precipitation occurrence, Gamma distribution to model precipitation amount and first-order autoregressive model to model solar radiation and daily extreme temperatures. Daily generator may be optionally conditioned on the monthly generator (Dubrovsky et al., 2004) which generates monthly means of the four variables using the 1st order autoregressive model. Parameters of the generator are allowed to exhibit annual cycle. Met&Roll is used mainly to provide synthetic series for crop growth model simulations – both in present and changed climates. It is also used to provide weather series for the hydrological SAC-SMA model (Buchtele et al., 1999). Met&Roll was also validated by Huth et al. (2001, 2003) and Kysely and Dubrovsky (2005) in terms of the extreme temperature characteristics.

Interpolation

In this paper, we focus on the nearest neighbours interpolator. The interpolated value is defined as a weighted average of values related to the surrounding stations. The bell-shaped weight function and corrections for the zonal, meridional, and altitudinal trends are taken into account during the interpolation of WG parameter:

$$Y^{\wedge}(\lambda,\varphi,z) = \sum_{i=1..K} [Y_i + a.(\lambda-\lambda_i) + b.(\varphi-\varphi_i) + c.(z-z_i)] \times w_i(\lambda,\varphi,z) \qquad (1)$$

where

- $Y^{\wedge}(\lambda,\varphi,z)$ is an interpolated value
- Y_i is a value of the parameter derived from the i-th station's weather series
- λ, φ, and z are longitude, latitude and altitude
- $w_i(\lambda,\varphi,z)$ is a bell-shaped weight function accounting for the distance $d_i(\lambda,\varphi,z)$ between the i-th station and the station defined by $[\lambda,\varphi,z]$ coordinates:
  $w_i(\lambda,\varphi,z) = [1 - (d_i(\lambda,\varphi,z)/D)^3]^3$ for $d_i(\lambda,\varphi,z) < D$
  $w_i(\lambda,\varphi,z) = 0$ for $d_i(\lambda,\varphi,z) \geq D$
- a, b, c are parameters of a tri-variate linear regression model ($Y = a.\lambda + b.\varphi + c.z + d$), which are estimated using data from all available stations (except for the one, for which we interpolate – during the cross-validation test)
- D defines the surroundings of the location for which we interpolate. The value of D is a subject of optimisation. We found, that D~100 km provides optimal results in the present experiment.

To show the importance of accounting for the altitude effect, we will also use simpler interpolator, which differs from the previous one by neglecting effect of altitude: in that case c is set to zero in eq.(1) and a and b are determined using bi-variate regression with λ and φ being independent variables. The two interpolators will be referred to as WG_{xy} and WG_{xyz} (Table 1).

Experiment

1. In the first step, all WG parameters are derived for the 45 stations.
2. The WG parameters are interpolated for each of the 45 stations using data from the remaining 44 stations. Each parameter is interpolated independently of the others, using both interpolation approaches: with/without altitude effect.
3. 40-year synthetic series are generated using site-calibrated WG (thus producing WG_0 series) and interpolated WGs (producing WG_{xy} and WG_{xyz} series).

Table 1 Types of weather series used in the present experiments.

acronym	weather series
OBS	observed weather series
WG_0	synthetic series produced by WG calibrated with the site-specific observed data
WG_{xy}	synthetic series produced by WG, whose parameters were interpolated (not accounting for the effect of altitude)
WG_{xyz}	synthetic series produced by WG, whose parameters were interpolated (accounting for the effect of altitude)

4. The four weather series (OBS, WG_0, WG_{xy} and WG_{xyz}) available for each station are analysed in terms of the heat and cold waves. The heat wave (Huth et al., 2000) is defined here as the longest continuous period (i) during which the maximum daily temperature reached at least T_{H1} in at least three days, (ii) whose mean maximum daily temperature was at least T_{H1}, and (iii) during which the maximum daily temperature did not drop below T_{H2}. The threshold temperatures T_{H1} and T_{H2} are set to 30 and 25ºC, respectively. Similarly, the cold wave is defined as the longest continuous period (i) during which the minimum daily temperature dropped to or below T_{C1} in at least three days, (ii) whose mean minimum daily temperature was T_{C1} or lower, and (iii) during which the minimum daily temperature did not exceed T_{C2}. T_{C1} and T_{C2} thresholds are set to −12 and −5ºC, respectively.
5. The four weather series are fed into the WOFOST model to simulate wheat yields. Note that the WOFOST model is used here as a "black box" which transforms weather series and site-specific information (cultivar characteristics, field attributes, soil characteristics, planting details, management factors) into the crop yields. The site-specific information is the same for all 45 stations. Although the latter setting is not realistic, it is justifiable in our experiment, which aims to validate the WG and the interpolation method.

3. Results

The station-specific frequencies of the heat and cold waves derived from the four weather series are displayed in Figures 2 and 3, respectively; the mean crop yields simulated by WOFOST crop growth model fed by the four types of the weather series are shown in figure 4. The displayed characteristics obtained using various input weather series are compared graphically in Figure 5, and quantitatively in Table 2 in terms of three measures: Mean Bias Error (*MBE*), Root Mean Square Error (*RMSE*) and Reduction of Variance (*RV*), all being expressed in percents:

$$MBE = 100\times\{\mathrm{AVG}(y_i - y_{i,\mathrm{ref}}) / \mathrm{AVG}(y_{i,\mathrm{ref}})\}$$

$$RMSE = 100\times\{[\mathrm{AVG}(y_i - y_{i,\mathrm{ref}})^2]^{1/2} / \mathrm{AVG}(y_{i,\mathrm{ref}})\}$$

$$RV = 100\times\{1 - \mathrm{AVG}(y_i - y_{i,\mathrm{ref}})^2 / \mathrm{AVG}[\mathrm{AVG}(y_{i,\mathrm{ref}}) - y_{i,\mathrm{ref}}]^2\}$$

where

y_i = characteristic of the i-th station (tested weather series is used)
$y_{i,\mathrm{ref}}$ = characteristic of the i-th station (reference weather series is used)
AVG = average of the characteristic across the set of 45 stations

The perfect fit between the two samples would be indicated by $MBE = 0$, $RMSE = 0$ and $RV = 100$.

Having results related to the four different weather series, we focus on two comparisons: (i) WG_0 *vs*. OBS, and (ii) WG_{xy} *vs*. WG_0 and WG_{xyz} *vs*. WG_0. (Note that *X*-axis is used for WG_0 characteristics in Figure 5, as WG_0 plays a role in both comparison tests). In the former test (panel B *vs*. panel A in Figures 2-4) the differences are due to the imperfections of WG.

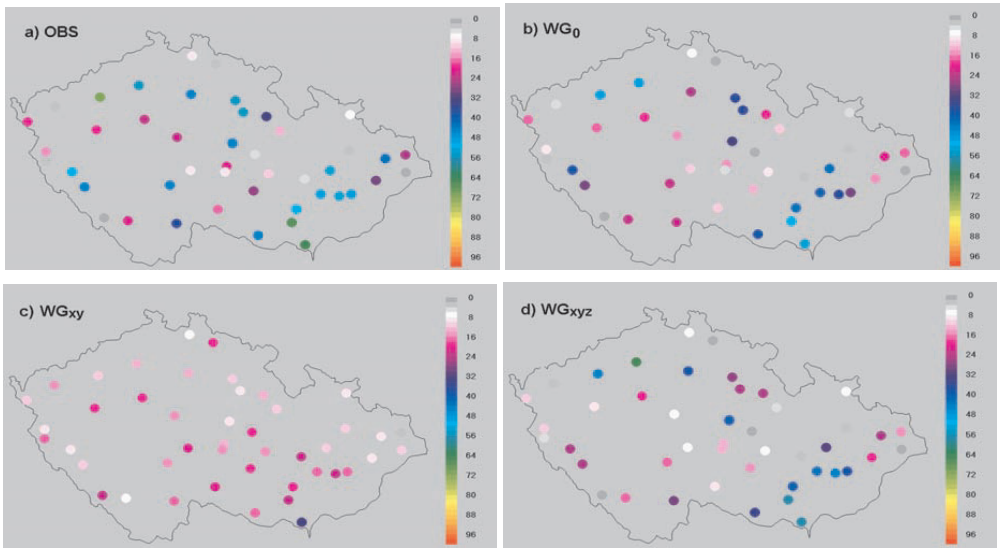

Figure 2 *Number of heat waves in the 40-year weather series of four types (see Table 1 for specifications of the weather series).*

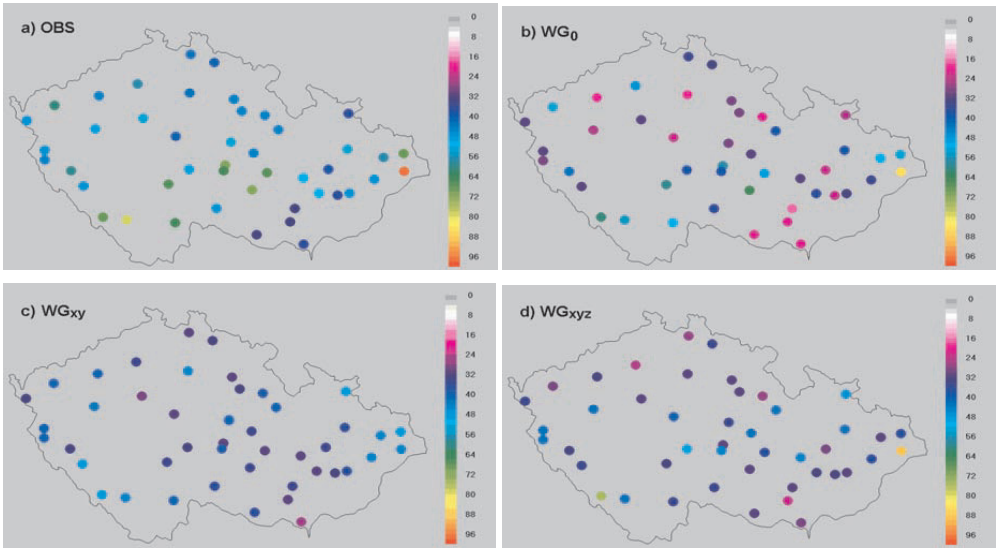

Figure 3 *The same as previous figure but for the frequency of cold waves.*

Ideally, the climatic characteristics should be the same in both observed weather series and weather series produced by the site-calibrated weather generator, except for the deviations due to stochasticity of the generator. In case of the perfect fit, the grey circles in Figure should follow the 1:1 line. In the latter test (compare panels C *vs.* B and D *vs.* B in Figures 2-4), results obtained with the interpolated generator are compared with those obtained with the site-calibrated generator. In this case, the differences show how the interpolation imperfections affect results obtained with the synthetic weather series. The perfect fit, which would be indicated by triangles lying on 1:1 line in Figure 5, would mean that the interpolation error is either zero or it does not affect results obtained with the interpolated generator. Altogether, in case of the perfect performance of WG and interpolator, the mean characteristics obtained with observed weather series, synthetic series produced by site-calibrated weather generator, and synthetic series produced by the interpolated generator should be the same. In reality, however, the results obtained by individual weather series differ. Figures 2-5 together with Table 2 show:

Table 2. Comparison of characteristics (number of heat waves, number of cold waves, and wheat yields simulated by WOFOST crop growth model) obtained with the four weather series (see Table 1 for specifications) in terms of mean bias error (*MBE*), root mean square error (*RMSE*) and reduction of variance (*RV*).

input weather series	with respect to OBS			with respect to WG_0		
	MBE[%]	*RMSE*[%]	*RV*[%]	*MBE*[%]	*RMSE*[%]	*RV*[%]
a) frequency of heat waves						
WG_0	-29	38	71			
WG_{xy}	-52	90	-61	-32	84	-28
WG_{xyz}	-29	43	64	-1	32	82
b) frequency of cold waves						
WG_0	-29	31	-47			
WG_{xy}	-28	37	-113	2	39	2
WG_{xyz}	-28	37	-112	1	37	12
c) model wheat yields						
WG_0	3	5	79			
WG_{xy}	7	13	-46	4	12	-8
WG_{xyz}	3	8	43	1	7	58

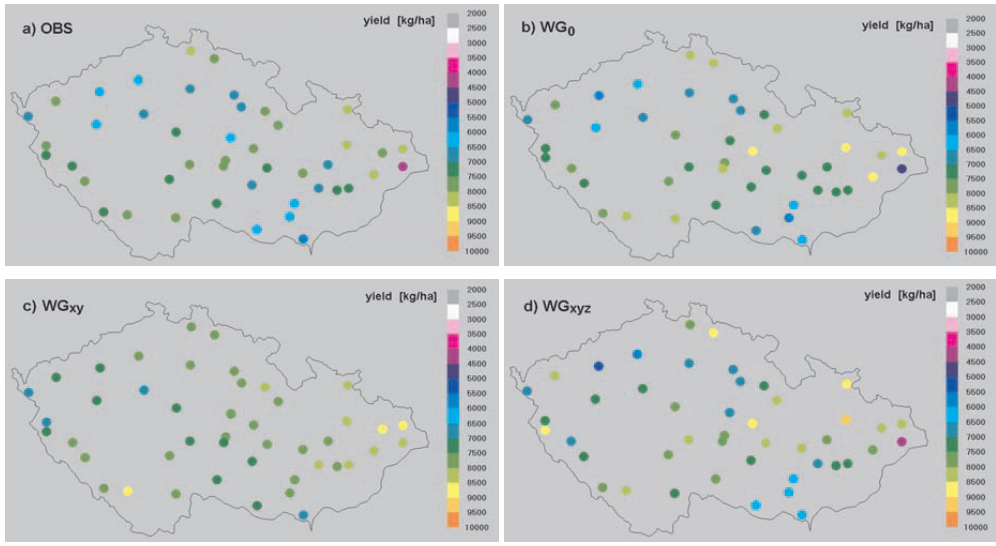

Figure 4 *Mean 39-year crop yields simulated by WOFOST crop growth model using the same weather series as those employed in Figures 2 and 3.*

a) Observed weather series vs. site-calibrated WG

- Weather generator reproduces heat waves better than the cold waves (indicated by *RV* values in Table 2). However, frequencies of both heat waves and cold waves are underestimated by the generator (indicated by negative values of *MBE* in WG_0 *vs.* OBS comparison).
- The good fit between mean model yields obtained with OBS and WG_0 weather series (indicated by low values of *MBE* and *RMSE* and high value of *RV* in WG_0 *vs*. OBS comparison) suggest applicability of WG in crop modelling: WOFOST model does not exhibit sensitivity to WG imperfections.

b) Site-calibrated vs. interpolated WGs

- The interpolator, which does not account for the altitude effect, fails. This is seen in figures (panels C *vs.* B in Figures 2-4; empty triangles in Figure) and indicated by low values of *RV* in WG_{xy} *vs.* WG_0 comparison.
- In accounting for the altitude effect, frequencies of heat waves in the weather series produced by the interpolated generator (WG_{xyz} series) are comparable with those found in weather series produced by the site-calibrated generator. The values of *RMSE* indicate that the error due to interpolation (*RMSE*(WG_{xyz} *vs.* WG_0) = 32%) is slightly lower than the error due to weather generator imperfections (*RMSE*(WG_0 *vs.* OBS) = 38%).
- Cold waves are poorly reproduced by the interpolated generator.
- Errors due to WG interpolation affect the model yields to a greater extent than the WG imperfections (*RMSE*(WG_{xyz} *vs.* WG_0) = 7%; *RMSE*(WG_0 *vs.* OBS) = 5%).

a)

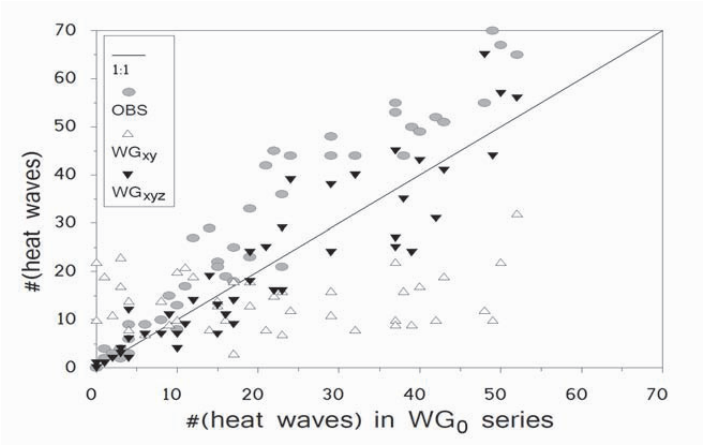

b)

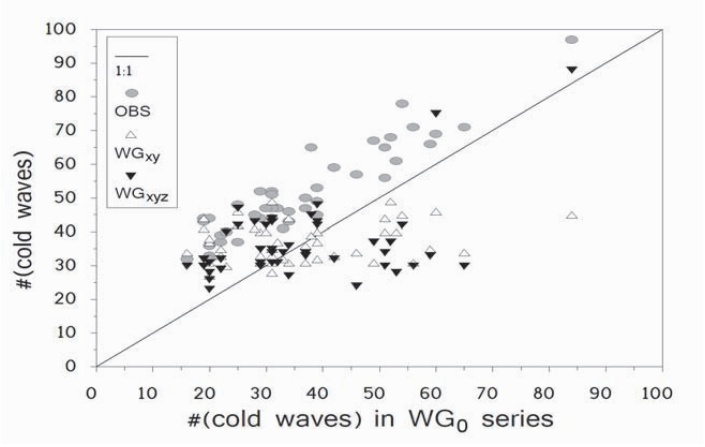

c)

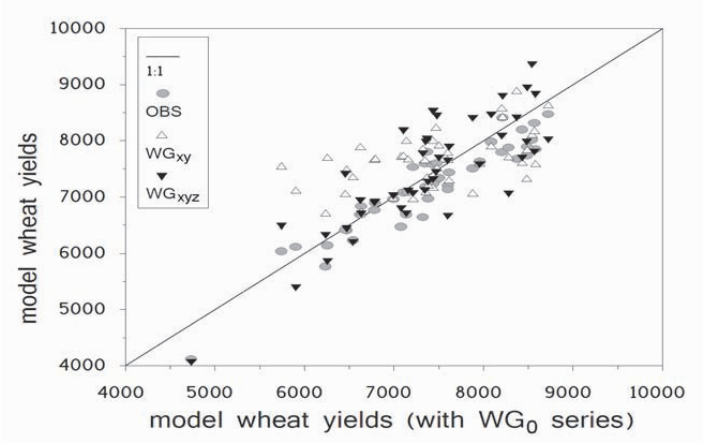

Figure 5 *Comparison of the station-specific (45 stations) characteristics obtained with the four types of weather series: a) number of heat waves, b) number of cold waves, c) wheat yields simulated by WOFOST crop growth model. (WG_0 series is used as a reference).*

4. Conclusions

The results shown in this paper originate from the experiments made in the first year (2005) of the CaliM&Ro project. These have shown that the interpolated WG performs reasonably well for some climatic characteristics (heat waves, in our case) as well as for the wheat yields modelled by WOFOST crop model. The new experiments, which follow the first ones, are now being made using updated experiment settings:

(i) 125 Czech stations with observed daily weather series are now available.
(ii) More interpolation techniques is tested (including co-kriging and neural networks).
(iii) More impact models (crop growth models and rainfall-runoff models) are fed by the observed and synthetic weather series.
(iv) More characteristics (mean, variability, extremes) will be employed in validating WG and interpolators. In addition, statistical significance of differences between results obtained with different weather series will be assessed.

Acknowledgement: CaliM&Ro project is supported by the Grant Agency of the Czech Republic, project 205/05/2265.

References

Buchtele J., Buchtelova M., Fortova, M., Dubrovsky M., 1999: Runoff changes in Czech river Basins - the outputs of rainfall - runoff simulations using different climate change scenarios. *Journal of Hydrology and Hydromechanics* **47**, 180-194.

Dubrovsky M., 1997: Creating Daily Weather Series With Use of the Weather Generator. *Environmetrics* **8**, 409-424.

Dubrovsky M., Zalud Z. and Stastna M., 2000: Sensitivity of CERES-Maize yields to statistical structure of daily weather series. *Climatic Change* **46**, 447- 472.

Dubrovsky M., Buchtele J., Zalud Z., 2004: High-Frequency and Low-Frequency Variability in Stochastic Daily Weather Generator and Its Effect on Agricultural and Hydrologic Modelling. *Climatic Change* **63**, 145-179.

Huth R., Kysely J., Pokorna L., 2000: A GCM simulation of heatwaves, dry spells, and their relationships to circulation. *Climatic Change* **46**, 29–60.

Huth R., Kysely J., Dubrovsky M., 2001: Time structure of observed, GCM-simulated, downscaled, and stochastically generated daily temperature series. *Journal of Climate* **14**, 4047-4061.

Huth R., Kysely J., Dubrovsky M., 2003: Simulation of Surface Air Temperature by GCMs, Statistical Downscaling and Weather Generator: Higher-Order Statistical Moments. *Studia Geophysica et Geodaetica* **47**, 203-216.

Kysely J., Dubrovsky M., 2005: Simulation of extreme temperature events by a stochastic weather generator: effects of interdiurnal and interannual variability reproduction. *Int.J.Climatol.* **25**, 251-269.

Trnka M., Dubrovsky M., Semeradova D., Zalud Z., 2004: Projections of uncertainties in climate change scenarios into expected winter wheat yields. *Theoretical and Applied Climatology* **77**, 229-249.

Trnka M., Dubrovsky M., Zalud Z., 2004: Climate Change Impacts and Adaptation Strategies in Spring Barley Production in the Czech Republic. *Climatic Change* **64**, 227-255.

Trnka M., Zalud Z., Eitzinger J., Dubrovsky M., 2005: Global solar radiation in Central European lowland estimated by various empirical formulae. *Agricultural and Forest Meteorology* **131**, 54-76.

Zalud Z., Dubrovsky M., 2002: Modelling climate change impacts on maize growth and development in the Czech Republic. *Theoretical and Applied Climatology* **72**, 85-102.

Weather type and wave height distribution changes in Tyrrhenian and Adriatic basins

G. De Chiara, A. Crisci , F.P. Vaccari, G. Maracchi

Institute of Biometeorology, Florence, Italy, (g.dechiara@ibimet.cnr.it / Phone: +390553033711)

Abstract

The automated classification scheme, developed by Jenkinson and Collison (1977), has been used to characterize the daily circulation pattern over the Italian area and in particular over the Tyrrhenian and Adriatic seas between the 1953 and 2003. The results in terms of circulation type and direction have been then compared with the wind and sea wave direction. An analysis of extreme wind speed and wave height events compared with the circulation type has also been made.

Weather types classification, in particular condition, can be representative of the local situation.

1. Introduction

The atmospheric circulation variability plays an important role in regional and local climate. An alternative way to describe climate variability, with respect to classical time series trend analysis, is the weather type approach. Using an adequate classification method, it is possible to recognize a specific daily circulation pattern in order to identify the most representative weather types in the Mediterranean basin. Furthermore it is possible to investigate changes in circulation patterns, in occurrence and persistence in the last decades. These phenomena have led to significant changes in many surface parameters, such as wave height distribution.

Different studies (Conway *et al*, 1998) have analysed the relationship between the weather type circulation and local climate conditions showing a connection between each other.

In this study the relationships between different circulation patterns and the local marine and atmospheric conditions (such as local wind and wave height) in the Tyrrhenian and Adriatic Basins have been investigated.

An objective classification scheme, developed by Jenkinson and Collison, based on the subjective Lamb Weather type classification over the British Isles, has been used. The Jenkinson classification uses daily grid-point sea level pressure data to characterize the daily circulation pattern (Jones *et al*.,1993; Goodess, 2000) in terms of type and direction of surface circulation. The direction of the surface circulation has been, then, compared with the direction of local winds and sea wave propagation to understand the connection between the synoptic classification and the local conditions. Furthermore an analysis of extreme wind speed and wave height with the different weather types has been made.

2. Circulation pattern classification

The Jenkinson and Collison (1977) method is an automated version of the Lamb weather type catalogue initially developed for the British Isles. The Jenkinson and Collison classification, chosen for its computational simplicity, is based on a single atmospheric variable, the Sea Level Pressure (SLP). With this method, using daily sea level pressure, it is possible to calculate the daily geostrophic flow and the vorticity over an area (Dessouky *et al*, 1975). By comparison between these two parameters, the type and direction of the daily surface circulation are obtained (Jones *et al*, 1993).
Daily gridded SLP data (2.5° x 2.5°) from NCEP-NCAR were used for the period 1959-2003 over a 52-point grid defined from 32.5°N to 47.5°N and from 5°W to 22.5° W (Fig.1).

The Jenkinson and Collison method considers 26 circulation types such as the 8 directional types, the cyclonic and anticyclonic types, the hybrid type (Cyclonic and Anticyclonic) and the unclassified types (Trigo *et al*., 2000). Only 10 basic circulation types have been considered in this study, as first approach:

- 8 directional types (N, NE, E, SE, S, SW, W, NW);
- Cyclonic type;
- Anticyclonic type.

3. Circulation pattern and local climate comparison

The relationship between weather types and local meteorological and marine conditions are then examined by means of the following data:

- Daily wind data from 1959 to 2003 of two meteorological stations located in Ponza, (an island placed in the middle of the Tyrrhenian Basin) and Bari (situated along the coast of the lower Adriatic basin) (Fig.1);
- Daily sea wave data from 1989 to 2003 of two buoys of the Sea Wave Measurement Network (Rete Ondametrica Nazionale – RON) located offshore the cities of Ponza and Bari (Fig.1).

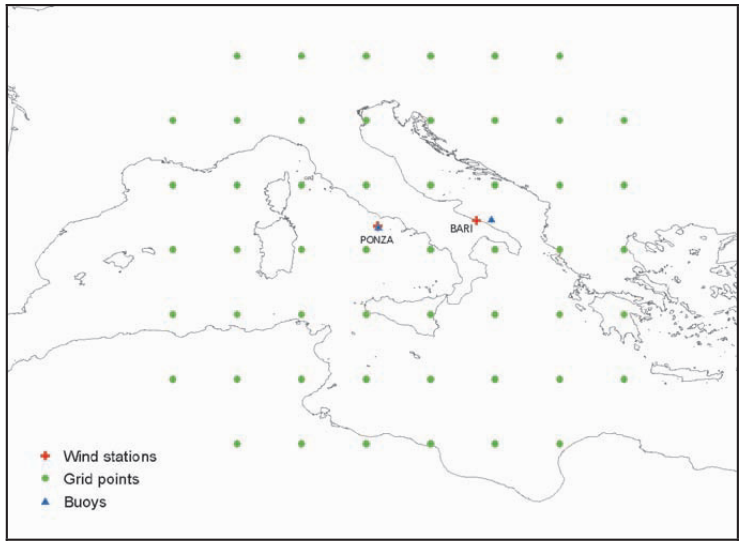

Figure 1. *SLP gridded data (in green), Buoy stations (blue) and Wind stations (in red).*

At first, for each directional circulation pattern, the daily wind and wave directions have been compared with the daily surface circulation direction (only for the 8 directional weather types) using the confusion matrix (a matrix plot which shows the frequency of occurrence of two variables). For each day of the analyzed period, the local wind direction (and the local wave direction), and the 8 directional synoptic circulation correspondences are shown. In an ideal case, in which for each days the two directions would be the same, all data should be along the diagonal. Disagreement to the principal diagonal represents a spreading of the two variables.

The first study based on Ponza winter wind data (1959 - 2003) shows there is a small dispersion from the principal diagonal (Fig.2); it means that there is a quite good agreement between local wind direction and directional circulation pattern. Wave analysis (from 1989 to 2003) shows a weaker agreement than the wind analysis.

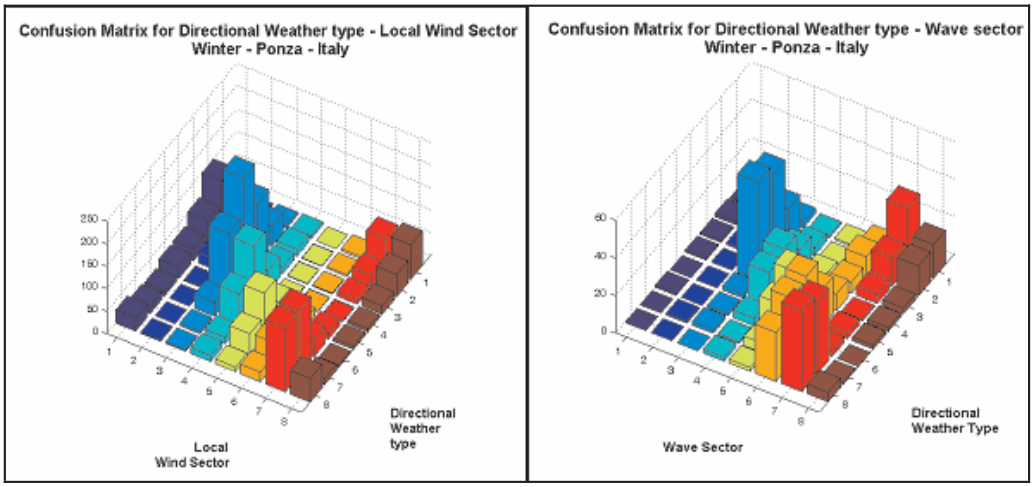

Figure 2. *Confusion matrix for winter season - Ponza*

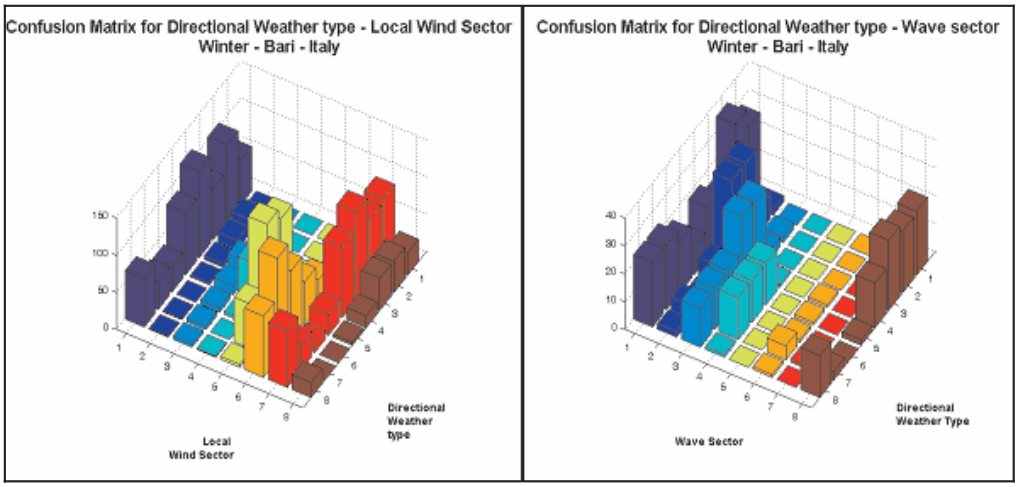

Figure 3.*: Confusion matrix for winter season – Bari*

The same investigation based on Bari winter data (Fig.3) reveals a poor agreement between the circulation pattern and both wind and wave directions. In particular, the southerly, south-westerly and westerly circulations are not captured by wave direction; the north-easterly, easterly and south-easterly circulations are not characterized by wind directions. The bigger circulation-wave disagreement for Bari with respect to Ponza could be caused by the presence of the Italian coast which poses stronger constrain for the air and sea fluxes as compared to the small Ponza Island.

Analysis repeated for spring season data reveal less agreement than the winter ones.

Further analysis has been carried out to verify the correlation between the wind direction distribution and the wave height distribution for each weather type classification. In this way it is possible to verify the wind direction influence on the wave height for different circulation patterns. In particular, a linear-circular correlation between them has been calculated for each season. The results show a relationship between Bari wind direction and wave height which

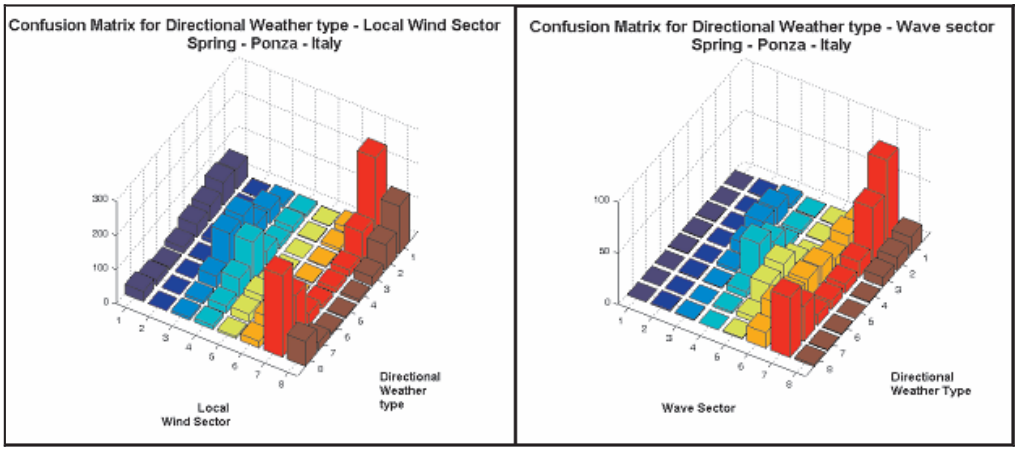

Figure 4. *Confusion matrix for spring season - Ponza*

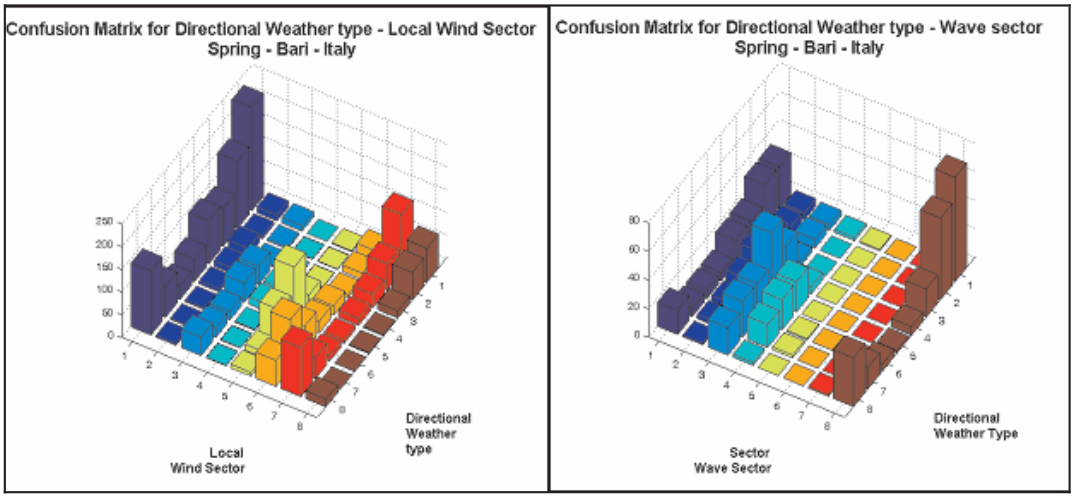

Figure 5. *Confusion matrix for spring season – Bari*

Table 1 Linear – circular correlation between wave height and the wind direction

	WINTER		SPRING		SUMMER		AUTUMN	
CWT	Bari	Ponza	Bari	Ponza	Bari	Ponza	Bari	Ponza
N	N	***Y***	***Y***	***Y***	***Y***	***Y***	N	***Y***
NE	N	***Y***	N	***Y***	***Y***	***Y***	N	***Y***
E	N	***Y***	N	***Y***	***Y***	***Y***	N	***Y***
SE	N	***Y***	***Y***	***Y***	N	***Y***	N	***Y***
S	N	***Y***	***Y***	***Y***	***Y***	***Y***	N	***Y***
SW	***Y***	***Y***	N	***Y***	N	***Y***	N	***Y***
W	***Y***	***Y***	N	***Y***	***Y***	***Y***	***Y***	***Y***
NW	N	***Y***	N	***Y***	N	***Y***	N	***Y***
C	N	***Y***	***Y***	***Y***	***Y***	***Y***	N	***Y***
A	***Y***	***Y***	***Y***	***Y***	N	***Y***	N	N

depends on the season and the circulation pattern. In fact there is a significant correlation (Tab.1) only for specific circulation patterns in each season. For the Ponza dataset wave height distribution and wind direction always show a significant correlation.

4. Analysis of extreme events

A typical statistical approach for hydrological extreme events has been used to analyze the relationship between synoptic and local climate. For each weather type circulation, a Generalized Extreme Value distribution function has been applied to the maximum wave height (recorded in days characterized by that specific circulation pattern). A Weibull distribution function has been applied for the maximum daily local wind speed, for each circulation pattern.

The analysis of winter season data of Ponza station (Fig.6) shows that both for wave height and wind speed the most extreme events (characterized by more vertical distributions curve) are forced by directional weather type from North, South-West, West and North-West, which are the directions characterized by the greatest fetch (the longest wind path without obstacles) for Ponza station. This means that local sea state and meteorological extreme conditions agree with the synoptic conditions.

The same analysis for Bari winter data (Fig. 7) shows that both wind speed and wave height are forced by directional weather types from North and North-East, the direction with the greatest fetch for western lower Adriatic sea. Highest wave heights occur also with southerly and easterly circulation whereas strongest wind speeds occur also with south-westerly circulation type.

Analysis repeated for summer season for the same sites reveal less agreement between wave height and wind speed response to the circulation types with respect to the winter season. In fact, the summer analysis for Ponza (Fig. 8) shows that extreme wind speed and wave height are both forced by a westerly circulation. Wind speed also from northerly and north-westerly circulation; wave height from south-westerly, north-easterly and cyclonic circulation.

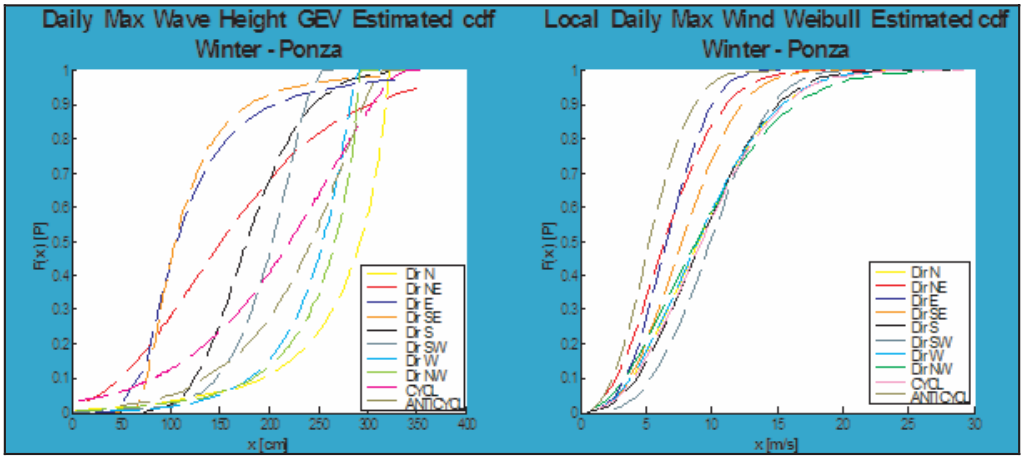

Figure 6. *Ponza – winter: Daily Maximum Wave Height GEV distribution; Daily maximum wind speed Weibull distribution.*

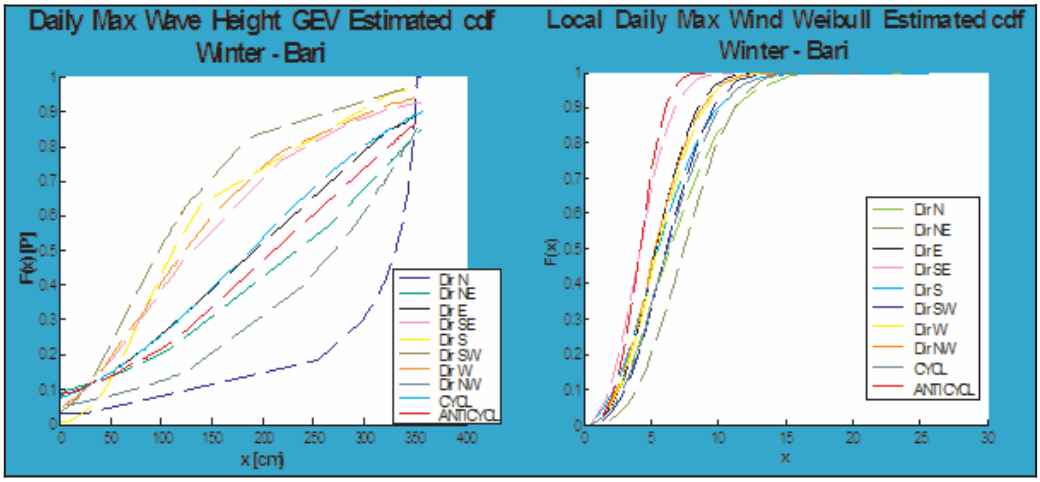

Figure 7. *Bari – winter: Daily Maximum Wave Height GEV distribution and Daily maximum wind speed Weibull distribution.*

Results for Bari summer analysis (Fig. 9) reveal that both extreme wave height and wind speed are forced by a north-westerly circulation. Wave height also from northerly and north-easterly circulation; wind speed from easterly, westerly and cyclonic circulation.

5. Trends in circulation weather type frequency

The analysis of the trend in daily circulation pattern frequency for the period 1959 to 2003 show an increase in the number of days with cyclonic circulation in spring and summer season and a corresponding decrease in the number of days with Anticyclonic circulation.

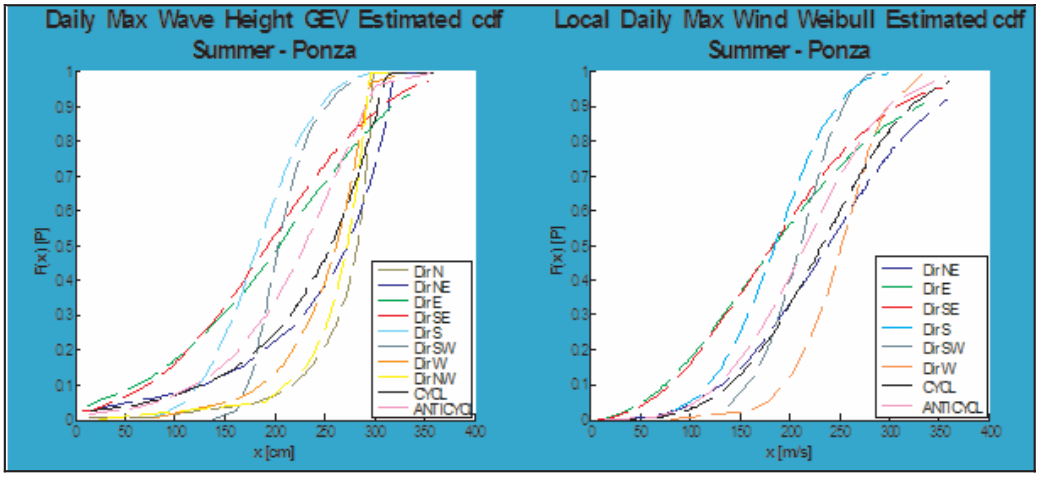

Figure 8. *Ponza – summer: Daily Maximum Wave Height GEV distribution and Daily maximum wind speed Weibull distribution.*

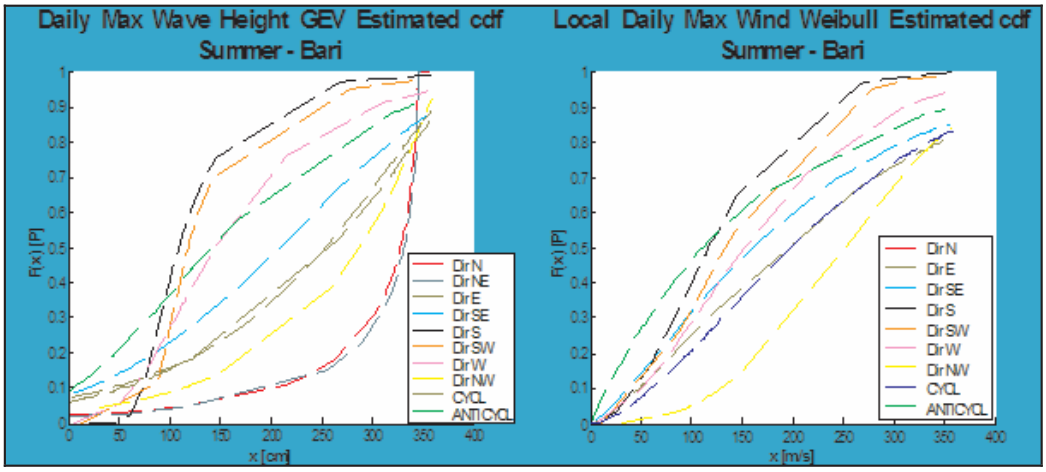

Figure 9. *Bari – summer: Daily Maximum Wave Height GEV distribution and Daily maximum wind speed Weibull distribution.*

6. Results and discussion

An analysis of a possible relationship between synoptic circulation and local climate has been presented. The aim of the study was to evaluate if a synoptic circulation pattern classification could be representative of meteorological and marine conditions.

A weather type classification developed by Jenkinson and Collison has been used to describe the daily weather types over the Italian area in the period 1959 - 2003. Daily circulation characterization has been compared with local wind and wave direction. Also statistical analysis of extreme winds and waves has been performed as well as an examination of frequency trends of different circulation types.

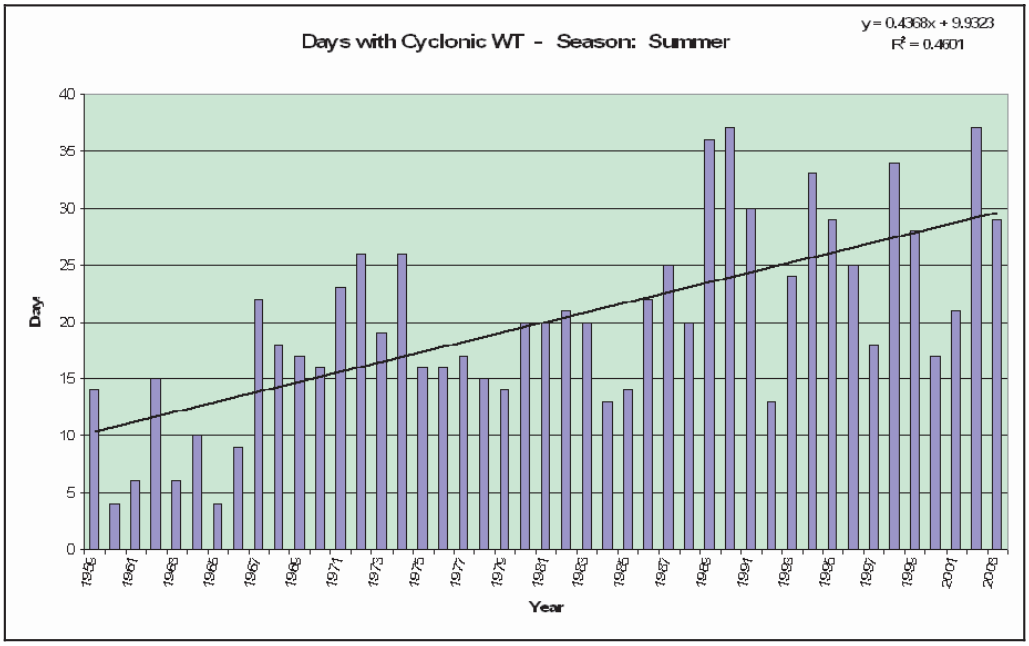

Figure 10. *Trend of cyclonic days in summer season*

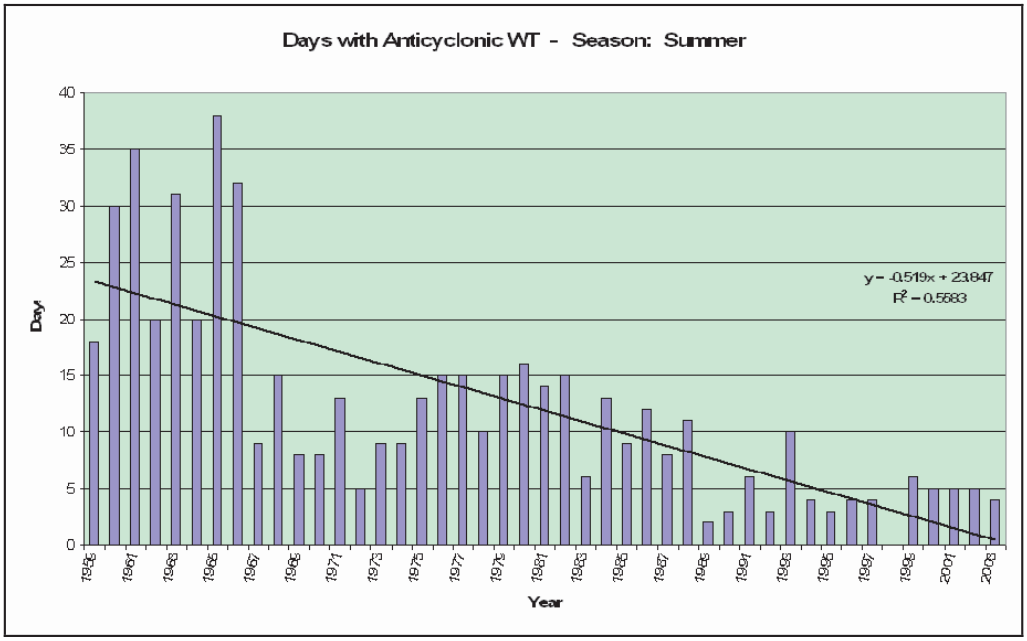

Figure11. *Trend of anticyclonic days in summer season*

Results show that the Weather Type Classification based on circulation pattern is a useful tool for the analysis of atmospheric behavior. Limitations of this classification arise when small scale features are dominant. In this study different topographic conditions (an island and a coastal site) gave different results. Also different seasonal response has been found. Winter

season demonstrate better agreement than spring and summer seasons between local and synoptic conditions probably due to stronger and more defined atmospheric fluxes.

The Circulation weather type classification could give reasonable information also in the case of extreme events analysis both for wind and wave heights.

Analysis of trend shows evidence of changing of the frequency of Cyclonic and Anticyclonic occurrences; these results are interesting and need further analysis with different data sets or other type of analysis (i.e. storm track).

References

Conway D., P.D. Jones, The use of weather type and air flow indices for GCM downscaling, Journal of Hydrology 212-213, 1998

Dessouky T.M. E., A.F. Jenkinson, An objective Daily Catalogue of Surface Pressure, Flow and Vorticity Indices for Egypt and It's use in Monthly Rainfall Forecasting, Meteorological Research Bulletin, Egypt, 1975.

Goodess C., The construction of daily rainfall scenarios for Mediterranean sites using a circulation-type approach to downscaling, PhD Thesis, University of East Anglia, 2000

Jenkinson A.F., F. P. Collison, An initial climatology of gale over the North Sea, Synoptic Climatology Branch Memorandum No. 62, Meteorological Office, Bracknell, 1977.

Jones P.D., M. Hulme, K.R. Briffa, A comparison of Lamb circulation types with an objective classification scheme, International Journal of climatology, vol.13, 655 – 663 (1993)

Trigo R.M., C.C. DaCamara, Circulation Weather types and their influence on the precipitation regimes in Portugal, International Journal of climatology, 20: 1559-1581 (2000)

European Commission

EUR 22594 – COST Action 733 – Proceedings from the 5th annual meeting of the european meteorological society – Session AW8: weather types classifications – COST Domain: Earth System Science and Environmental Management (ESSEM)

Luxembourg: Office for Official Publications of the European Communities

2007 — 117 pp. — 17.6 x 25 cm

ISBN 978-92-898-0025-9